Master's thesis

NTNU
Norwegian University of Science and Technology
Faculty of Natural Sciences
Department of Materials Science and Engineering

Cathrine Nøstvold

Mass and Energy Balanced Life Cycle Assessment of Metallurgical Grade Silicon Production

Master's thesis in Nanotechnology
Supervisor: Gabriella Tranell
Co-supervisor: Johan Berg Pettersen and Elisa Pastor Vallés
August 2022

NTNU
Norwegian University of
Science and Technology

Cathrine Nøstvold

Mass and Energy Balanced Life Cycle Assessment of Metallurgical Grade Silicon Production

Master's thesis in Nanotechnology
Supervisor: Gabriella Tranell
Co-supervisor: Johan Berg Pettersen and Elisa Pastor Vallés
August 2022

Norwegian University of Science and Technology
Faculty of Natural Sciences
Department of Materials Science and Engineering

NTNU
Norwegian University of
Science and Technology

Preface

The work presented in this thesis, constitutes the deliverable to TMT4910 - Nanotechnology, Master's Thesis. The project have been conducted throughout the spring and summer of 2022, aiming to create a baseline for the SisAl project, and contributing to new and improved ways of producing silicon metal.

I would like take the opportunity to thank my supervisor on silicon metal production at the Department of Materials Science and Engineering, Gabriella Tranell, for introducing me to the world of metals and materials. I greatly appreciate the guidance, opportunities and lifelong memories given me throughout this project. I would also like to direct a huge thanks to my supervisor on LCA at the Department of Energy and Process Engineering, Johan Berg Pettersen, for guiding me through the landscape of life cycle assessments. The discussions have been vital for broadening my perspective.

Furthermore, I would like to acknowledge my co-supervisor on life cycle assessments, Elisa Pastor Vallés, at the Department of Energy and Process Engineering. I sincerely appreciate all the help I have been given, and I am forever thankful for all guidance and support throughout my project. I would also like to extend my gratitude to Vegar Andersen at the Department of Materials Science and Engineering. The help I received during the mass and energy balance, have been of uttermost importance to me and this thesis, which I am truly grateful for.

Finally, I would like to acknowledge my man, Eirik Robert Reynolds. For supporting me, encouraging me, and loving me, through the ups and the downs, and everything in-between. One simply does not fulfil a master's degree without you.

This work was supported by the SisAl Pilot Consortium under Grant Agreement No. 869268.

Sammendrag

På grunn av forsyningsrisiko og en uerstattelig anvendelse innenfor et bredt spekter av lavkarbonteknologier, er silisium ansett som et kritisk råmateriale. Metallet fremstilles ved reduksjon av SiO_2 i kvarts, ved bruk av karbon som tradisjonelt sett er en blanding av både bio- og fossilt karbon. I forbindelse med overgangen til et lavkarbonsamfunn, vurderes det å erstatte det fossile karbonet som tilsettes med bio-karbon. Flere studier har undersøkt miljøpåvirkningen fra silisiumproduksjon ved bruk av en tradisjonell karbonmiks, men ikke like mange har betraktet en karbonblanding utelukkende bestående av biokarbon.

For å undersøke hvilken effekt det har å erstatte den tradisjonelle karbonmiksen med en biobasert miks, har en livsløpsvurdering blitt gjennomført. Livsløpsregnskapet ble gjennomført som en masse- og energibalanse av silisiumproduksjon, inkludert gjenvinning av energi og silika fra avgassen, og raffinering av metallet. To ulike karbonblandinger ble brukt i vurderingen: Én som representerer den tradisjonelle blandingen, og én utelukkende bestående av bio-karbon. For å undersøke hvordan silisiumutbytte påvirker ytelsen, ble tre forskjellige utbytter for hver blanding undersøkt, noe som gav totalt seks scenarier. Livsløpseffektvurderingen viste at bruk av en ren biobasert karbonblanding reduserte miljøpåvirkningen for 10 av 18 effektkategorier på midtpunktnivå, og for alle tre effektkategorier på endepunktnivå. For fem av de åtte mest fremtredende effektkategoriene på midtpunktnivå, presterte den bio-baserte karbonblandingen bedre enn den konvensjonelle. Bidragsanalysen viste også ved å implementere avgassbehandling, og velge biobaserte råvarer fra bærekraftig produksjon, kan i tilfellene hvor den biobaserte blandingen scoret høyest, redusere effekten ytterligere.

Abstract

Silicon metal is a critical raw material due to its supply risk, and its wide range of applications withing technologies needed for transferring to a low carbon society. It is produced by reduction of SiO_2 in quartz, by the use of carbon which, conventionally, is a mix of both fossil and biogenic carbon. As a part of transitioning to a low carbon future, the fossil carbon added to the process is considered completely replaced with biogenic carbon. Several studies have investigated the environmental impact of silicon production concerning the conventional carbon mix, however, little is found on switching to a purely bio based carbon mix.

To investigate the impact of going from a mixture of both fossil and biogenic carbon, to an purely bio based carbon mix, a life cycle assessment have been conducted. The inventory analysis was conducted as a mass and energy balance of metallurgical grade silicon production, including recovery of energy and silica from the off gas, and refining of the metal. The analysis was conducted for two different charge mixes. One representing the conventional mix, and one purely based on biogenic carbon. To further investigate how silicon yields affect the performance, three different yields for each mix was investigated, resulting in a total of six scenarios. The results showed that using a completely bio based carbon mix, reduced the impact for 10 of 18 midpoint impact indicators, and for all three endpoint indicators. Of the eight most prominent midpoint impact categories, bio performed better than the conventional mix on five of them. The contribution analysis also revealed that off gas treatment, and careful selection of biogenic raw materials from sustainable production, could further lower the impact categories where the bio based mix scored higher than the conventional charge mix.

Nomenclature

Chemical compounds

C	Carbon
CH_4	Methane
CO	Carbon monoxide
CO_2	Carbon dioxide
N_2O	Dinitrogen monoxide
NO_X	Nitrogen oxides
PAH	Polycyclic Aromatic Hydrocarbon
Si	Silicon
SiO	Silicon oxide
SiO_2	Silicon dioxide, silica
SO_2	Sulphur dioxide
SO_X	Sulphur oxide
VOC	Volatile Organic Compound

Life cycle assessment impact category abbreviations

ED	Damage to Ecosystem Quality
EOF	Photo-chemical Oxidant (Tropospheric Ozone) Formation: Ecosystems
FE	Freshwater Eutrophication

FET Freshwater Ecotoxicity

FF Fossil Fuel

GW Global Warming (climate change)

HH Damage to Human Health

HOF Photo-chemical Oxidant (Tropospheric Ozone) Formation: Humans

HTc Human Toxicity, carcinogenic

HTnc Human Toxicity, non-carcinogenic

IR Ionising Radiation

LO Land Occupation

ME Marine Eutrophication

MET Marine Ecotoxicity

OD Stratospheric Ozone Depletion

PMF Particulate Matter Formation

RA Damage to Resource Availability

SO Surplus Ore

TA Terrestrial Acidification

TET Terrestrial Ecotoxicity

WC Water Consumption

Life cycle assessment abbreviations

AoP Areas of Protection

CF Characterisation Factor

F.U. Functional Unit

LCA Life Cycle Assessment

LCI Life Cycle Inventory Analysis

LCIA Life Cycle Impact Assessment

OF Ozone Formation

Other abbreviations

GHG Greenhouse Gas

LHV Lower Heating Value

MT Metric ton

NCV Net Calorific Value

PM Particulate Matter

SEAF Submerged Electric Arc Furnace

Contents

List of Figures

List of Tables

Chapter 1

Introduction

1.1 Background

Silicon (Si), the second most abundant element in Earth's crust [1], plays a key role in decarbonising the society. It is directly used in low carbon technologies, such as photovoltaic panels and Li-Ion batteries, and indirectly used in a wide range of renewable energy technologies through chemical and metallurgical applications [2–9].

Even though silicon is a metalloid, it is usually referred to silicon metal due to its metallic look. It is produced from the silica (SiO_2) rich mineral quartz, by a reduction reaction using a carbon (C) source as a reducing agent. The smelting happens in an submerged electric arc furnace (SEAF) [6], and when heat is added to the reaction, carbon binds to the oxygen and liquid Si is tapped from the process [10]. After a refining step, the purity of this metal is usually in the range of $96\% - 99.99\%$, and is named metallurgical grade silicon (MG-Si) [4, 10–13]. If the silicon metal is to be used in solar or electronic applications, further purification is needed [14, 15].

Despite an global abundance of quartz [16], silicon is considered a Critical Raw Material (CRM) in the European Union due to its high economic importance and supply risk [17]. This is because all major producers of silicon metal are situated outside of the union, making it highly dependent upon import [7]. One of these is Norway, the third largest producer worldwide [18, 19], and also one of the main exporters to the European Union [7].

1.2 Current status and future trends

Today, the main end use of silicon metal in the EU is divided into four streams: chemical applications (54%), aluminium alloys (38%), solar applications (6%) and electronic applications (2%) [7]. At first glance, it may seem like silicon metal only plays a small role in decarbonising the society. However, through chemical applications and aluminium alloys, silicon have a wide range of applications: from chargers of electrical vehicles and wind turbine generators, to improving insulation and reducing heat loss in buildings [8, 20, 21].

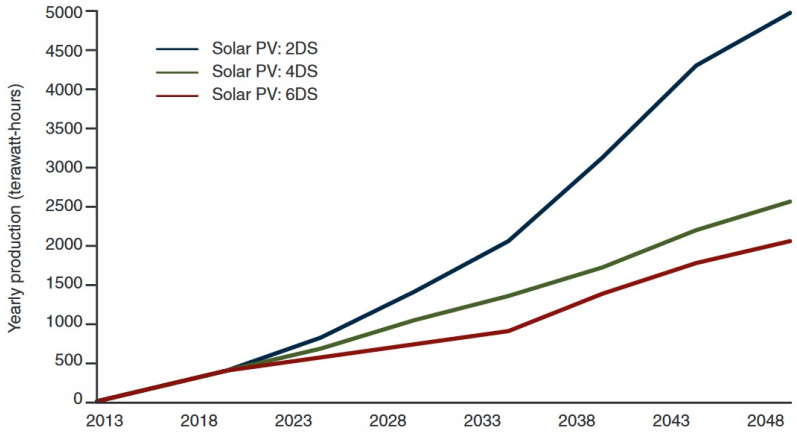

Figure 1.1: Projected production of solar PV for three different scenarios: 2 °C (2DS), 4 °C (4DS), and 6 °C (6DS) increase. From *The Growing Role of Minerals and Metals for a Low Carbon Future*, by World Bank Group, 2017, World Bank Publications © [3].

The demand for silicon metal is expected to increase [3, 17]. This is connected with a growing global population, and the shift towards a climate neutral society, amongst others, and will demand more technology and renewable energy sources, like solar photovoltaic for electricity production, illustrated in Figure 1.1. Even though there are studies on recycling silicon metal from metal powder [22] and slag [23, 24] formed during the production process, and recovery of silicon metal from solar cell scrap [25, 26], the end-of-life recycling rate is 0%, and is expected to continue to be so [7]. This, combined with there being no substituting elements for silicon in chemical applications or in aluminium alloys, and replacing silicon metal by another element in solar or electronic applications results in serious loss of performance [7], underlines the expected increase in silicon metal demand and thus increased production.

1.3 Emissions from Si production

Producing silicon metal comes with emissions to air [27]. A strong affinity between silicon and oxygen atoms in silica, requires large amounts of energy to break the bonds [28]. The energy is added as heat through carbonaceous electrodes, which are consumed during the production.

Decomposing the electrodes and reducing agents, results in direct emissions of greenhouse gases like CO_2 and CH_4, contributing to global warming and climate change [10, 27]. The carbon mix usually contains fossil carbon, thus the problem can be addressed by switching from fossil to biogenic carbon [29]. Emissions of biogenic CO_2 is regarded as neutral, as long as the same amount of biomass consumed is regrown [30]. However, indirect greenhouse gas emissions are still associated with biogenic carbon, due to land use and land use change related to primary production of biogenic carbon [31].

Improvements within the sector have reduced the carbon material demand close to a stoichiometric limit [6]. Disregarding the discussion in the above section, further reductions of CO_2 emissions can only happen by using clean energy, recover heat and capture carbon from the off-gas. Because electricity production results in greenhouse gases emissions [32], silicon metal production have indirect emissions through the energy consumption. By recovering process energy, the overall energy is reduced, hence also the overall emissions [4].

Production of silicon metal is also a source of other hazardous emissions than greenhouse gases. Storage, handling, pre-treatment and smelting of quartz and carbon leads to emission of dust and particulate matter [4, 27]. Heavy metals, poly-cyclic aromatic hydrocarbons, volatile organic compounds, dioxins, CO, SO_2 and NO_x, originating from the raw materials or electrodes, are also emitted during smelting and post-treatment [27].

In addition to emissions to air, solid waste and by-products are produced together with silicon metal. SiO gas from the furnace oxidises when it meets air, and forms solid SiO_2 particles travelling with the off-gas. This is named micro-silica [33], due to the microscopic size of the particles, and is most commonly used as a component within the cement industry [12]. Another significant by-product is slag [10]. Even though production of MG-Si is almost slag free, SiO_2 rich slag can be used as a raw material in ferro-alloy production.

Even though the by-products from silicon metal production, microsilica and slag, can be utilised, recycling of silicon metal would further lower the energy consumption [28]. Unfortunately, as already mentioned in section 1.2, the end-of-life recycling input rate of silicon metal is 0%. Another possible solution, investigated by the SisAl pilot project, is to substitute the carbonaceous reducing agent with aluminium (Al), thus eliminating the direct emissions associated with the reducing agents [34].

1.4 Environmental assessments of MG-Si

As discussed in the previous section, one of the main contributors to emissions from silicon metal production, is the consumption of electricity. Silicon metal production is quite energy intensive, with a consumption of electricity of around $11 - 13\text{MW h}$ per MT silicon metal [10]. A study by Sævarsdottir, Magnusson and Kvande found an carbon footprint increase of MG-Si due to a shift towards more fossil-based electricity, underscoring the importance of the energy source for the environmental performance of silicon production [35].

Another topic discussed in section 1.3, was emissions from the raw materials. The environmental impacts of carbonaceous materials is already discussed, but quartz also plays a key role. Heidari and Anctil investigated the carbon footprint of MG-Si, focusing on quartz quality. They found an increase in both cumulative energy demand (CED) and carbon footprint when the purity of quartz decreased, highlighting the importance of raw material quality for environmental performance of the production [36].

Several life cycle assessments have been conducted in order to asses the environmental impact of silicon production, but most studies concern silicon used in solar or electronic applications [37–42]. This means that the studies either follows another process route than, or includes further refinement steps after, the process described in section 1.1. One study conducting an LCA of MG-Si, is found in the master's thesis by Vallés, comparing two different ways of reducing quartz to silica [43]. However, among other parameters, energy to be recovered or different charge mixes were not covered by this thesis, which, in light of the discussion in section 1.3, could be important parameters for the environmental performance of MG-Si.

1.5 Goal and Scope

As discussed throughout the introduction, silicon metal is an essential material for the transition to a more sustainable society. Its demand is predicted to grow, and considering the pollution emitted during production, makes it necessary to further investigate parameters influencing the environmental impact, and how these could vary under different production conditions.

Thus, in this thesis, the goal is to investigate the environmental performance of conventional silicon production, through a mass and energy balanced life cycle assessment, to identify hot-spots of pollution and which parameters they depend upon. The aim by doing so, is to contribute to the SisAl project by providing a baseline for comparison of new and improved ways of producing MG-Si [34]. From this, a research questions is derived:

> **From a mass and energy balanced life cycle assessment: how does a carbon mixture based on biogenic carbon only, perform compared to a more conventional mixture of both fossil and biogenic carbon, and how does altering the yield affect the results?**

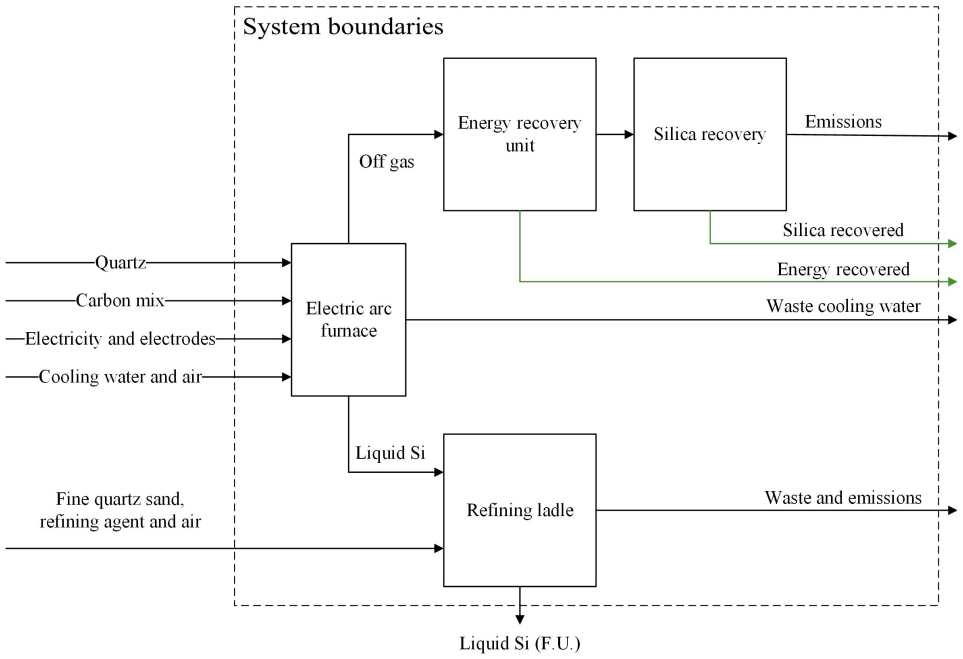

Figure 1.2: System boundaries of the investigated production process.

The scope covers the system illustrated in Figure 1.2: the furnace, refining ladle and recovery of energy and microsilica from the off gas. The functional unit, or reference unit, is 1 tonne refined silicon metal, with a final product consisting of no more than 0.2% aluminium, and no more than 0.05% calcium after refining. The study is limited to a Norwegian context, in terms of data collection and input variables to the LCA software. Data is collected mainly from published material, supplemented with unpublished internal data from the Department of Materials Science and Engineering at the Norwegian University of Science and Technology. The environmental impact will be assessed according to the midpoint and endpoint impact categories of the ReCiPe method [44]. Finally, the assessment will be evaluated on uncertainty and sensitivity, before conclusions and recommendations are made.

The structure of the thesis is as follows: after the introduction section, theory on silicon production and the nature of life cycle assessment follows, following the method section. Finally, the results are presented and discussed, before a final conclusion and recommendations for further work.

Chapter 2

Theory

2.1 The Process of Producing Metallurgical Grade Silicon

If not otherwise stated, the following subsections are based on the book *Production of High Silicon Alloys* by Schei, Tuset and Tveit [10].

2.1.1 The Furnace

As mentioned in section 1.1, the input raw materials for production of silicon metal is quartz and carbon, the latter in the form of a mixture of two or more of coke, coal, charcoal and wood chips. This is called a charge mix. While coke and coal are fossil carbon sources, charcoal and wood chips are termed biogenic, or bio based, carbon, simply because these products originate from biomass. Energy enters the furnace either through the raw materials as chemical energy, or through consumable electrodes as electric energy [45, 46], as seen in Figure 2.1. Since both heat and carbon are vital to break the bonds between oxygen and silicon in SiO_2, it is named a carbothermic reduction reaction. The overall reaction equation within the furnace is given as:

$$\mathrm{SiO_{2(s)}} + 2\,\mathrm{C_{(s)}} \longrightarrow \mathrm{Si_{(l)}} + 2\,\mathrm{CO_{(g)}}\,. \tag{2.1}$$

Here, the Si yield is 100%, namely that all silicon entering the furnace through quartz, leaves as liquid silicon. However, this is rarely the case, as there

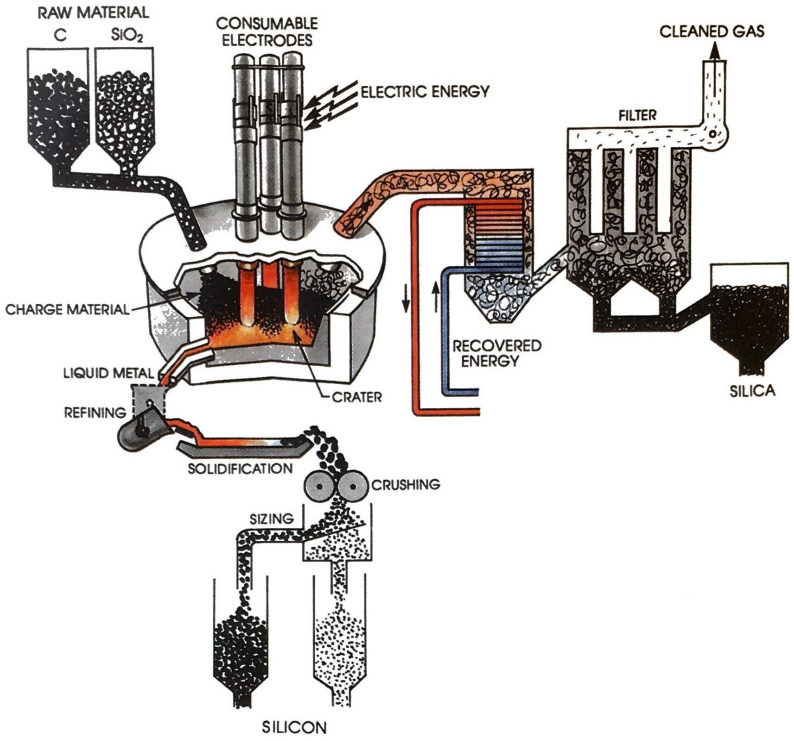

Figure 2.1: Illustration of a typical silicon production plant. Reproduced with permission from *Production of High Silicon Alloys*, by Schei, Tuset and Tveit, 1998, Fagbokforlaget [10].

is some loss of Si to the off gas. This depend upon the SiO reactivity of the carbonaceous raw materials, and how the furnace is operated [12]. The following reaction equation shows how $SiO_{(g)}$ is formed:

$$SiO_{2(s)} + C_{(s)} \longrightarrow SiO_{(g)} + CO_{(g)}\,. \tag{2.2}$$

By multiplying Equation 2.1 by the Si yield, x, and Equation 2.2 by the Si yield loss, $(1-x)$, and adding these two reactions together, an overall reaction equation within the furnace, taking yield and loss into account, is given by:

$$SiO_{2(s)} + (1+x)\,C_{(s)} \longrightarrow x\,Si_{(l)} + (1-x)\,SiO_{(g)} + (1+x)\,CO_{(g)}\,. \tag{2.3}$$

2.1.2 The Off Gas

The $SiO_{(g)}$ and $CO_{(g)}$ produced in the melt, rise to the upper part of the furnace at a temperature around 1400 °C. Here, air in excess is let in, and a combustion occurs according to:

$$SiO_{(g)} + CO_{(g)} + 2\,O_{2(g)} \longrightarrow SiO_{2(s)} + CO_{2(g)} + O_{2(g)}\,. \tag{2.4}$$

This lowers the temperature of the off gas a little, but by adjusting the inlet air to keep the gas temperature above 600 °C, microsilica is produced.

After the combustion within the furnace, the off gas continues to an energy recovery unit. The hot off gas heats up water within a boiler, such that superheated steam is produced. This steam is fed to a turbine, making the turbine rotate, which in turn forces an attached generator to produce electricity. Approximately 30% of the energy recovered from the off gas ends up as electricity, the rest is lost [4].

The off gas leaves the energy recovery unit, and enters the silica filter at a temperature of about 150 °C. Here, the microsilica produced during combustion is filtered out, and the rest of the off gas leaves through the stack and enters the environment. As previously mentioned in section 1.3, undesirable compounds originating from handling, smelting and combustion of raw materials, accompany the off gas and are emitted to air.

2.1.3 The Refining Ladle

The liquid silicon product in Equation 2.3 is tapped into a refining ladle from the furnace, at a temperature about 1600 °C. Oxygen enriched air is bubbled through the melt in the ladle, forming an oxide film, also called slag, at the metal surface according to:

$$\mathrm{Si_{(l)}} + \mathrm{O_{2(g)}} = \mathrm{SiO_{2(s)}}\,. \tag{2.5}$$

Due to the high affinity Ca and Al have to oxygen, the two following reactions will also occur:

$$2\,\mathrm{Ca_{(l)}} + \mathrm{SiO_{2(s)}} = 2\,\mathrm{CaO_{(s)}} + \mathrm{Si_{(l)}}\ , \tag{2.6a}$$

$$4\,\mathrm{Al_{(l)}} + 3\,\mathrm{SiO_{2(s)}} = 2\,\mathrm{Al_2O_{3(s)}} + 3\,\mathrm{Si_{(l)}}\,. \tag{2.6b}$$

Oxidation of Ca and Al is also mutually linked:

$$3\,\mathrm{Ca_{(l)}} + \mathrm{Al_2O_{3(s)}} = 3\,\mathrm{CaO_{(s)}} + 2\,\mathrm{Al_{(l)}}\,. \tag{2.7}$$

In order to minimise the loss of Si to the slag from the reaction in Equation 2.5, the principle of Le Châtelier is utilised. Le Châtelier's principle states that, by any external perturbation to a system, for instance by increasing the concentrations of reactants in a chemical reaction, the system will move towards

the opposite direction, consequently increasing the concentration of products while simultaneously lowering the concentration of the reactants, until a new equilibrium is reached [47]. Therefore, by adding SiO_2 to the ladle in the form of fine quartz sand, Equation 2.5 will shift towards the left side, while Equation 2.6a and Equation 2.6b will shift towards the right side. Depending on the composition of the silicon metal tapped from the furnace, and the desired composition of the refined metal, $CaO_{(s)}$ is added during refinement as well, to avoid too much loss of $Si_{(l)}$ to $SiO_{2(s)}$.

2.2 Life Cycle Assessment

If not otherwise stated, section 2.2 and appurtenant subsections, are based on ISO standards 14040:2006 and 14044:2006 [48, 49].

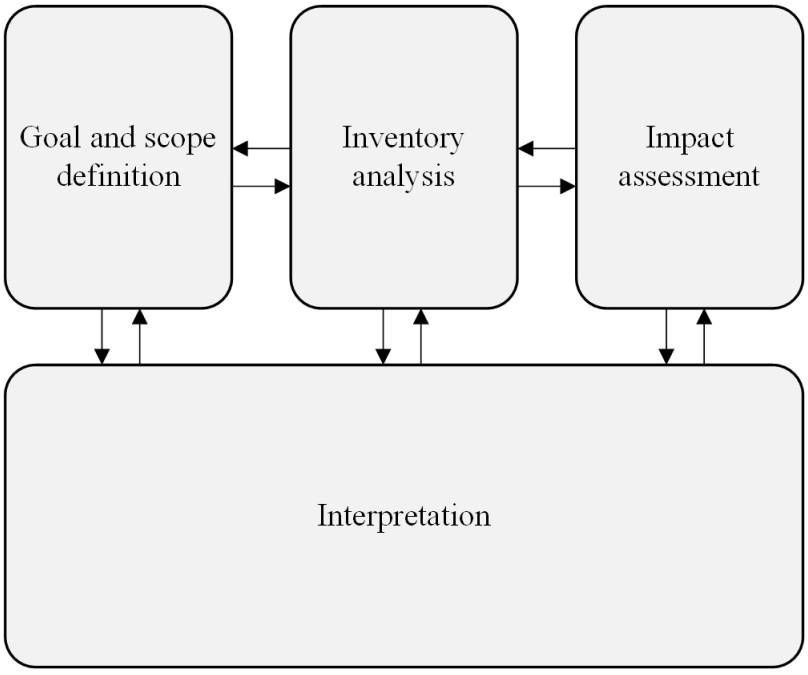

Figure 2.2: The four phases of an LCA, adapted from ISO Standard No. 14040:2006 [48].

Life cycle assessment (LCA) is a tool that can aid in increasing the awareness of possible environmental impacts associated with a product or a service, by identifying the main contributors to emissions during the life cycle of the system studied. This is conducted in a 4-step iterative process, as illustrated in Figure 2.2. It is an iterative technique because, as one makes progress through

the different phases, one may discover that a modification of previous or coming phases is required. The following subsections gives a short description of each of the four phases, and the inventory and impact phases will be further elaborated in subsequent sections.

2.2.1 Goal and Scope

This is the first phase of an LCA, and sets the scene for the study. The goal of the study describes the motive for conducting the study, the intended application, and how and to whom it is to be presented. The scope focuses more detailed on the system investigated, and describes the product or service that is to be studied. This covers, amongst others, describing system boundaries, which impact assessment methodology and categories that are used, assumptions, limitations, and information regarding the data used. The scope also covers describing the functional unit (F.U.), which is the reference unit to which all inputs and outputs are normalised. Depending on the system studied, the F.U. can be based on the performance, property or reference flow of a material [50]. However, great care should be taken when deciding the F.U., as different F.U.s for the same system can result in large variations within the different impact categories [51, 52].

2.2.2 Inventory Analysis

The second phase of an LCA is the life cycle inventory analysis (LCI), which covers data collection and processing, as well as allocation of flows and emissions. When modelling the inventory, a distinguishing between the foreground and background system is made [53]. The foreground system consists of the processes within the scope of the study, while the background system holds all the processes entering the foreground system. When conducting an LCA, the background system, making up about 99% of the unit processes within the studied system [54], is modelled using a database, while data of the foreground system is collected and calculated [55].

2.2.3 Impact Assessment

Life cycle impact assessment (LCIA) is the third phase of an LCA. During the LCIA phase, impact categories, category indicators and characterisation models are selected. These are used to classify and characterise the LCI results, and are necessary steps of the impact assessment to provide the LCIA results, also called an LCIA profile. Further optional steps are to do a normalisation, grouping or weighting of the LCIA profile.

2.2.4 Interpretation

The fourth phase is the interpretation. At this point of the assessment, results from the LCI and the LCIA are regarded jointly. This way, significant issues can be identified, and conclusions, limitations and recommendations can more easily be given. Completeness, sensitivity and consistency of the LCA should also be evaluated during this phase. Completeness is controlled by evaluating whether all relevant data and information regarding the interpretation is complete and accessible. If it's not, one must either consider revising the previous phases, or justify why the missing information is unnecessary, if that be the case. A sensitivity check is conducted to evaluate the reliability of the interpretation. The aim of this check is to demonstrate how data uncertainties, calculations or other steps during the previous phases, affect the results. Thirdly, the focus on consistency is to check if data, assumptions and methods are in accordance with the goal and scope defined in the first phase.

2.3 Inventory by Mass and Energy Balance

One way of carrying out the life cycle inventory analysis, is by conducting a mass and energy balance.

2.3.1 Mass Balance

The mass balance is based on stoichiometric calculations by use of the relationship

$$n = \frac{m}{M}\,, \tag{2.8}$$

where n is the number of mole in [mol], m is the mass in [g], and M the molar mass of a given element or compound, given in [g/mol] [56]. By knowing the mass of at least one of the compounds included in a chemical reaction, the mass of the other compounds are calculated by the molar relationship between the compounds. The molar mass of elements can easily be found, for instance in *Aylward and Findlay's SI Chemical Data* [57], and the molar mass of a mixture is calculated from

$$M_{mix} = \sum_i x_i M_i\,, \tag{2.9}$$

where x is the mole fraction, and i the different constituents of the mixture.

2.3.2 Energy Balance

As already mentioned in subsection 2.1.1, energy is supplied to the furnace either as electric or chemical energy. The amount of electric energy going into the furnace, depends on the power of the furnace, which can be in the range of $10 - 45$ MW [46]. The amount of chemical energy entering the furnace, can be estimated using a modified version of Dulong's formula [58]:

$$\mathrm{LHV}\,[\mathrm{kJ/g}] = 38.2 m_{\mathrm{C}} + 84.9\left(m_{\mathrm{H}} - \frac{m_{\mathrm{O}}}{8}\right) - 0.62\,. \tag{2.10}$$

m_{C}, m_{H} and m_{O} are the percentages of carbon, hydrogen and oxygen, respectively, in the raw materials. LHV is short for lower heating value, also known as net calorific value (NCV), which gives the energy when all the water produced during the process, remains as water vapour instead of condensing back to liquid [59]. If the analysis provide data of dried raw materials, and the raw materials are not dried before utilised in the production, a conversion from dry based to wet based LHV is necessary [60]:

$$\mathrm{LHV_{WB}}[\mathrm{kJ/g}] = \mathrm{LHV_{DB}} \cdot \left(\frac{100\% - MC\%}{100\%}\right) - (24.43 \cdot MC\%)\,. \tag{2.11}$$

Here, $\mathrm{LHV_{WB}}$ and $\mathrm{LVH_{DB}}$ are the wet based and dry based lower heating values, respectively, where $\mathrm{LVH_{DB}}$ is calculated from Equation 2.10. $MC\%$ is the moisture content in percentage of the material.

Energy leaves the furnace through the off gas or the silicon metal, or as miscellaneous losses [45, 46]. When energy is transferred between two mediums due to a temperature difference, it is called heat. This is the case for energy lost or recovered from off gas, and can be calculated by:

$$Q = mc_{\mathrm{p}}\Delta T\,, \tag{2.12}$$

where Q is energy transferred in [J]. m is the mass in [kg] of the medium which undergo a temperature change, ΔT is the temperature change in [K], and c_{p} is the specific heat capacity at constant pressure, p, of the medium, which is given in $[\mathrm{J\,kg^{-1}\,K^{-1}}]$ [56]. For a mixture of compounds, the specific heat capacity can be calculated according to:

$$c_{\mathrm{p},mix} = \frac{1}{M_{mix}} \sum_i x_i c_{\mathrm{p},i} M_i\,. \tag{2.13}$$

Here, i are the different constituents of the mixture, and x their respective mole fraction. If the mass fraction z is given instead of the mole fraction, Equation 2.13 is rewritten to

$$c_{\mathrm{p},mix} = \sum_i z_i c_{\mathrm{p},i}\,. \tag{2.14}$$

The energy leaving the furnace with the tapped silicon metal can be divided into chemical and thermal energy. The chemical energy is found by considering average bond enthalpies, ΔH, found in *Aylward and Findlay's SI Chemical Data*, while the thermal energy of tapped silicon at 1600 °C is found using databases like *HSC Chemistry® 9*.

2.4 Impact Assessment using ReCiPe

As previously described in subsection 2.2.3, impact assessment is about classify and characterise the LCI results. One way of assessing the life cycle impact, is through the ReCiPe2016 method [62]. The method concerns 18 midpoint impact categories, and three endpoint impact categories, as seen in Figure 2.3.

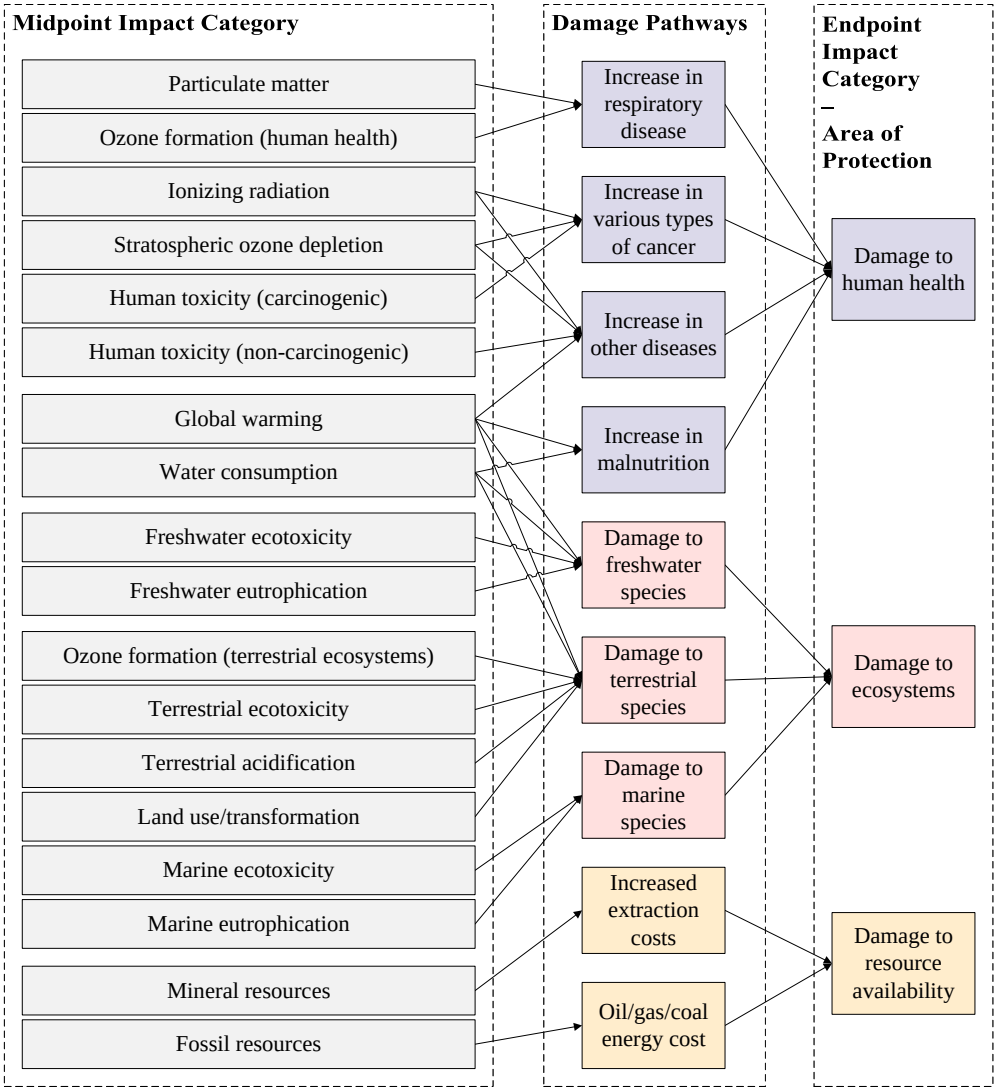

Figure 2.3: Overview of how the midpoint and endpoint indicators are linked. Adapted from *ReCiPe 2016 v1.1. Report I: Characterization*, by Huijbregts et al., 2017, National Institute for Public Health and the Environment [44].

Emissions and extraction of resources are translated into impact scores through characterisation factors, expressed as impact per unit stressor. Impacts at midpoint level are calculated using

$$I_m = \sum_i CF_{m,i} \times M_i \,, \tag{2.15}$$

where I_m is the midpoint impact for impact category m in $[\mathrm{kg}x - \mathrm{eq}]$, M is the magnitude of inventory flow i in [kg], and CF the characterisation factor that connects flow i with midpoint impact category m in $[\mathrm{kg}x - \mathrm{eq}\,/\mathrm{kg}]$ [63]. x is the reference substance of each midpoint impact category.

Endpoint impacts can be calculated from midpoint impacts by

$$I_e = \sum_m CF_{e,m} \times I_m \,, \tag{2.16}$$

where I_m is the midpoint impact calculated in Equation 2.15, and $CF_{e,m}$ the characterisation factor connecting midpoint impact m to endpoint impact e. The three endpoint impact categories have different units, as also the midpoint impact categories have. Damage to human health is given in [year], disability-adjusted loss of life years, damage to ecosystem quality is given in [species · year], time-integrated species loss, and damage to resource availability is given in [US$], surplus cost [44].

The characterisation models are a source of uncertainty, and this is targeted by dividing uncertainty and choices into three different scenarios, where one of the perspectives is chosen during data processing [44, 63–65]:

- **Individualist perspective:** Risk-seeking with a short-term perspective. Only undisputed impacts, from proven cause-effect relations, are considered, giving little uncertainty in data used.
- **Hierarchist perspective:** Risk-accepting, where the perspective of the time-frame and plausibility of impact mechanisms are based on scientific consensus.
- **Egalitarian perspective:** Risk-aversive with a long-term perspective. Follows the precautionary principle, where nothing is left out, but all data available is included. This gives the most complete, but also the most uncertain, data set.

The endpoint impact categories are closely linked to three areas of protection (AoP) identified in the ReCiPe method: human health, natural environment, and resource scarcity. To compare the endpoint impact categories with each-other, the endpoint impact results can be weighted [49]. The weighting can either be done according to the perspective, or with an average approach. The latter weight human health and ecosystems equally, 40% each, and resource availability is weighted by 20%.

Chapter 3

Methodology

All calculations are based on fixed carbon content (% Fix C), given in metric units, at 1 atm and 25 °C. The functional unit, F.U., of the LCA is 1 tonne refined Si. During calculations, three assumptions were made:

1. Complete combustion in the combustion zone of the furnace, i.e., all $CO_{(g)}$ is converted to $CO_{2(g)}$. This is for simplicity, because incomplete combustion can lead to a wide range of compounds which would be too comprehensive to include in this thesis [66–68].

2. During combustion, the amount of Ar and N_2 entering with air, was assumed to remain equal when leaving with the off gas, and not react during combustion. Ar was not considered because it is an inert gas. The behaviour of nitrogen during combustion is dependent upon several factors, amongst others the temperature and the SiO behaviour [27, 69–73]. Further, nitrogen is not included in the distribution tables used in this thesis, thus both nitrogen entering with air and from raw materials were left out of the calculations. Nitrogen compounds were added to the LCA analysis as emission factors instead, which will be covered later in this chapter.

3. Because carbothermic reduction of SiO_2 to Si is considered a slag free process [10], it was assumed that no slag was created in the furnace. Therefore, all slag in the mass balance was assumed to originate from oxidation within the ladle.

Mass and energy balance was calculated for two different charge mixes, as stated in section 1.5, for three different yields: 85%, 90% and 95%. This resulted in a total of six different scenarios for life cycle assessment. The biogenic carbon mix (BIO) is based on an internal report on charge mixtures from Kallfeltz, sited in Myrvågnes's doctoral thesis [74], while the mix representing the conventional charge mix (MIX) is found in 'Pilot Scale Test of Flue Gas Recirculation for the Silicon Process' by Andersen et al. [75], and are shown in Table 3.1.

Table 3.1: Charge mixtures, given as share of % Fix C. Gathered from [74, 75].

	Coke	**Coal**	**Charcoal**	**Wood Chips**
BIO	0%	0%	80%	20%
MIX	15%	40%	30%	15%

Proximate analysis of the raw materials was used to calculate the share of each carbon source in the charge mix based on % Fix C. Ultimate analysis was used to calculate the amount energy entering the furnace through the raw materials, and the amount of C and H leaving the furnace after combustion, as CO_2 and H_2O respectively. Ash analysis was used to estimate amount of trace elements entering the furnace through the raw materials, and the distribution of the trace elements between metal, slag, fume and off gas was estimated by distribution tables.

3.1 Raw Materials Data

Proximate, ultimate, and ash analysis, on coke, coal, charcoal and wood chips, were provided by Vegar Andersen [76]. These analyses were dry based, and gathered from internal experiments at the Department of Material Sciences at NTNU, and used in a recent publication [75]. Because the ash analysis did not include all elements listed in the distribution tables mentioned in the previous section, values gathered from Phyllis' database was supplemented [77–80]. Proximate and ultimate analysis of the electrode material was found in a SINTEF report [81], while ash analysis for the electrode material found

in the doctoral thesis of Myrhaug [82]. Ash analysis on quartz was gathered from the doctoral these of Myrhaug and Aasly [82, 83].

Table 3.2: Wet based proximate analysis of carbonaceous materials. The values for the electrode are dry based, since the moisture content is 0 %. Adapted from [76, 81].

	Moisture	**FixC**	**Volatiles**	**Ash**
Coke	11.70 %	82.36 %	5.37 %	1.79 %
Coal	10.80 %	52.08 %	36.82 %	1.35 %
Charcoal	4.70 %	81.38 %	12.13 %	2.01 %
Wood chips	40.00 % [1]	17.86 %	-	-
Electrode	0.00 %	96.00 %	0.70 %	3.00 %

To account for the moisture in the raw materials, the dry based proximate analysis was converted into wet based using the formula $\frac{100\%}{100\%+MC\%}$, where MC is the moisture content of the respective raw material. The original, dry based proximate analysis is found in Appendix A.

Table 3.3: Dry based ultimate analysis of carbon materials, from [76, 81].

	Coke	**Coal**	**Charcoal**	**Wood chips**	**Electrode**
C [%]	89.30 %	78.00 %	83.00 %	50.70 %	96.60 %
N [%]	1.78 %	1.58 %	0.39 %	0.20 %	-
O [%]	3.83 %	12.00 %	9.60 %	41.40 %	-
H [%]	1.83 %	5.79 %	3.71 %	6.48 %	-
S [%]	0.42 %	0.52 %	0.05 %	0.11 %	0.30 %

The dry based ultimate analysis was used directly, without any conversion with respect to moisture, to calculate the energy entering the furnace through the raw materials. The ultimate analysis is seen in Table 3.3. However, when calculating the CO_2 and H_2O leaving the furnace after combustion, the rows of C and H were converted to wet based values using the same formula as for Table 3.2 to account for moisture in the raw materials. These wet based values can be found in Appendix A.

[1] Value provided by Vegar Andersen through personal communication, as wood chips are dried before analysis but not before used in charge mixtures [84].

Table 3.4: Dry based ash analysis of raw materials showing trace element content. Be aware of different units. Adapted from [76–80, 82, 83]. More information on how these values were determined, can be found in Appendix B.

		Quartz	**Coke**	**Coal**	**Charcoal**	**Wood chips**	**Electrode**
Al	[%]	0.25	0.13	0.78	0.02	0.01	0.39
As	[ppm]	0.30	0.20	1.36	3.30	0.03	2.50
B	[ppm]	37.50	-	45.50	15.70	5.90	37.50
Ba	[ppm]	13.00	40.40	56.20	43.05	27.70	62.00
Be	[ppm]	0.10	0.36	0.22	0.02	0.04	0.25
Bi	[ppm]	0.25	0.00	-	-	-	1.50
Ca	[%]	0.004	0.05	0.25	1.01	0.38	0.15
Cd	[ppm]	0.04	0.03	0.06	2.42	0.19	1.20
Cl	[%]	-	0.69	0.02	0.03	0.01	-
Co	[ppm]	37.00	0.89	1.65	0.17	0.21	10.00
Cr	[ppm]	14.50	2.00	6.92	6.08	2.08	19.00
Cu	[ppm]	1.50	15.43	6.47	6.72	2.85	12.00
Fe	[%]	0.10	0.26	0.39	0.03	0.01	0.34
Hg	[ppm]	0.00	0.03	0.03	0.03	0.01	0.04
K	[%]	0.06	0.08	0.10	0.31	0.08	0.02
Mg	[ppm]	50.50	322.00	657.30	917.05	322.19	473.00
Mn	[%]	0.01	0.004	0.003	0.03	0.02	0.29
Mo	[ppm]	6.00	0.85	0.99	0.19	0.07	2.00
Na	[ppm]	79.00	449.00	514.70	306.20	47.03	288.00
Ni	[ppm]	4.50	3.59	4.70	14.73	1.18	31.00
P	[ppm]	25.00	28.80	36.80	1300.30	131.34	163.00
Pb	[ppm]	3.00	10.91	1.53	3.41	0.97	46.00
S	[%]	0.09	0.65	0.66	0.01	0.07	0.20
Sb	[ppm]	0.25	-	-	5.10	0.11	0.60
Sc	[ppm]	1.00	1.01	0.77	0.07	0.02	-
Se	[ppm]	0.25	-	5.60	-	0.03	0.25
Si	[%]	46.20	1.53	2.03	0.11	0.06	-
Sn	[ppm]	0.25	0.07	0.36	0.69	0.03	1.60
Sr	[ppm]	12.00	22.00	23.60	38.95	5.27	39.00
Ti	[ppm]	200.00	89.60	284.80	8.91	5.64	-
Tl	[ppm]	0.25	-	-	-	-	0.25
V	[ppm]	3.00	9.65	15.31	0.52	0.27	37.00
W	[ppm]	75.80	0.18	0.09	0.11	0.01	0.50
Zn	[ppm]	4.00	13.15	11.31	91.70	78.55	48.00
Zr	[ppm]	24.15	4.47	3.22	0.93	0.50	1.70

Sulphur, S, is given in both the ultimate analysis (Table 3.3) and the ash analysis (Table 3.4). In order to keep consistency throughout the trace element distributions, the latter value was chosen for the mass balance.

As previously mentioned, Phyllis' database was used to supply information on trace elements in the carbonaceous raw materials [77–80]. In addition, two sources of trace element composition of quartz was used [82, 83]. To see how values were chosen for the trace element composition of the raw materials, please refer to Appendix B for further information. The final ash analysis of trace elements in the carbonaceous materials is shown in Table 3.4. Stoichiometric calculation of the Si content in quartz found in Table 3.4, resulted in quartz purity of 99.50 % SiO_2.

3.2 Mass Balance

Following is a brief explanation on how the mass balance was conducted. Detailed calculations can be found in Appendix C.

3.2.1 Submerged Electric Arc Furnace

Daily quartz consumption was calculated from a 45 MW furnace [46] and an energy consumption of 4.6 MWh/t quartz [85], resulting in $m_{quartz} = 234.78\,t/d$. From this, the mass balance was calculated in unit [d^{-1}]. When the mass balance was complete, and the final amount of refined, liquid Si produced per day was found, all previous values were divided by this number to get the unit [t^{-1} Si].

The amount of SiO_2 entering through quartz, was calculated from m_{quartz} and a quartz purity of 99.50 % SiO_2, giving $m_{SiO_2} = 0.95 \cdot m_{quartz} = 233.61\,t/d$. When quartz is reduced, it is only the fixed carbon (Fix C) in the raw materials that participate in the reaction [86]. Thus, all upcoming calculations regarding the carbonaceous raw materials, were based on their Fix C content.

The total amount of Fix C needed to reduce the SiO_2, was found by stoichiometric calculations of Equation 2.3, by using Equation 2.8. From this, the amount of each carbon material in the charge mix, was found using the ma-

terial's FixC%, and the percentage the raw material constituted in the charge mix. Electrode consumption of $100\,\mathrm{kg/t_{Si}}$ was used in the calculations as well [81]. As it is industrial practice to not include carbon from electrodes in the input calculations, but to include carbon from electrodes when calculating CO_2 emissions [87], this was also done for this thesis.

The amount of products from Equation 2.3, was found by stoichiometric calculations using Equation 2.8 and the calculated input of Fix C and $SiO_{2(s)}$. For the carbonaceous raw materials and electrodes, a distinction between C from fossil or biogenic sources were made. Coke, coal and electrodes were considered fossil sources, while charcoal and wood chips were treated as biogenic sources.

Trace elements entering the furnace through the electrodes and the raw materials, were distributed between tapped Si, silica fume and off-gas according to Table 3.5. Si entering the furnace from other sources than quartz, where distributed to tapped Si or gaseous SiO according to this table. The table is mainly based on data from the doctoral thesis of Kamfjord [88], but for the trace elements Bi, Sc, Sn, W and Zr, values are added from Myrhaug's doctoral thesis [82]. All elements leaving with off gas or silica fume were calculated as elements, i.e. Bi, except from sulphur, which was assumed to oxidise during combustion to SO_2 [89].

The amount of cooling water for the furnace was estimated by Equation 2.12. Incoming river water temperature was set to 5 °C, an estimated yearly average in a Norwegian river [90]. See Appendix D for graphical information on how this value was estimated. Outgoing cooling water temperature was set to 70 °C [91], and $Q = E_{\text{loss to cooling water}}$.

3.2.2 Off Gas: Combustion Zone and Silica Recovery

The amount of air let in to the combustion zone, was calculated from Equation 2.12, aiming for a final off gas temperature leaving the furnace at 750 °C [92]. By assuming an incoming air temperature of 25 °C, $\Delta T = 725\,\mathrm{K}$. Combustion zone gas energy was found from the energy balance, and the heat capacity was found using Equation 2.13 on Table 3.6. Heat capacities at $T = 400\,°\mathrm{C}$ was chosen as it was close to the middle temperature of the two temperature ranges where $C_{p,\,\text{air}}$ and $C_{p,\,\text{off gas}}$ were used, giving $C_{p,\,\text{air}} = 1.07\,\mathrm{MJ/(t \cdot K)}$.

Table 3.5: Element distribution within the furnace [82, 88].

Element	To metal	To silica fume	To off gas
Al	91 %	9 %	0 %
As	8 %	92 %	0 %
B	68 %	32 %	0 %
Ba	90 %	10 %	0 %
Be	64 %	36 %	0 %
Bi	70 %	30 %	0 %
Ca	79 %	21 %	0 %
Cd	28 %	69 %	3 %
Cl	0 %	33 %	67 %
Co	92 %	7 %	1 %
Cr	96 %	4 %	0 %
Cu	79 %	20 %	1 %
Fe	96 %	4 %	0 %
Hg	0 %	100 %	0 %
K	0 %	100 %	0 %
Mg	3 %	97 %	0 %
Mn	51 %	21 %	28 %
Mo	83 %	16 %	1 %
Na	0 %	100 %	0 %
Ni	96 %	4 %	0 %
P	21 %	79 %	0 %
Pb	0 %	98 %	2 %
S	0 %	4 %	96 %
Sb	2 %	97 %	1 %
Sc	80 %	20 %	0 %
Se	15 %	85 %	0 %
Si	80 %	20 %	0 %
Sn	80 %	20 %	0 %
Sr	79 %	21 %	0 %
Ti	100 %	0 %	0 %
Tl	12 %	88 %	0 %
V	99 %	1 %	0 %
W	100 %	0 %	0 %
Zn	4 %	90 %	6 %
Zr	99 %	1 %	0 %

Table 3.6: Heat capacities of the main air constituents, and silica, at 400 °C. C_p values were found by using *HSC Chemistry® 9*, molar masses in *Aylward and Findlay's SI Chemical Data* and the composition of air from *luft* [57, 61, 93].

	$\mathbf{C_p}$ [MJ/(t · K)]	**Molar mass**		**Mole fraction**
$\mathbf{N_{2(g)}}$	1.091	28.02	g/mol	78.08 %
$\mathbf{O_{2(g)}}$	1.024	32.00	g/mol	20.95 %
$\mathbf{H_2O_{(g)}}$	2.068	18.02	g/mol	1.00 %
$\mathbf{Ar_{(g)}}$	0.520	39.95	g/mol	0.94 %
$\mathbf{CO_{2(g)}}$	1.113	44.01	g/mol	0.04 %
$\mathbf{SiO_{2(g)}}$	0.910	60.09	g/mol	-

Gaseous SiO_2 (silica fume) and CO_2 leaving the combustion zone, was calculated by stoichiometry from gaseous SiO and CO entering the combustion zone, according to Equation 2.4 and Equation 2.8. Water vapour released from the combustion of raw materials was calculated as well. This was done by multiplying the amount of each raw material with their respective moisture content from Table 3.2. In addition, the hydrogen content from the wet based ultimate analysis (shown in Table A.2) was multiplied with the amount of the respective carbon material and added to the total water vapour output.

The amount of water vapour, SiO_2, and CO_2 created during combustion, was added to the calculated inlet mass of air. The amount of oxygen needed for complete combustion of SiO and CO was subtracted, which was found from stoichiometric calculations. As stated in the beginning of the method section, Ar and N_2 entering the furnace through air was not considered.

The new heat capacity of the off gas was calculated according to Equation 2.14, where the new off gas composition was found by dividing each compound's new mass by the total mass, giving the mass fraction. These values differed between different yields and different charge mixes.

For silica recovery, fume filter efficiency was set to 99.96% [94]. According to Table 3.5, this means that not only elements going to the off gas were emitted, but also 0.04% of the microsilica with its trace elements attached where assumed emitted.

3.2.3 Liquid Si refining

For refining of the tapped Si, the final content of Al and Ca was set to be 0.2% and 0.05%, respectively [95], and is indicated in Figure 3.1 by a blue dot. The Al and Ca content of the metal tapped from the furnace, was calculated using Table 3.5. This was done by adding all inputs of each trace element from each raw material, and use the table to calculate the amount of each trace element entering the refining ladle. The initial compositions are marked in Figure 3.1, where the green dots mark the bio based mix, while the purple dots indicate the conventional charge mix. The minimum amount of Al_2O_3 and CaO needed to be extracted with the slag to reach the desired Al and Ca content, was calculated according to:

$$m_{Al_2O_3} = (Al\%_{in} - 0.2\%) \cdot m_{tap} \cdot \frac{M_{Al_2O_3}}{2M_{Al}}, \tag{3.1}$$

and

$$m_{CaO} = (Ca\%_{in} - 0.05\%) \cdot m_{tap} \cdot \frac{M_{CaO}}{M_{Ca}}. \tag{3.2}$$

From the minimum amount of oxides extracted calculated in Equation 3.1 and Equation 3.2, the total slag mass was found by dividing the surplus compound by its percentual slag mass. The percentual slag mass for each oxide extracted, is indicated by red lines in Figure 3.1, giving a slag composition of 62% SiO_2, 24% Al_2O_3, and 14% CaO. The slag composition is set higher than the desired purity (blue dot), because it reduces the time needed to reach the desired Al and Ca content [96].

When total amount of slag was found, the amount of the remaining slag components were found by multiplying the total slag mass by the respective mass fractions indicated by the red lines in Figure 3.1. If the deficit compound from Equation 3.1 and Equation 3.2 was CaO, quicklime was added, but if the deficit compound was Al_2O_3, nothing was added during refining. In addition, as about 30% of the final slag mass consist of metallic silicon, the calculated total slag mass was divided by 0.7 to get final slag mass [97].

Since half of the amount of SiO_2 in slag, is a result of oxidation of liquid Si, and the other half is caused by addition of fine quartz sand, the amount of the latter was found by dividing the final slag mass of SiO_2 into two. The amount of oxygen needed was found by multiplying half the final slag mass by the molar ratio of O_2/SiO_2. The amount of refined liquid Si tapped from

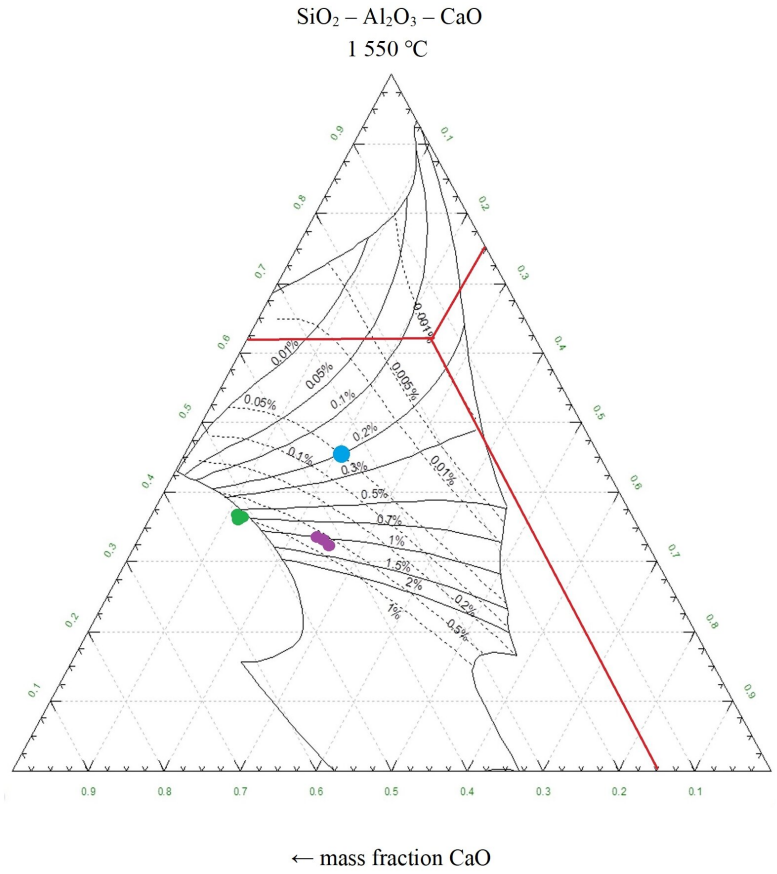

Figure 3.1: Phase diagram of the SiO_2-Al_2O_3-CaO slag system at 1550 °C and 1 atm. Dotted lines indicate Ca%, and solid lines indicate Al%. Red lines indicates slag composition by mass fraction, blue dot shows maximum content of Al and Ca for the final silicon product, purple dots are the initial composition of the non-bio based mixtures, and the green dots are the initial composition of the bio based mixes. Adapted from *Principles of Metal Refining and Recycling*, by Engh, Sigworth and Kvithyld, 2021, Oxford University Press [95].

the ladle was calculated by considering that half of the SiO_2 in the slag came from oxidation of the metal, and through stoichiometry changing this into m_{Si}, subtracting this from the input value of liquid Si.

How trace elements entering the refining ladle from the furnace were distributed, was estimated using Table 3.7, after Næss et al. [98]. Some elements entering the ladle from the furnace according to Table 3.5, are not dealt with in Table 3.7. These elements, like Bi and Cd, were assumed to remain in the metal or slag, and not leave with the fume as emissions to air [4].

Table 3.7: Element distribution within the refining ladle [98].

Element	To slag	To ladle fume	To refined metal
Al	21 %	1 %	78 %
As	13 %	4 %	83 %
B	15 %	0 %	85 %
Ba	98 %	0 %	2 %
Be	97 %	0 %	3 %
Bi	-	-	-
Ca	94 %	2 %	4 %
Cd	-	-	-
Co	8 %	1 %	91 %
Cr	26 %	0 %	74 %
Cu	8 %	10 %	82 %
Fe	8 %	1 %	91 %
Mg	35 %	37 %	28 %
Mn	12 %	1 %	87 %
Mo	13 %	0 %	87 %
Na	-	-	-
Ni	9 %	0 %	91 %
P	9 %	3 %	88 %
Sb	-	-	-
Sc	23 %	0 %	77 %
Se	-	-	-
Si	-	-	-
Sn	13 %	6 %	81 %
Sr	97 %	1 %	2 %
Ti	9 %	0 %	91 %
Tl	-	-	-
V	9 %	0 %	91 %
W	21 %	1 %	78 %
Zn	7 %	21 %	72 %
Zr	8 %	0 %	92 %

3.3 Energy Balance

As already written in subsection 2.1.2, the temperature of the off gas is assumed to remain above 100 °C until it leaves the stack. Therefore, energy content of the raw materials were calculated according to Equation 2.11, meaning that water from combustion remained as vapour until leaving the stack.

3.3.1 Submerged Electric Arc Furnace

Electric energy input was calculated by multiplying the furnace power by 24 h/d, and convert units from MWh/d to MJ/d by multiplying with 3600, giving $E_{\text{el,in}} = 3\,888\,000.00$MJ/d. Chemical energy input was found by calculating the energy contribution from each raw material, which was found by using Equation 2.10 on Table 3.3, and converting from dry based to wet based LHV using Equation 2.11. These values can be seen in Table 3.8.

Table 3.8: Wet based net calorific value of the carbon sources in the furnace.

	Coke	**Coal**	**Charcoal**	**Wood chips**	**Electrode**
[MJ/kg]	30.58	29.27	31.65	11.90	36.28

Energy loss from the 45 MW furnace was set to be 8% and 13% to heat and cooling water, respectively [46]. Energy leaving the furnace through tapped silicon, was found to be $\text{E}_{\text{chemical}} = 32.2$ MJ/kg [57], and $\text{E}_{\text{thermal}} = 3.26$ MJ/kg at 1600 °C [61]. Thermal energy leaving with the off gas, available for energy recovery, was the input energy minus losses and energy leaving with the tap.

3.3.2 Energy Recovery Unit

The off gas entering the energy recovery unit, was assumed to have an temperature of 750 °C [92]. This gave $\Delta T = 600$ K, because as already mentioned in subsection 2.1.2, an final off gas temperature of 150 °C is common. As also mentioned in subsection 2.1.2, about 30% of recovered heat is converted into electrical energy, the rest is lost, which was assumed in this thesis.

3.4 Life Cycle Assessment

For life cycle assessment, *SimaPro* [99] software was used with the ecoinvent 3 database - allocation at point of substitution - unit [54], and the ReCiPe2016 method with an hierarchist approach [62].

To include important emissions from the silicon metal industry not covered by the mass balance, emissions factors were calculated based on yearly emissions reported at www.norskeutslipp.no for the three Norwegian producers of metallurgical silicon: Elkem Salten, Elkem Thamshavn and Wacker Chemicals [100–102]. Yearly emissions from 2016 to 2021 was gathered, and an average over the time period from the three producers were calculated, and then divided by 365 to go from yearly to average daily emission. The compounds with their respective emission factors are listed in Table 3.9.

Chlorine, Cl, isn't a part of the ReCiPe2016 method [44], so it was excluded from the LCA, even though it was included in the mass balance. Since dioxins and PAHs are some of the forms chlorine can take after combustion [103], these numbers from Table 3.9 replaced Cl in the analysis.

The mass balance assumed complete combustion due to excess air, hence only CO_2 emissions were calculated to leave the stack. However, in real life, incomplete combustion occurs despite of excess air [104], creating pollutants such as CO, CH_4, N_2O and NO_X [105]. Because the sum of CO, CH_4, PAHs and dioxins made up less than 0.1% than the combined CO_2 emissions from the mass balance, these values were inputted without any further mass balance because they made up such a small part of the total CO_2 emissions.

Numbers from the mass and energy balance, and the emission factors, were divided by the amount of refined silicon to give all values a unit per metric ton silicon. Final yield was found by multiplying the yield of silicon tapped from the furnace with the yield of silicon tapped from the refining ladle, where the former is the chosen yields of $85\% - 90\% - 95\%$, and the latter is found by dividing the amount of liquid silicon leaving the refining ladle by the amount of liquid silicon entering the refining ladle.

Table 3.9: Daily average emission factors for compounds not included in the mass balance. Pink rows show emissions to air, blue rows shows emissions to water. The emission factors are calculated from three data sets over a time period of five years [100–102].

Compound	**Amount**	**Unit**
NO_X	3.95	[t/d]
N_2O	7.05	[kg/d]
CH_4	20.67	[kg/d]
CO	480.64	[kg/d]
Dioxins	3.49	[µg/d]
PAH_{air}	272.60	[g/d]
PAH_{water}	6.40	[g/d]
Suspended particles	77.53	[kg/d]

Chapter 4

Results & Discussion

The structure of this chapter is as follows: first, the inventory based on mass and energy balance is presented. Following the inventory, is the impact assessment on endpoint and midpoint level. Then, a sensitivity analysis is presented, and finally an uncertainty estimation.

4.1 Inventory Analysis

Table 4.1: Final yield after refining of the six scenarios.

	BIO			**MIX**		
	85	**90**	**95**	**85**	**90**	**95**
Final yield [%]	75.4	80.1	84.9	78.2	83.2	88.1

Table 4.1 shows the final yield after refining for the six different scenarios. It shows an overall higher final yield for the charge mixture MIX, which contains both fossil and biogenic carbon. This is probably related to the trace element composition of the raw materials, as the refining calculations revealed a shortage of Al for the BIO mixtures and a shortage of Ca for the MIX mixtures. From Table 3.4, which shows substantial larger amounts of Ca in charcoal and wood chips than coke and coal, and the opposite for Al, this was thus expected. For the MIX scenarios, the calculations included adding CaO during refining to compensate for the shortage of CaO, but not for the BIO scenarios as there where no shortage of Ca in this case.

Table 4.2 and Table 4.3 show the inventory of the six scenarios. All values are given per tonne refined silicon metal. Input of *silica sand* is used for input of quartz to the furnace, as there were no option for input of quartz in the ecoinvent database. The input of *silica sand* accounts for both quartz entering the furnace, and fine quartz sand entering the refining ladle. Dioxins are given as *Hydrocarbons, chlorinated* in the LCI. This is because dioxins aren't a part of the ReCiPe2016 method, but chlorinated hydrocarbons are [44], which is just another name for dioxins [106].

Table 4.2: Life cycle inventory of bio based mixes.

		BIO85%	**BIO90%**	**BIO95%**
Product (F.U.)				
Silicon, metallurgical grade	ton	1.00	1.00	1.00
Avoided products				
Silica sand {GLO} | market for | APOS, U	kg	425.70	267.24	126.51
Electricity, medium voltage {NO} | market for | APOS, U	MJ	9 808.85	9 003.57	8 288.41
Inputs from nature				
Water, river, NO	m3	47.01	44.90	43.02
Air	ton	48.08	43.83	40.05
Inputs from technosphere				
Silica sand {GLO} | market for | APOS, U	kg	2 848.22+35.31	2 679.40+34.07	2 529.47+32.96
Coke {GLO} | market for | APOS, U	MJ	0.00	0.00	0.00
Hard coal {Europe, without Russia and Turkey} | market for hard coal | APOS, U	kg	0.00	0.00	0.00
Charcoal {GLO} | market for | APOS, U	kg	1 030.25	995.38	964.41
Wood chips, wet, measured as dry mass {Europe without Switzerland} | market for | APOS, U	kg	1 173.72	1 133.99	1 098.71
Graphite {GLO} | market for | APOS, U	kg	112.74	112.29	111.89
Quicklime, in pieces, loose {RoW} | market for quicklime, in pieces, loose | APOS, U	kg	0.00	0.00	0.00
Electricity, medium voltage {NO} | market for | APOS, U	MJ	47 166.58	44 370.86	41 888.02
Emissions to air				
Silicon dioxide (silica)	g	170.35	106.94	50.63
Carbon dioxide, fossil	kg	399.09	397.50	396.09
Carbon dioxide, biogenic	kg	4 550.42	4 396.40	4 259.61
Water	kg	1 625.78	1 554.53	1 491.25
Aluminium	g	70.93	67.03	63.56
Arsenic	mg	16.29	15.69	15.16
Boron	mg	17.17	16.26	15.45
Barium	mg	4.84	4.64	4.47
Beryllium	µg	54.19	51.44	48.99
Bismuth	µg	105.74	100.59	96.03

Table 4.2 continued from previous page

		BIO85%	BIO90%	BIO95%
Calcium	g	240.48	232.37	225.17
Cadmium	mg	89.52	86.53	83.88
Cobalt	g	2.06	1.94	1.83
Chromium	µg	834.35	790.33	751.24
Copper	g	1.42	1.36	1.31
Iron	g	34.33	32.60	31.06
Mercury	µg	17.21	16.61	16.07
Potassium	g	2.35	2.25	2.17
Magnesium	g	17.46	16.85	16.30
Manganese	g	335.01	324.24	314.67
Molybdenum	mg	177.11	166.81	157.66
Sodium	mg	251.26	240.85	231.61
Nickel	µg	525.88	504.53	485.58
Phosphorus	g	10.48	10.11	9.79
Lead	mg	374.64	360.69	348.30
Antimony	mg	64.02	61.69	59.62
Scandium	µg	235.22	221.46	209.25
Selenium	µg	261.66	246.93	50.10
Tin	mg	78.65	75.37	72.47
Strontium	mg	677.76	648.93	623.32
Thallium	µg	260.56	245.67	232.44
Vanadium	µg	54.27	52.06	50.10
Tungsten	g	2.16	2.03	1.92
Zinc	g	13.99	13.51	13.08
Zirconium	µg	282.11	265.59	250.92
Sulfur oxides	kg	7.19	6.83	6.51
Nitrogen oxides	kg	47.88	45.04	42.52
Dinitrogen monoxide	g	85.47	80.40	75.90
Methane	g	250.74	235.88	222.68
Carbon monoxide	kg	5.83	5.49	5.18
PAH, polycyclic aromatic hydrocarbons	g	3.31	3.11	2.94
Hydrocarbons, chlorinated	ng	42.35	39.84	37.61
Emissions to water				
PAH, polycyclic aromatic hydrocarbons	mg	77.63	73.03	68.94
Suspended solids, unspecified	g	940.54	884.79	835.28
Cooling water	m3	47.01	44.90	43.02
Waste to treatment				
Slag from metallurgical grade silicon production {GLO} | market for | APOS, U	kg	162.71	156.99	151.91

Comparison of Table 4.2 and Table 4.3 reveals that the total amount of CO_2 emissions are lower for the bio based mix. However, the material and electricity demand for the conventional mix is lower, and the amount of energy recovered is higher. This is related to the low heating value of wood chips, which is about one third compared to the other carbon materials (Table 3.8), since the bio based mix have a higher wood chips share than the conventional mix.

Table 4.3: Life cycle inventory of conventional mixes.

		MIX85%	MIX90%	MIX95%
Product (F.U.)				
Silicon, metallurgical grade	ton	1.00	1.00	1.00
Avoided products				
Silica sand {GLO} | market for | APOS, U	kg	412.61	261.60	127.45
Electricity, medium voltage {NO} | market for | APOS, U	MJ	10 240.07	9 444.81	8 738.31
Inputs from nature				
Water, river, NO	m^3	47.28	45.20	43.35
Air	ton	50.46	46.26	42.53
Inputs from technosphere				
Silica sand {GLO} | market for | APOS, U	kg	2 710.57+24.57	2 550.37+23.24	2 408.06+22.05
Coke {GLO} | market for | APOS, U	MJ	5 721.36	5 528.72	5 357.58
Hard coal {Europe, without Russia and Turkey} | market for hard coal | APOS, U	kg	766.05	740.25	717.34
Charcoal {GLO} | market for | APOS, U	kg	367.67	355.29	344.29
Wood chips, wet, measured as dry mass {Europe without Switzerland} | market for | APOS, U	kg	837.74	809.54	784.48
Graphite {GLO} | market for | APOS, U	kg	108.69	108.24	107.83
Quicklime, in pieces, loose {RoW} | market for quicklime, in pieces, loose | APOS, U	kg	2.42	2.04	1.71
Electricity, medium voltage {NO} | market for | APOS, U	MJ	44 886.99	42 234.18	39 877.43
Emissions to air				
Silicon dioxide (silica)	g	165.11	104.68	51.00
Carbon dioxide, fossil	kg	2 893.00	2 806.94	2 730.49
Carbon dioxide, biogenic	kg	2 179.80	2 106.41	2 041.20
Water	kg	1 614.79	1 544.98	1 482.96
Aluminium	g	122.88	117.31	112.37
Arsenic	mg	12.11	11.66	11.25
Boron	mg	19.37	18.40	17.54
Barium	mg	5.26	5.05	4.87
Beryllium	µg	82.16	78.51	75.28
Bismuth	µg	100.88	95.99	91.65
Calcium	g	180.08	169.90	160.85
Cadmium	mg	40.27	38.96	37.79
Cobalt	g	1.98	1.87	1.76
Chromium	µg	816.17	773.67	735.92
Copper	g	1.60	1.54	1.49
Iron	g	64.05	61.35	58.95
Mercury	µg	19.19	18.53	17.93
Potassium	g	1.73	1.65	1.59
Magnesium	g	15.59	15.05	14.56
Manganese	g	265.62	257.22	249.75
Molybdenum	mg	176.40	166.36	157.45
Sodium	mg	349.30	335.73	323.68

Table 4.3 continued from previous page

		MIX85%	MIX90%	MIX95%
Nickel	µg	419.54	402.04	386.49
Phosphorus	g	4.68	4.51	4.37
Lead	mg	374.01	360.21	347.95
Antimony	mg	28.15	27.05	26.06
Scandium	µg	282.10	267.09	253.75
Selenium	mg	1.71	1.64	1.59
Tin	mg	68.16	65.28	62.72
Strontium	mg	619.37	592.91	569.40
Thallium	µg	248.09	233.96	221.40
Vanadium	µg	104.20	100.34	96.91
Tungsten	g	2.06	1.94	1.83
Zinc	g	8.71	8.41	8.14
Zirconium	µg	278.75	262.73	248.50
Sulfur oxides	kg	18.32	17.59	16.95
Nitrogen oxides	kg	45.56	42.87	40.48
Dinitrogen monoxide	g	81.34	76.53	72.26
Methane	g	238.62	224.52	211.99
Carbon monoxide	kg	5.55	5.22	4.93
PAH, polycyclic aromatic hydrocarbons	g	3.15	2.96	2.80
Hydrocarbons, chlorinated	ng	40.30	37.92	35.80
Emissions to water				
PAH, polycyclic aromatic hydrocarbons	mg	73.88	69.51	65.63
Suspended solids, unspecified	g	895.08	842.18	795.19
Cooling water	m^3	47.28	45.20	43.35
Waste to treatment				
Slag from metallurgical grade silicon production {GLO} | market for | APOS, U	kg	113.21	107.08	101.63

The inventory analysis of the bio based mix, reveals a slag amount in the range of $151.91 - 162.71$kg/t Si for the different yields. For the conventional mix, the slag amount ranged from $101.63 - 113.21$kg/t Si for the different yields. The amount of slag has a direct impact on the results from the mass balance shown in Table 4.2 and Table 4.3. The more slag formed in the refining ladle, the less refined liquid silicon is tapped. The lesser the amount of tapped refined silicon is, the larger are all other values in Table 4.2 and Table 4.3, since these values are found by dividing daily values by daily production of refined silicon metal.

4.1.1 Chlorine

The mass balanced emissions to air of chlorine per tonne refined silicon, are seen in Table 4.4. These values are much higher than the values of PAH and dioxins together, which can be seen in Table 4.2 and Table 4.3. While the values of PAH and dioxins are given in the range [g] to [ng], the calculated chlorine values are in the magnitude of [hg] and [kg].

Table 4.4: Emission of chlorine to air per ton refined silicon, according to the mass balance.

	BIO			**MIX**		
Yield	85 %	90 %	95 %	85 %	90 %	95 %
Cl [kg/t]	0.255	0.247	0.239	1.064	1.028	0.996

This could be due to an overestimation of the chlorine content of the carbonaceous raw materials, as shown in Table 3.4. However, chlorine can form many different compounds during combustion [103], and according to Malmgren and Riley, the majority of chlorine in carbon materials ends up as HCl after combustion [89]. Since HCl is not reported to www.norskeutslipp.no by the silicon metal producers, this might explain the discrepancy. Further, increasing the off gas temperature to above 800 °C destroys most of PAHs and dioxins [107], but secondary formation of dioxins and PAHs might occur [108, 109]. This too could explain the mismatch between mass balanced values of chlorine, and reported values of dioxins and PAHs. Nonetheless, since $HCl_{(g)}$ is an acidic gas, it will contribute to terrestrial acidification when emitted to air [110]. Thus, the fate of chlorine in the silicon production process could be of interest for further investigation.

4.2 Impact Analysis on Endpoint Level

Figure 4.1 shows the comparison of the weighted endpoint impact results per MT refined silicon metal, given in unit [Pt], according to the hierarchist average where resource availability is weighted 20%, and the two other impact categories are weighted 40% each.

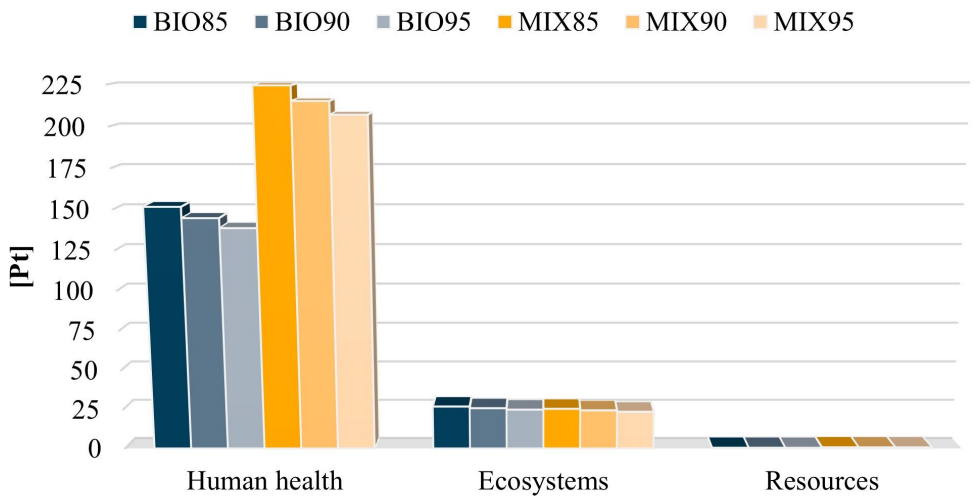

Figure 4.1: Comparison of endpoint impact results for the six scenarios, given in weighted points.

Even though human health and ecosystem is weighted equally, there are large differences between them. The bio based mixes scores almost six times higher on damage to human health than on damage to ecosystems, and the non-bio based mixes scores nearly nine times higher on damage to human health compared to damage to ecosystems. For both ecosystems and resources, there are small differences between the six scenarios. The largest difference between a bio based and non-bio based mix is seen in the human health category. For the same yield, the non-bio based mix scores about 1.5 times higher than the bio based mix.

To investigate the contribution to the damage categories, each category will be assessed with respect to contribution from midpoint impact categories. Thus, as seen in Figure 2.3, this thesis will start by assessing the endpoint impacts, then follow the damage pathways backwards to assess the midpoint impacts, where most emphasis will be put on the categories found to contribute the most to the endpoint impacts. Due to the linear relationship between different yields of the same charge mix, only the 90% yield of each mix will be considered in further endpoint impact analysis. Tables of endpoint impact values are found in Appendix E.

4.2.1 Human Health

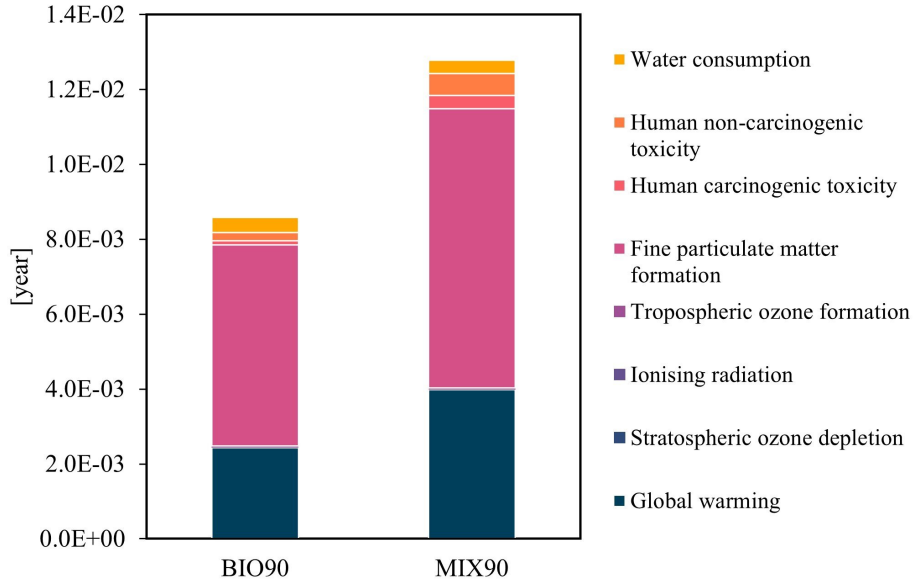

Figure 4.2: Contribution of midpoint impact categories to damage to human health, given in [year].

Figure 4.2 shows the calculated disability-adjusted loss of life years for BIO90 and MIX90. BIO90 have a total score of 8.59×10^{-3} year, while the total score of MIX90 is 1.28×10^{-2} year. As already mentioned in section 4.2, MIX90 scores 1.5 times higher than BIO90. This is mainly due to a larger potential for global warming and fine particulate matter formation, but MIX90 also scores higher on human toxicity potential, both carcinogenic and non-carcinogenic. The potential for water consumption, on the other hand, is slightly larger for BIO90. The contributions from stratospheric ozone depletion, ionising radiation and tropospheric ozone formation, are in the range 1×10^{-5} to 1×10^{-7} and too small to show in the graph, and thus negligible compared to the other midpoint impact categories.

4.2.2 Ecosystems

Figure 4.3 shows the time-integrated species loss for BIO90 and MIX90. BIO90 have a total score of 4.63×10^{-5} species $\cdot$ year, while MIX90 has a total score of 4.38×10^{-5} species $\cdot$ year. The main reason for BIO90 having the highest total score, is the land use potential, which is about 1.6 times larger for BIO90 than

for MIX90. Even though terrestrial acidification and global warming potential, both noticeable contributions for both mixes, are smaller for BIO90 compared to MIX90, they don't make up for the large contribution from the land use potential. Compared to each-other, MIX90 have a noticeable contribution from freshwater eutrophication, while BIO90 have a higher contribution from water consumption. There is also a significant contribution of tropospheric ozone formation potential on both mixes, while the contribution of marine eutrophication, and the ecotoxicity categories, are minimal relative to the other categories, as they are in the range 1×10^{-8} to 1×10^{-11} and thus not visible in the graph.

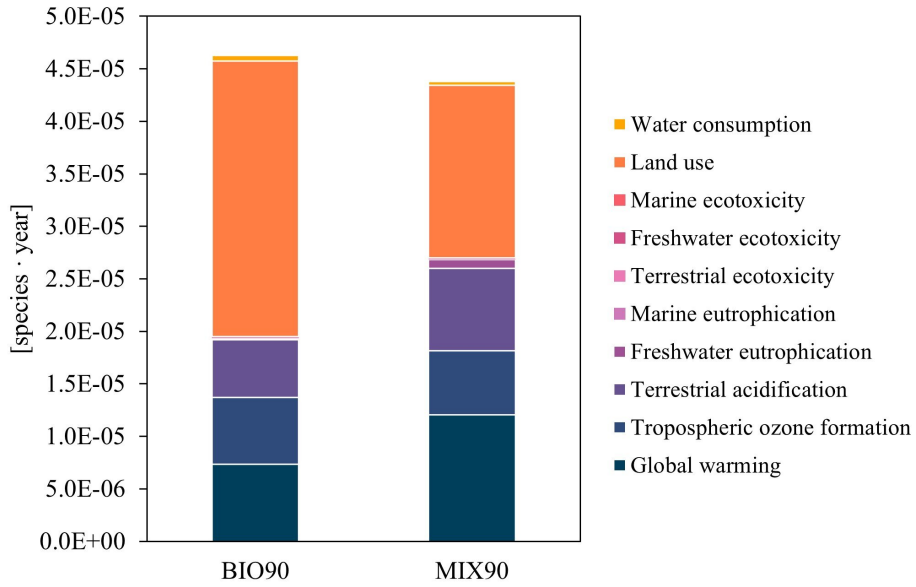

Figure 4.3: Contribution of midpoint impact categories to damage to ecosystems, given in [species · year].

4.2.3 Resource Availability

Figure 4.4 illustrates the surplus cost due to damage to resource availability for BIO90 and MIX90. BIO90 have a total score of 54.29 $ and MIX90 a total score of 92.19 $. MIX90 have a slightly higher score on mineral resource scarcity, which is confirmed in Table 4.2 and Table 4.3, where it can be seen that the input of quartz is higher for the non-bio based mixes compared to the bio based mixes. MIX90 also scores much higher on fossil resource scarcity, thus resulting in the highest total score.

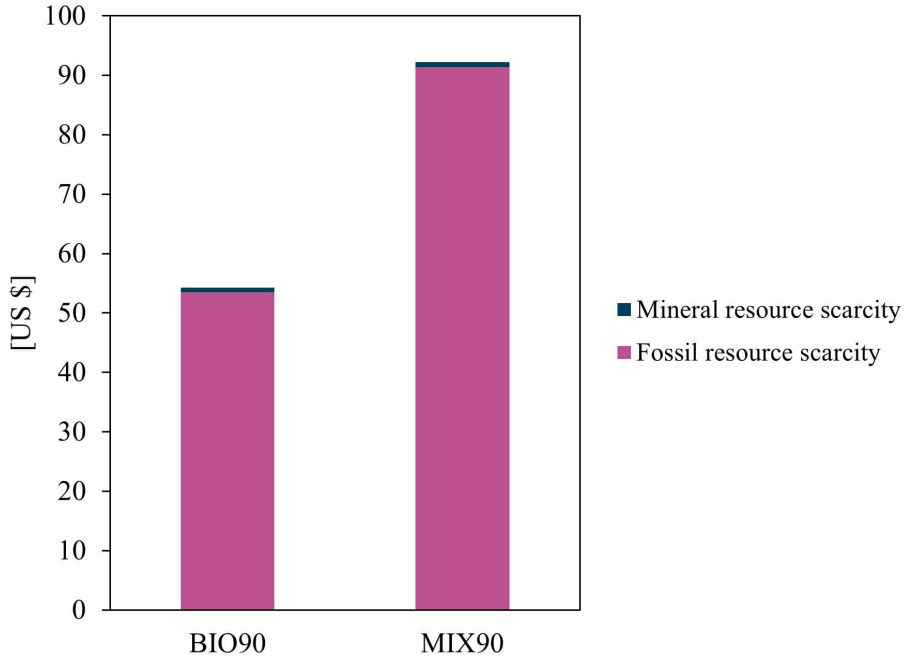

Figure 4.4: Contribution of midpoint impact categories to damage to resource availability, given in [US $].

4.3 Impact Analysis on Midpoint Level

Figure 4.5 shows the relative percentual midpoint impact results of the six scenarios per MT refined silicon metal. The differences in performance of bio based and conventional charge mixes are small to none for the impact categories ionising radiation, and mineral resource scarcity. The conventional charge mixes perform slightly better in impact categories tropospheric ozone formation, both on human health and terrestrial ecosystems, terrestrial ecotoxicity, and water consumption, and outperforms the bio based mixes in impact categories stratospheric ozone depletion, and land use. For the last 10 impact categories, the bio based charge mixes outperform the conventional charge mixes. As pointed out in section 4.2, there's a linear relationship between the different yields for the same charge mix, which is clearly visualised in Figure 4.5, showing how the impacts are lowered when the yield is increased. Due to this linearity, only 90% yield of each mix will be assessed on midpoint impacts as well.

To investigate what contributes to each midpoint impact category, each of them will be assessed. Emphasis will be put on the midpoint impact categories that

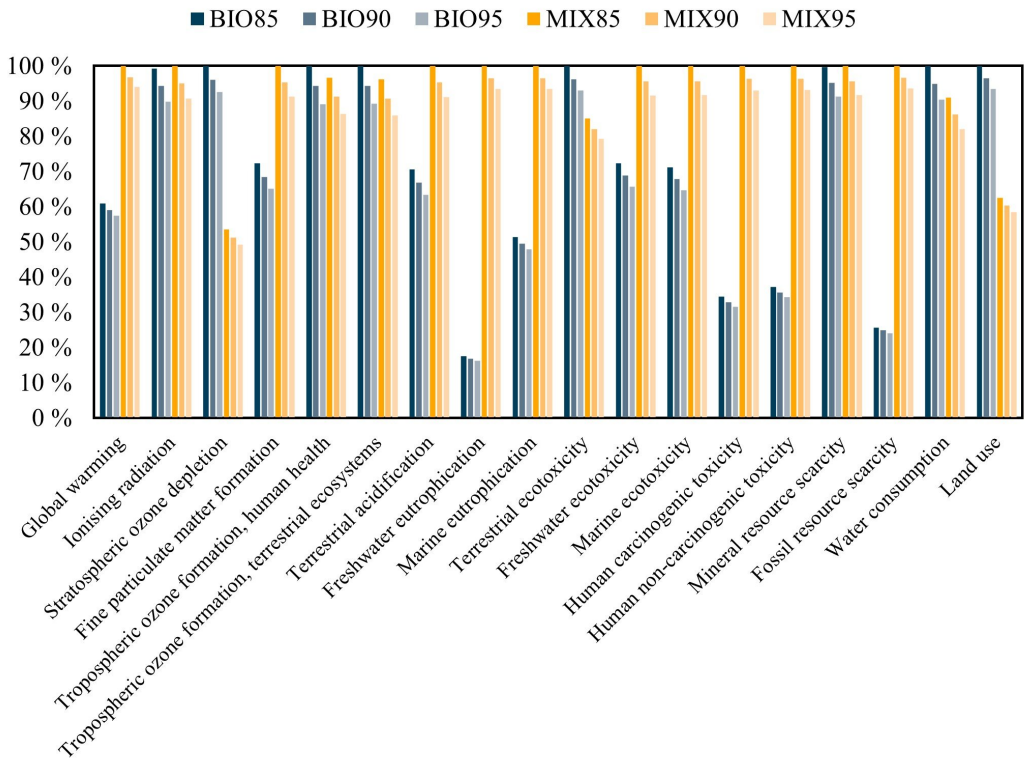

Figure 4.5: Comparison of overall midpoint impact results for the six scenarios, given in relative percentages.

contributed the most to the endpoint impacts: global warming, fine particulate matter formation, ozone formation, terrestrial acidification, human toxicity, and land use. Water consumption had an noticeable impact on damage to both human health and ecosystems, but since water scarcity in general is not a big issue in Norway, this will only briefly be assessed. Since the endpoint impact category *Resources* scored low compared to the two other endpoint impact categories, fossil scarcity and mineral scarcity will also only briefly be assessed.

When each midpoint impact category is presented, the total amount of emission equivalents is given, which is the sum of positive contributions minus the negative emissions related to recovery of energy and silica fume. Impacts from coke, coal and carbon electrodes are aggregated together to *fossil carbon*, while impacts from charcoal and wood chips are aggregated together to *biogenic carbon*.

4.3.1 Global Warming

As can be seen from Figure 4.6, BIO90 has an overall better performance than MIX90, where the latter scores about 1.6 times higher than the former. The main contributors to the overall score of BIO90, are biogenic carbon (69%), process emissions (16%) and electricity (9.7%), while the main contributors to MIX90 are process emissions (65%), biogenic carbon (15.7%), and fossil carbon (10.5%).

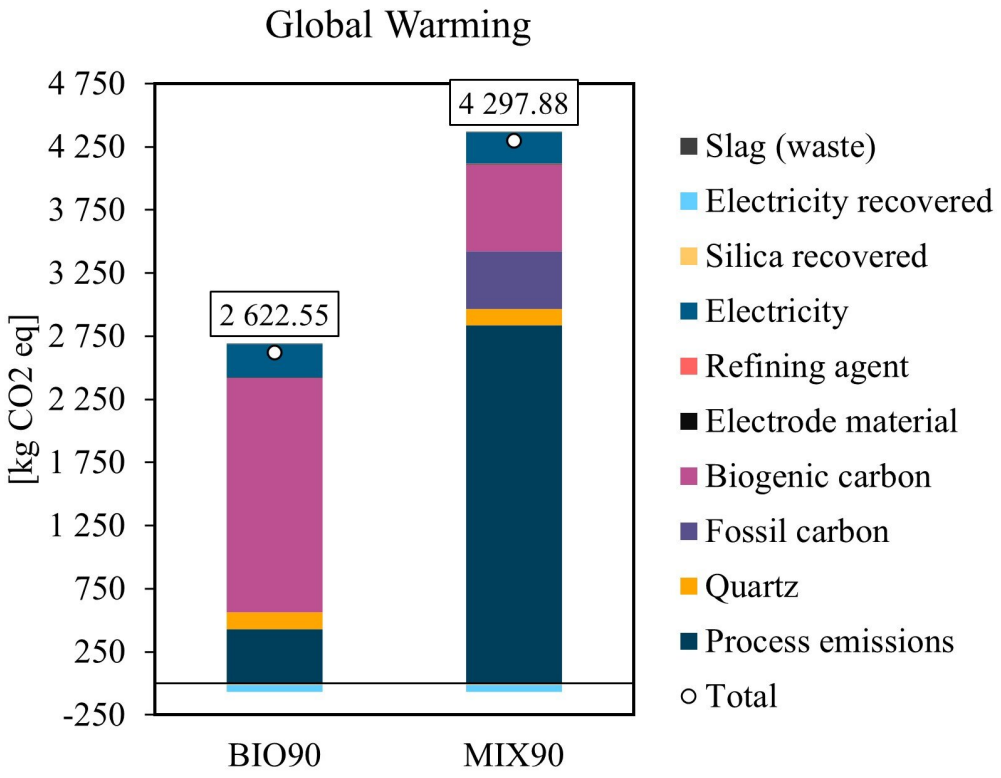

Figure 4.6: Comparison of impact on climate change for BIO90 and MIX90.

The contribution of biogenic carbon to the overall global warming potential, is highly associated with the production of charcoal. The process emissions of BIO90 are due to CO_2 being emitted during consumption of the electrodes, as biogenic CO_2 emissions are not accounted for [2], while the high process emissions for MIX90 also include emission of CO_2 from consumption of coke and coal. As the amount of electrode material consumed is almost equal for both BIO90 and MIX90 (see Table 4.2 and Table 4.3), the large difference between the process emissions is due to the coke and coal consumption. Further, the main reasons for the fossil carbon contribution to the overall global

warming potential, are the emissions arising from mining of coal and coking of coke. Finally, voltage transformation is the main reason for the electricity contribution to the overall impact on climate change.

One way of tackling climate change, is by addressing the direct emissions from the production by switching to biogenic carbon. Figure 4.6 illustrates how this would lower the direct emissions. However, this also leads to an increase in indirect emissions from production of, i.e., charcoal. Even though manufacturing of the raw materials fed to the investigated production process is outside of the scope of this thesis, this illustrates how emissions associated with a product can be shifted from one process to another. As new and improved methods for charcoal production is developed [111], the overall global warming impact associated with silicon metal production decreases, and can possibly be considered CO_2 neutral by choosing charcoal from sustainable production [112].

4.3.2 Fine Particulate Matter Formation

The formation of fine particulate matter is estimated to be lower for BIO90 than MIX90, as shown in Figure 4.7. This is mainly due to a higher impact from process emissions for MIX90, than of BIO90. For BIO90, process emissions accounts for almost 80% of the overall impact, while this number is 82% for MIX90. The second largest contributor to fine particulate matter formation of BIO90, is biogenic carbon, while fossil and biogenic carbon are the second and third largest contributors of MIX90, respectively.

The driving force behind the high process emissions, is formation and emission of NO_x and SO_x during production, which forms secondary $PM_{2.5}$ particles in air [44]. $PM_{2.5}$ is a collective term for particles with a diameter smaller than 2.5 µm, and has gained increased concern later years [113]. This is because smaller particles have much more numerous ways of entering the human body than larger particles, which also increases the potential damage $PM_{2.5}$ aerosols pose. However, particles of diameter larger than 2.5 µm can also pose a health risk [44].

The input values of SO_x are mass balanced, while the values of NO_x are calculated emission factors, as seen in Table 4.2 and Table 4.3. Compared to

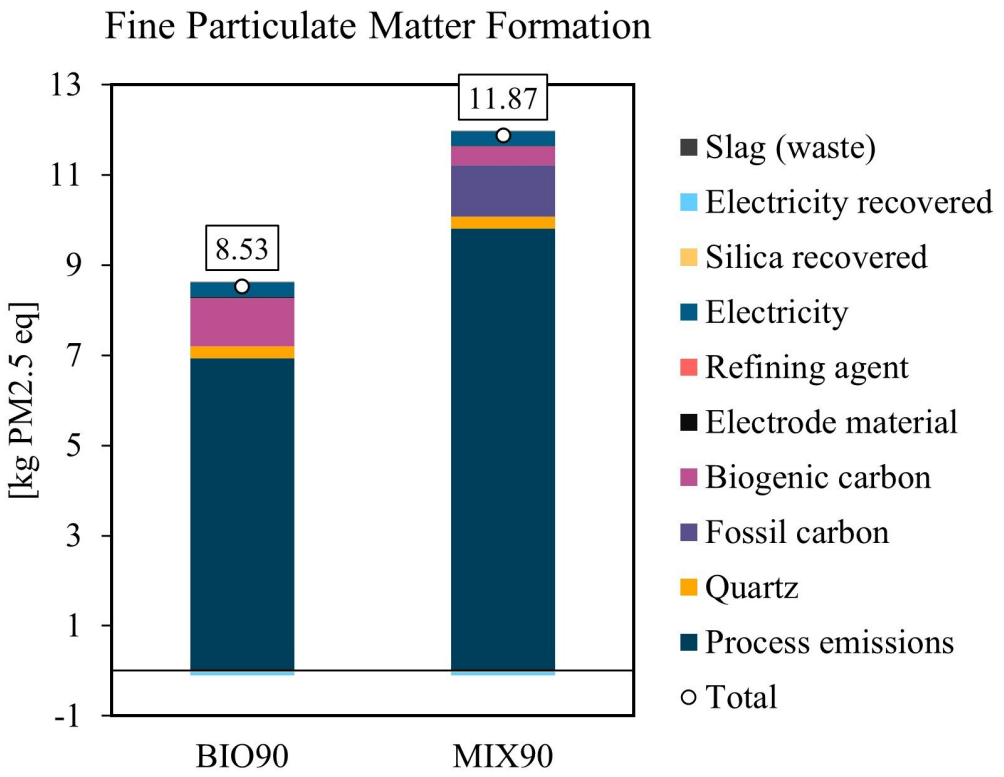

Figure 4.7: Comparison of impact on fine particulate matter formation for BIO90 and MIX90.

the emission factors reported by Kero, Grådahl and Tranell for NO_x and SO_x, which were in the range of $11 - 22\,kg/t$ and $11 - 13\,kg/t$, respectively [27], the values used for NO_x in this thesis is very high. Depending on charge mix and yield, the calculated NO_x values in this thesis range from $40.48\,kg/t$ to $47.88\,kg/t$, which is about twice as high as the numbers reported by Kero, Grådahl and Tranell. For BIO90, the SO_x values in this thesis range from $6.51\,kg/t$ to $7.19\,kg/t$, which is less than the reported numbers from Kero, Grådahl and Tranell. For MIX90 on the other hand, the values range from $16.95\,kg/t$ to $18.32\,kg/t$, which is quite much higher than given by Kero, Grådahl and Tranell. Compared to these reported numbers, the overall impact in Figure 4.7 might be overestimated.

4.3.3 Tropospheric Ozone Formation

The potential impact of tropospheric ozone formation on human health and terrestrial ecosystems, are seen seen visually in Figure 4.8. The overall score

is slightly higher for BIO90 than MIX90 for both impact categories, where the main contributor to is emissions from the production process. For BIO90, the process emissions account for over 90% of the overall impact for both impact categories. For MIX90, process emissions account for around 90% on both human health and terrestrial ecosystems. It can also be noted that the impact from biogenic carbon is slightly higher for impact on terrestrial ecosystems, than for impact on human health.

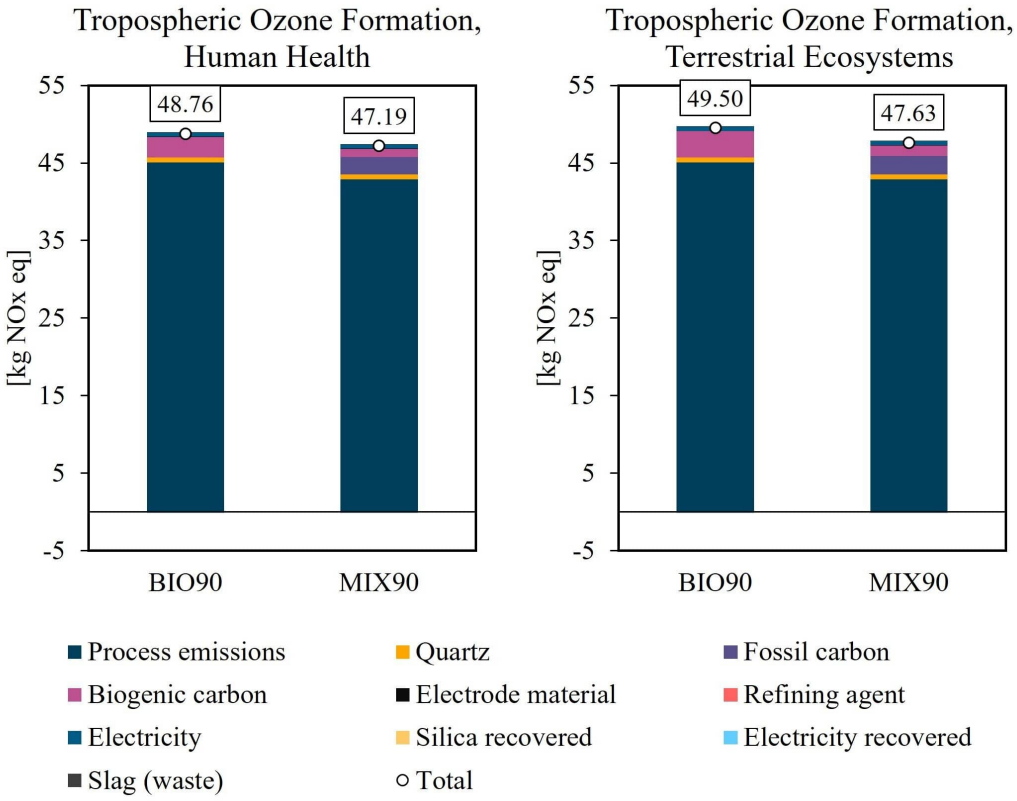

Figure 4.8: Comparison of impact on tropospheric ozone formation, on both human health and terrestrial ecosystems, for BIO90 and MIX90.

The main reason for the high score of process emissions to tropospheric ozone formation for both human health and terrestrial ecosystems, is the formation and release of NO_x. Through photo-chemical reactions, emission of NO_x, amongst others, leads to near-ground ozone formation [44], which is associated with negative health effects on humans [114] and on ecosystems [115].

The reason for BIO90 having a larger contribution from process emissions than MIX90, is related to the final yield from Table 4.1. Since the emission factor of NO_x was calculated by dividing an daily average by daily amount of

tapped, refined silicon metal, and the yield is lower for BIO90 than MIX90, the emissions of NO_x per tonne silicon metal is higher for BIO90 than MIX90. As already discussed in subsection 4.3.2, the NO_x emissions of this thesis are quite high relative to other sources [27], thus the impact from tropospheric ozone formation may be overestimated for both BIO90 and MIX90.

4.3.4 Terrestrial Acidification

From Figure 4.9 it can be seen that BIO90 performs better than MIX90. The main contributor to terrestrial acidification, is the process emissions, accounting for 88.5% of the total impact of BIO90, and 89% of the overall impact of MIX90. The reason for the high impact of the process emissions, are emissions of NO_x and SO_x. Since BIO90 and MIX90 emits almost the same amount of NO_x, but BIO90 emits less SO_x than MIX90 (seen in Table 4.2 and Table 4.3), BIO090 performs overall better on terrestrial acidification potential.

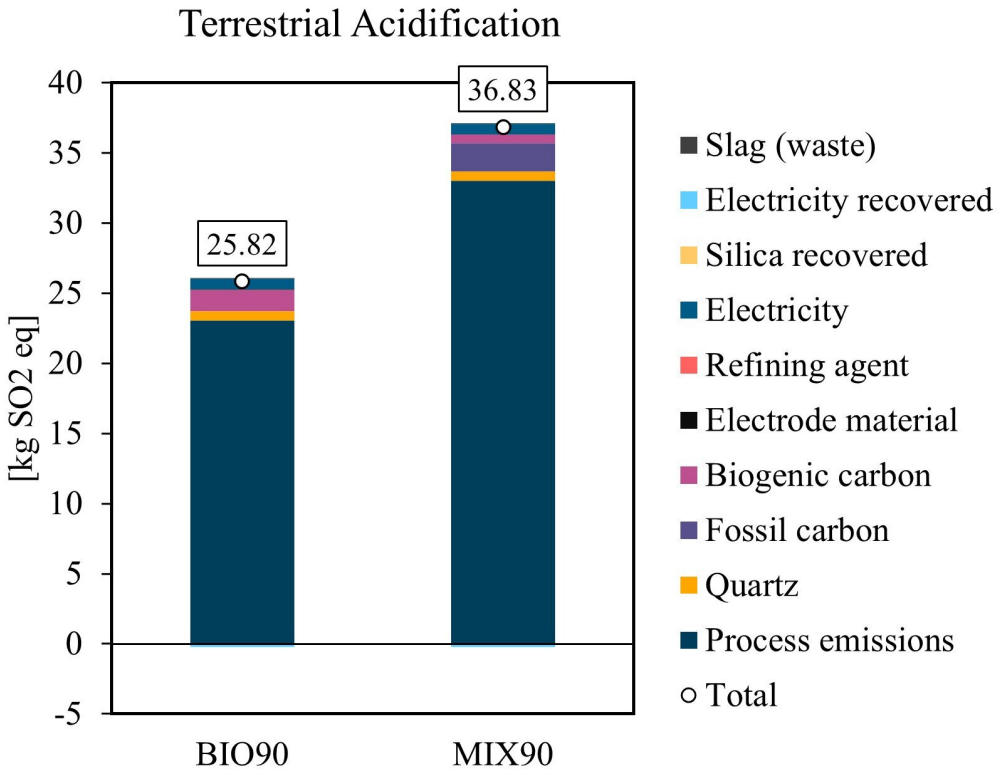

Figure 4.9: Comparison of impact on terrestrial acidification for BIO90 and MIX90.

NO_x and SO_x deposit onto soil after being emitted into the air, and then leach into soil, changing the pH towards a more acidic state, potentially causing vegetation to disappear [44]. As previously discussed in subsection 4.1.1, HCl also contributes to terrestrial acidification, but it is not a part of the method and thus not included here. It was also discussed in both subsection 4.3.2 and subsection 4.3.3, that the numbers for NO_x in this thesis are substantially larger than numbers reported by others [27], so the terrestrial acidification potential might in this case be overestimated.

4.3.5 Human Toxicity

The potential for carcinogenic and non-carcinogenic toxicity on human health from production of MG-Si, is depicted in Figure 4.10, where the impact from MIX90 is almost three times as high as the impact from BIO90 in both cases. For non-carcinogenic toxicity, the main contributors to BIO90's overall score are electricity (54.0%), biogenic carbon (24.5%), and process emissions (11.6%). The main contributors to MIX90's overall score on non-carcinogenic toxicity, are fossil carbon (68.8%) and electricity (20.5%).

For the carcinogenic toxicity on human health, the contribution from process emissions are so small they don't show in the graph. Thus, the overall impact on carcinogenic toxicity for BIO90 is dominated by electricity (66.7%) and biogenic carbon (24.2%). The main contributors to the overall carcinogenic toxicity impact of MIX90, are the same as for the non-carcinogenic toxicity: fossil carbon (69.1%) and electricity (23.9%).

The process emissions' contribution to non-carcinogenic human toxicity is due to emissions of heavy metals, PAHs and dioxins. For both carcinogenic and non-carcinogenic human toxicity potential, the large contribution from fossil carbon is owed to emissions and waste arising from coal mining, while the contribution from biogenic carbon is attributed to emissions caused by production of charcoal. The impact from electricity results from mainly from material demand for transmission, but also transformation, of voltage. This is highly related to the enormous metal need of the infrastructure, and also loss of power and SF_6 during transmission and transformation [116, 117], which is why energy recovery also lowers the overall impact considerably. For non-carcinogenic human toxicity, BIO90's and MIX90's overall impacts are reduced

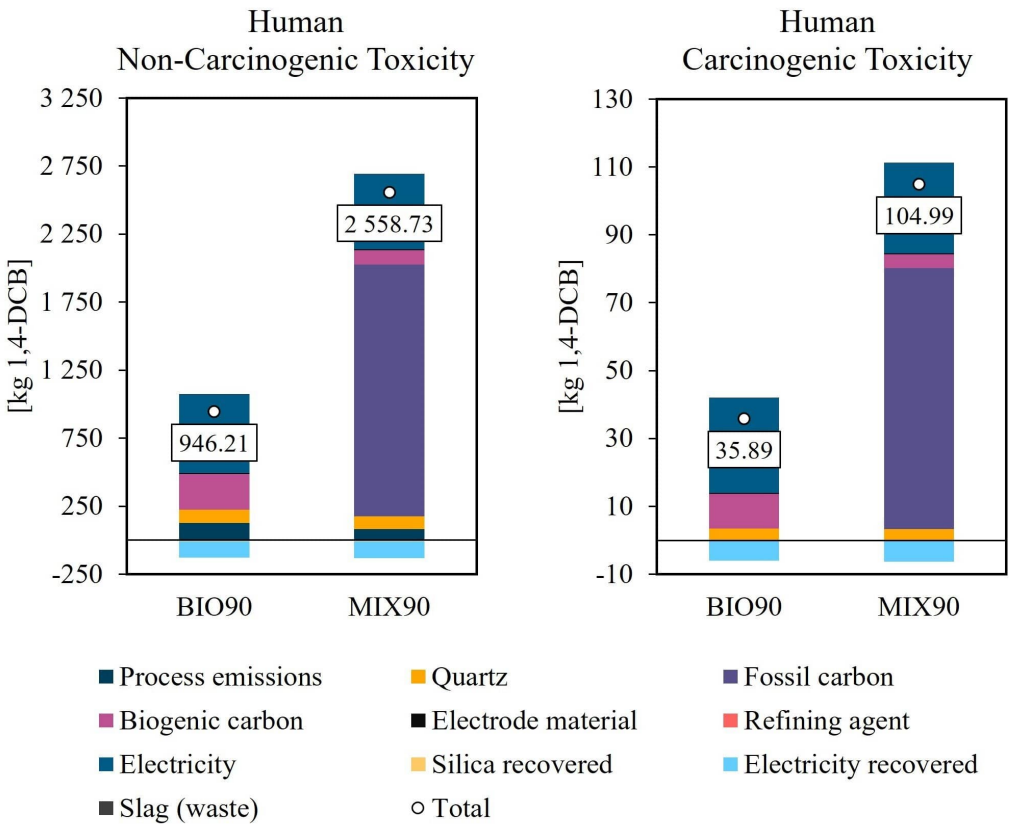

Figure 4.10: Comparison of impact on human toxicity for BIO90 and MIX90.

by −11% and −4.6%, respectively. The overall carcinogenic human toxicity potential is reduced by −13.5% and −5.3%, for BIO90 and MIX90 respectively. The energy recovered is slightly higher for the conventional mixes, than the bio based mixes, as seen in Table 4.2 and Table 4.3. Thus, the reason for the percentual energy recovery of BIO90 to be more than twice as large as that of MIX90 in this case, is due to the large contribution from fossil carbon.

4.3.6 Land Use

As seen in Figure 4.11, BIO90 outperforms MIX90 on land use by an overall impact score about 1.6 times higher. From the visualisation, it is clearly that biogenic carbon is the reason for the high impact, which accounts for 93.3% of the overall impact of BIO90, and 71.5% of the overall impact of MIX90. MIX90 also has a noticeable impact from fossil carbon (18.4%). The main contributor to the high impact from biogenic carbon, is forestry and timber cleaving for charcoal production, and forestry related to wood chips, while the

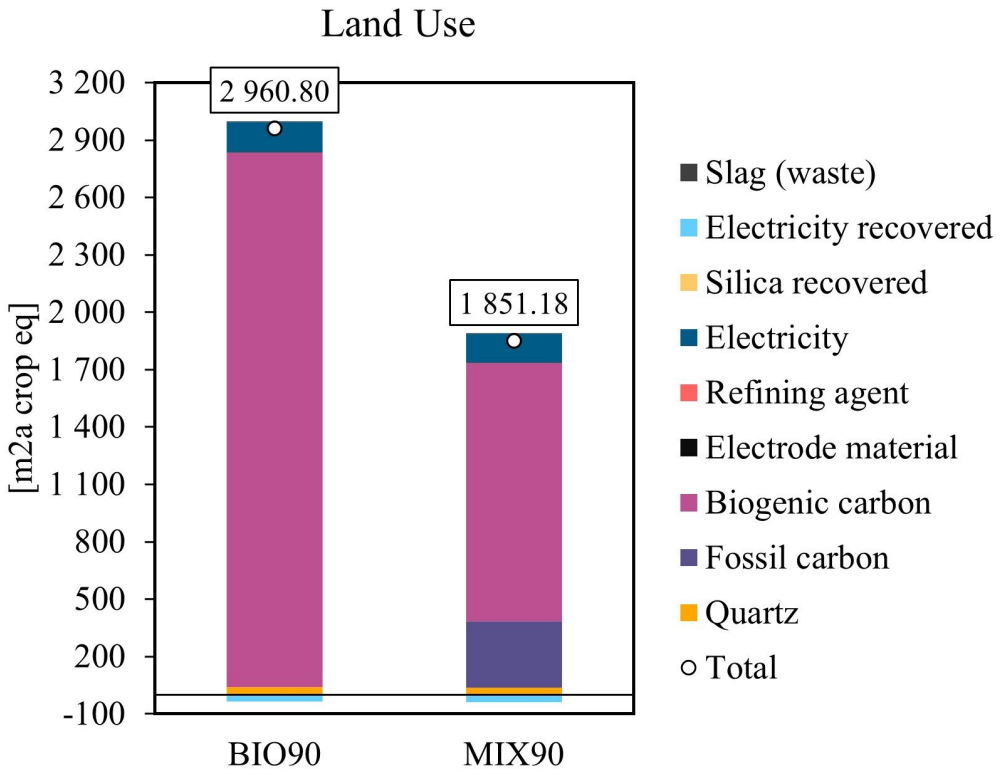

Figure 4.11: Comparison of impact on land use for BIO90 and MIX90.

contribution from fossil carbon owes it to mining of hard coal

The land use impact category is related to species loss due to land use, relative to a natural state [44]. As such, land use contribute to fragmentation and loss of habitat, thus reducing biodiversity of both animals and vegetation, but land use is also linked to hydrology, impacting surface water, groundwater, and evapotranspiration [118].

4.3.7 Ecotoxicity

From Figure 4.12, it can be seen that MIX90 performs better on terrestrial ecotoxicity than BIO90. BIO90 have a higher contribution from process emissions as well as from biogenic carbon. The process emissions of BIO90 make up about 40% and are due to emissions to air. The main contributors to MIX90 are process emissions (41.4%), electricity (27.6%), biogenic carbon (12.6%), and quartz (10.9%). In addition, MIX90 have a negative contribution from electricity recovery of about −6.2%.

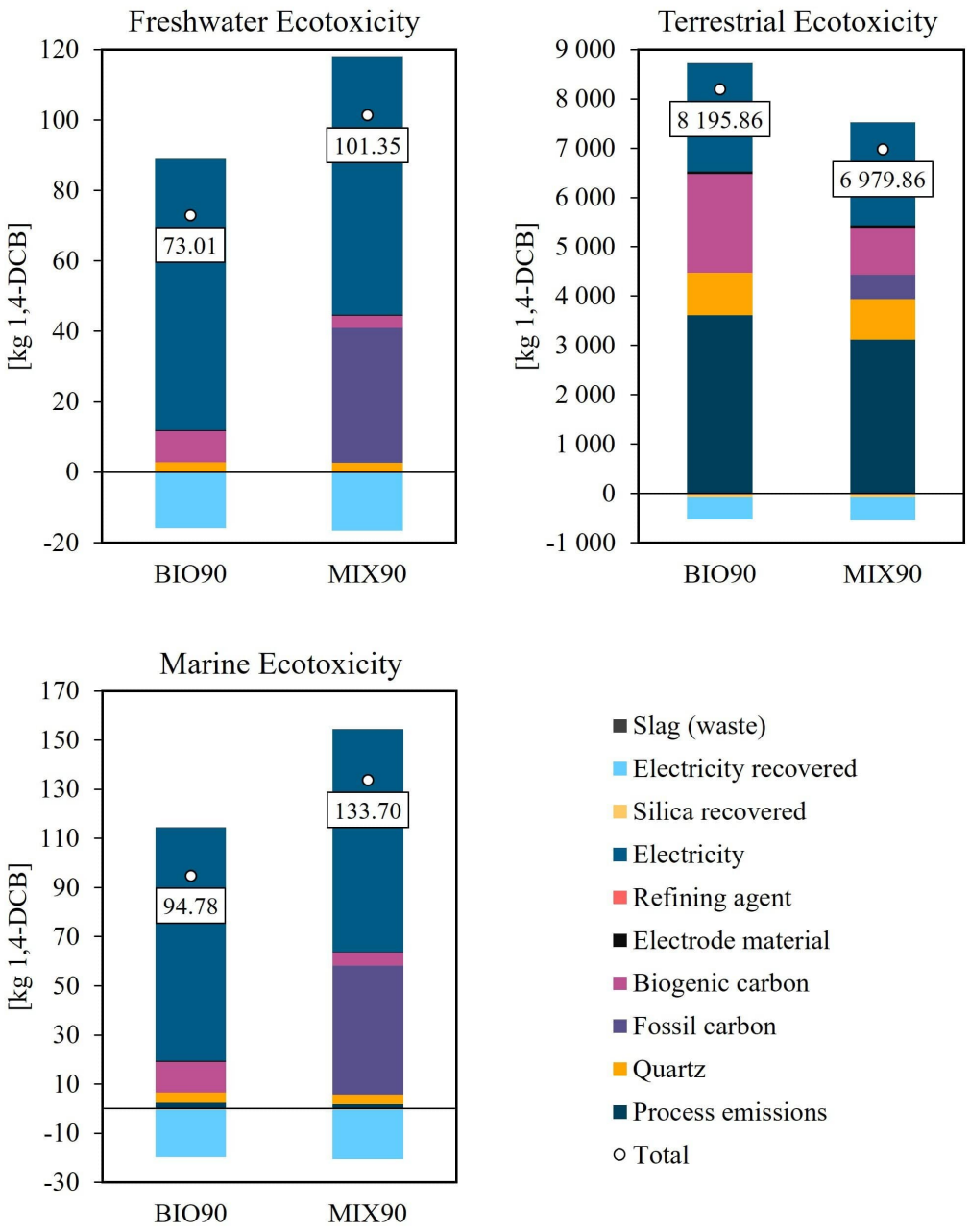

Figure 4.12: Comparison of impact on terrestrial, freshwater and marine ecotoxicity for BIO90 and MIX90.

For freshwater ecotoxicity potential, MIX90 scores higher than BIO90. The main contributors to MIX90 are electricity (62%) and fossil carbon (32.5%), but electricity recovery also has a noticeable contribution of −13.9%. BIO90 owes its overall score on freshwater ecotoxicity mainly to electricity (86.5%), but also to biogenic carbon (6.9%). The contribution from electricity recovery on BIO90 is of −17.6%.

The overall score on marine ecotoxicity is lower for BIO90 than MIX90. The main contributors to MIX90 are electricity (58.6%) and fossil carbon (34.0%), with a negative contribution from electricity recovery of −13.1%. The total score of BIO90 is mainly a result of the contribution from electricity (83.0%) and biogenic carbon (11.0%), where the recovery of electricity reduces the impact by −16.8%.

The process emissions related to terrestrial are high due to release of heavy metals, PAHs and dioxins during production. The impact of electricity to all ecotoxicity categories is associated with transformation and transmission of voltage, previously discussed in subsection 4.3.5. The contribution from biogenic carbon is connected to charcoal production and wood chips transportation, while mining of coal and quartz are the reasons for their noticeable contribution. In addition, coking of coke also have a small contribution to marine ecotoxicity.

4.3.8 Eutrophication

As seen in Figure 4.13, BIO90 outperforms MIX90 on freshwater eutrophication. MIX90 has an overall score almost six times as high as that of BIO90, owing it mostly to the contribution from fossil carbon (86.5%), but also through a noticeably contribution of electricity (8.4%). For BIO90, the main contributors to the overall score are electricity (46.1%) and biogenic carbon (43.1%). The impact from fossil carbon is mainly related to mining operations of hard coal, but also from coking of coke. The impact from electricity is due to transmission and transformation of voltage, while the impact from biogenic carbon owes it to charcoal production.

The overall score on marine eutrophication potential is also higher for MIX90 than BIO90, almost by a factor of two. As for freshwater eutrophication, the main reason for the high score of MIX90 on marine eutrophication is the contribution from fossil carbon (73.5%), but also biogenic carbon (15.2%) and electricity (9.4%) contribute noticeably. For BIO90, the main contributors are biogenic carbon (77.2%) and electricity (18.8%). The large contribution from fossil carbon is due to mining operations of hard coal, charcoal production is the main contributor to the impact from biogenic carbon, and electricity contribution owes its score from voltage transformation.

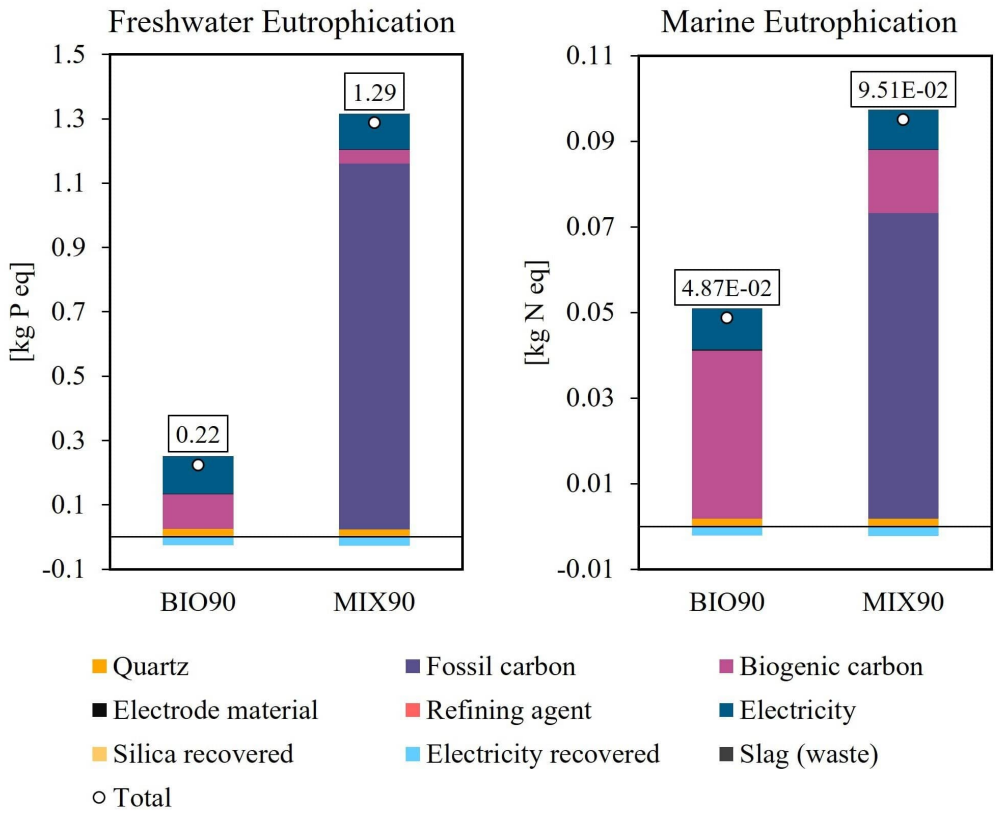

Figure 4.13: Comparison of impact on freshwater and marine eutrophication for BIO90 and MIX90. Be aware of different units.

For BIO90, electricity recovery reduces the impact of freshwater and marine eutrophication by -9.4% and -3.8% respectively, while for MIX90 the numbers are -1.9% and -2.1% respectively. As previously discussed in subsection 4.3.5, the higher percentual value for energy recovery of BIO90 than MIX90, is closely linked to the fact that the total positive impact is lower as well.

4.3.9 Abiotic Resources

Fossil Resource Scarcity

MIX90 has an overall fossil resource scarcity score almost four times higher than BIO90, as seen in Figure 4.14. The main contributor to the high impact of MIX90, is fossil carbon, which accounts for more than 81.6%. This is related to fossil fuel usage during mining operation and preparation of hard coal, in

addition to coking of coke. BIO90, on the other hand, owes its impact to biogenic carbon (52.8%), electricity (27.1%), and quartz (18.6%).

The reason for the high scores of biogenic carbon, quartz and electricty, is the usage of fossil fuel for production and transportation of charcoal and wood chips, for production of quartz, and voltage transformation of electricity. The negative contribution from electricity recovery is −5.5% for BIO90, and −1.6% for MIX90.

Mineral Resource Scarcity

Mineral resource scarcity is one of the impact categories where BIO90 and MIX90 scores almost equal. As seen in Figure 4.14, MIX90 scores slightly higher, due to the fossil carbon contribution (17.4%). However, electricity (65.6%) is the main contributor, with biogenic carbon (10.0%) the third largest contributor to the overall impact of MIX90. For BIO90, on the other hand, the main contributor is electricity (69.6%) and biogenic carbon (23.0%).

The impact of electricity is mainly related to construction, production, and transmission of electricity from hydro-power, while the contribution from fossil carbon is related to operations of hard coal mines. The contributions from biogenic carbon and quartz are related to material demand from production. The large impact of electricity also leads to a substantial impact from energy recovery, with −14.1% and −14.7% for BIO90 and MIX90, respectively.

Water Consumption

Regarding the water consumption potential, MIX90 has a slightly overall better performance than BIO90, as seen in Figure 4.14. The main difference in the scenarios lies within the biogenic carbon, which is higher for BIO90 than MIX90. Since BIO90 is based purely on biogenic carbon sources, while MIX90 is a mixture of fossil and biogenic carbon, this makes sense. However, the main contributor to the water consumption potential is the electricity, which makes up 84.4% of the positive impact on BIO90, and 86.1% of the impact from MIX90. Process emissions also have a substantial contribution to the overall water consumption potential, with 10.5% for BIO90 and 11.3% for MIX90.

Electricity owes its high contribution to the water consumption potential to electricity production, as the Norwegian electricity mix constitutes mainly of hydro-power. This is also why energy recovery affects the overall score as much as it does, by −17.1% for BIO90 and −19.3% for MIX90. The process emissions have a noticeable impact for both mixes due to the cooling water used within the furnace.

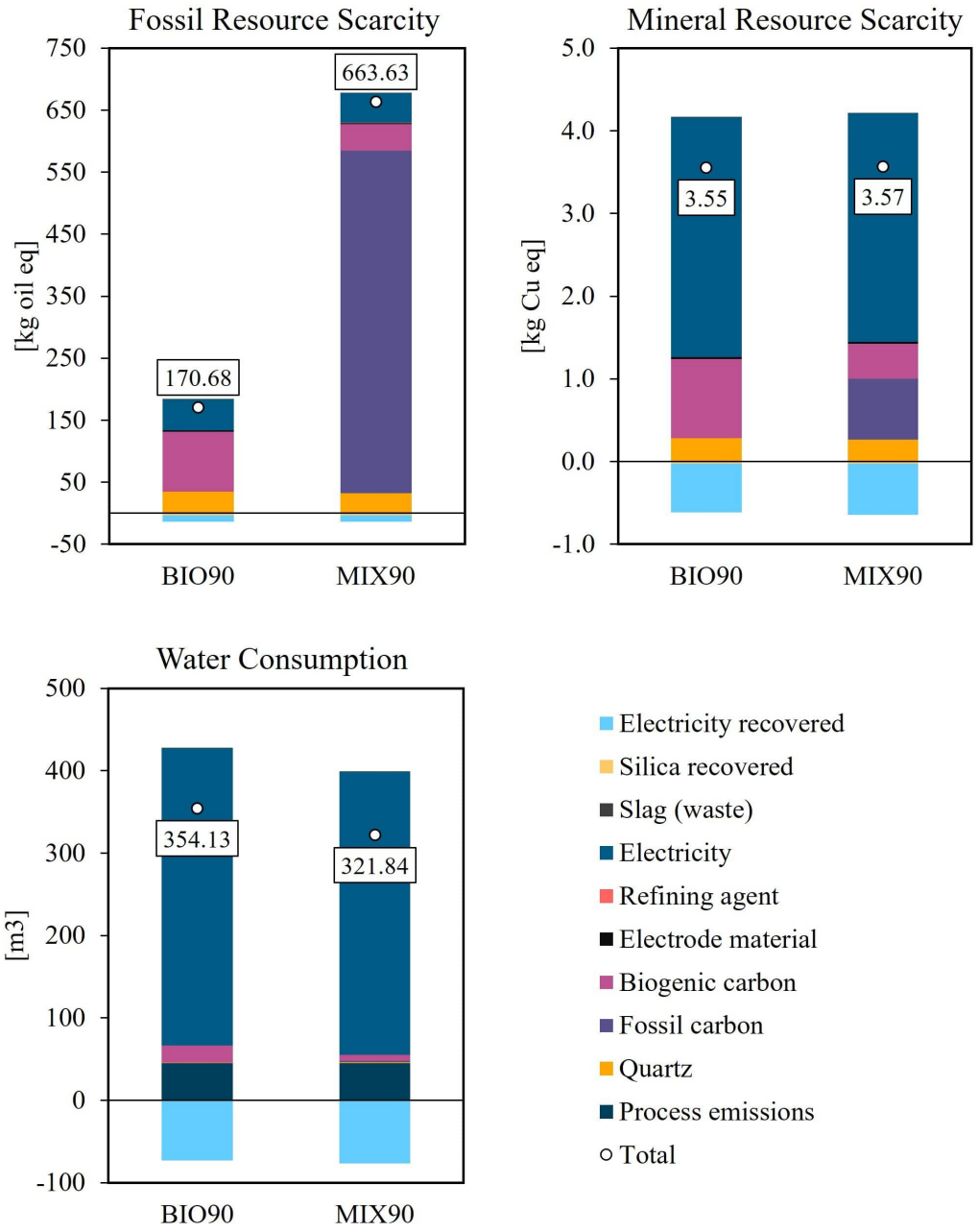

Figure 4.14: Comparison of fossil resource scarcity, mineral resource scarcity, and water consumption for BIO90 and MIX90. Be aware of different units.

4.3.10 Others

Stratospheric Ozone Depletion

As seen in Figure 4.15, MIX90 performs better than BIO90 on stratospheric ozone depletion, with almost half the amount of kg CFC-11 equivalents compared to BIO90. The reason for the high score of BIO90, is mainly the contribution from the biogenic carbon (74.0%), but process emissions and electricity also contributes with 12.7% each to the positive impact. Through electricity recovery, the impact is reduced by −2.6%. The main contributors to the total score of MIX90, are biogenic carbon (48.7%), process emissions (22.1%), and electricity (22.0%), and recovery of energy have a negative contribution of about −4.9%.

The large contribution from biogenic carbon results from forestry for charcoal production. The process emissions are due the release of N_2O and dioxins during production, while the electricity contribution is a results of voltage transformation.

Ionising Radiation

BIO90 and MIX90 score almost equal on ionising radiation, and as seen in Figure 4.15. MIX90 scores only a little higher due to the fossil carbon contribution (11.6%). The main contributor, however, is electricity, accounting for 88.2% and 82.6% of the impact of BIO90 and MIX90, respectively. BIO90 also has a contribution from biogenic carbon of about 9.9%. The negative impact from energy recovery reduces the impact of BIO90 by −17.9%, while for MIX90 the number is −18.5%.

The reason for the large contribution from electricity to the ionising radiation potential, is because of import of Swedish electricity to the Norwegian electricity mix. As Sweden produces some of its electricity from nuclear power, this is the source of the ionising impact of electricity. Nuclear power is also the source of the contribution from fossil and biogenic carbon, as the database assumes parts of the electricity mix used during mining and processing of coal, and production of charcoal, originate from nuclear power plants.

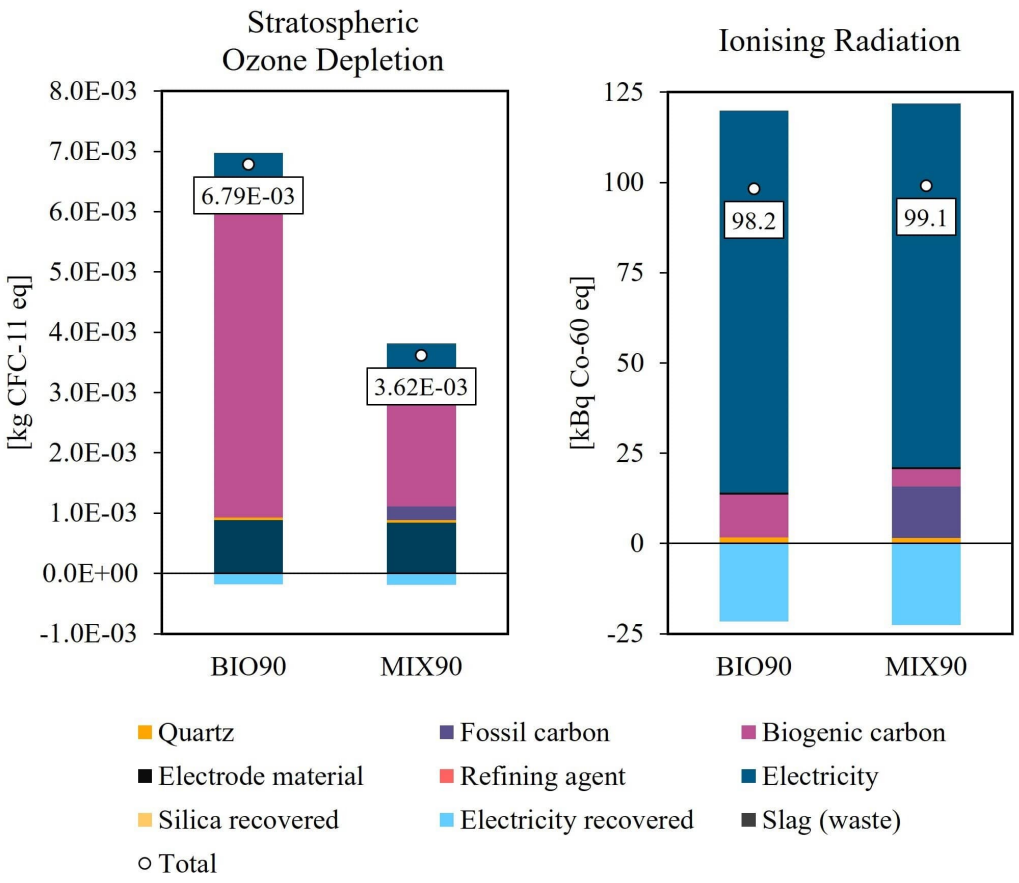

Figure 4.15: Comparison of impact on stratospheric ozone depletion and ionising radiation for BIO90 and MIX90. Be aware of different units.

4.4 Uncertainty Analysis

4.4.1 Data Uncertainty

Data regarding raw materials were easily available. Data regarding the refining ladle, on the other hand, was not as accessible. Slag composition is closely linked to the final product and inputs during refining, and is thus not usually shared by the industry.

There is also uncertainty related to the trace elements data in this thesis, especially regarding the biogenic carbon sources. The content of inorganic elements in biogenic materials vary seasonally and geographically [89]. Since the model is highly sensitive to the Al and Ca content during the refining stage, different sources of biogenic raw materials may change the results significantly.

The data used for raw materials' composition, has a huge time span, ranging from 1998 with the report *Delprosjekt 2. Produksjon av ferrosilisium og silisium metall i Norge* by Monsen, to internal data from Department of Materials Science and Engineering (NTNU) gathered in 2021 by Andersen. New and improved analysing techniques have most likely been developed during the last 24 years, and as data for quartz and electrodes used in this thesis are 14-24 years old, more recent data would be preferable.

4.4.2 Model Uncertainty

During calculations, complete combustion was assumed within the furnace. This leads to an overestimation of CO_2 emissions, and does not account for emissions of other compounds arising from incomplete combustion. This assumption was made because it would be too comprehensive to account for incomplete combustion, and the uncertainty would still be substantial, as assumptions would have to be made regarding how much of each compound being created.

To compensate for the missing compounds arising from incomplete combustion, data was gathered from www.norskeutslipp.no. However, these were based on an average over five years, then scaled down to a daily average. These emission factors were not mass balanced, and as could be seen for i.e., NO_x, they might be overestimated, at least when compared other numbers reported [27].

Nitrogen entering the furnace, either with air, or through the raw materials, was assumed to not react throughout the processes. This assumption was made because the fate of nitrogen within the furnace is not yet fully understood [73].

The last assumption made during calculations, were regarding the slag. Compared to other life cycle assessments of silicon production, the final slag amount after refining, was substantially lower in this thesis [43]. This might be a result from the assumption that no slag was leaving the furnace, but it could also be linked to the nature of the bio based mixture. The bio based mixes gave different compositions of the metal entering the refining ladle, than that of the more traditional charge mix. As the refining setup is based on addition of CaO due to Ca deficit, the uncertainty increases when the bio based mixes result in deficiency of Al instead of Ca.

The scope is limited to a Norwegian study, which yields uncertainties if applied outside of Norway. Since the goal and scope defines the study, with its system boundaries, this is not a full environmental assessment of the metallurgical grade silicon production process. Especially is this the case for the electricity used, as the Norwegian electricity mix is quite different from other mixes at it is mainly based on hydro-power. This will be further assessed in the sensitivity analysis, where the sensitivity to the electricity is assessed for this model setup.

4.4.3 Scenario Uncertainty

It is still common practice to add some fossil carbon to the charge mix when producing silicon metal, so the bio based charge mix scenario is mainly theoretical. The LCIA showed that the bio based charge mix had a deficit of aluminium before refining. This is usually not the case, which is also visualised in Figure 3.1, where the initial concentrations of Al and Ca is outside of the mapped diagram. This is related to the trace element composition of the raw materials. Thus, up-scaling the volume of silicon metal produced by biogenic carbon only, could potentially

Slag has already been discussed with respect to uncertainty regarding the assumptions made during calculations. Another uncertainty in the modelled scenario, is that it was output as waste. Slag from metallurgical grade silicon production is commonly sold to silicomanganese production [119]. Even though the impact from waste handling was minimal compared to the other processes, this could modify the results of this life cycle assessment.

4.5 Sensitivity Analysis

A sensitivity analysis is conducted in order to determine if the system is susceptible to change if one of the input parameters are altered, and the system is sensitive toward a parameter if small changes in parameters results in large changes of the system [120]. Here, the sensitivity of the system under study is tested for sensitivity toward source of wood chips, and the electricity mix.

4.5.1 Sensitivity to Wood Chips Source

Since Norwegian producers of metallurgical grade silicon get their raw materials from all over the world [121], a sensitivity analysis for wood chips was conducted. In order to assess the relative change, the sensitivity analysis was conducted for the BIO90 mix. BIO90|EwCh is the reference, with wood chips from Europe without Switzerland. BIO90|RoW is the comparison, with wood chips from a global mix.

As seen in Figure 4.16, the midpoint impact results do not change much when changing the source of the wood chips. If a change is seen, then the global alternative performs best. The largest change is seen for terrestrial ecotoxicity, where the impact is reduced by about 3% when using the global wood chips.

The relative difference between BIO90|EwCh and BIO90|RoW in Figure 4.16 varies from $0 - 3\%$, so it may seem like this model setup is insensitive to the source of the wood chips. Wood chips was also a minor contributor to all midpoint impact categories assessed in section 4.3.

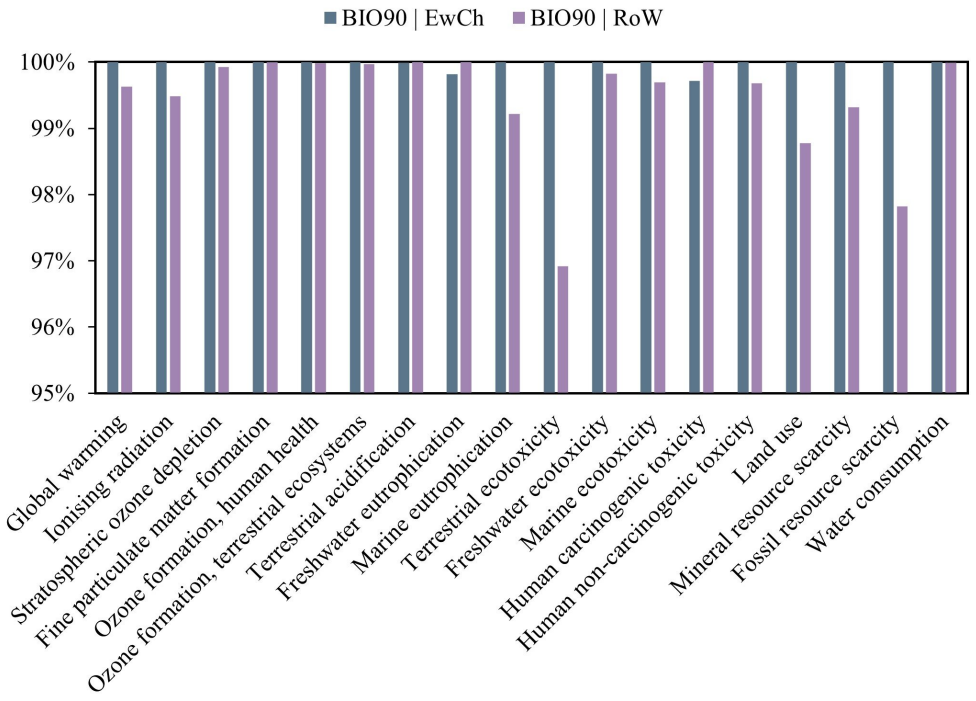

Figure 4.16: Sensitivity analysis comparing midpoint impact results, using wood chips from Europe without Switzerland (EwCh) or global wood chips mix (RoW). The analysis is conducted on BIO90. Pay attention to the y axis.

4.5.2 Sensitivity to Electricity Mix

Thesis is intended to contribute to the SisAl project, so a sensitivity analysis of electricity with respect to the European electricity mix, was conducted. In order to assess the relative change, the sensitivity analysis was conducted for the BIO90 mix. BIO90|NO is the reference with the Norwegian electricity mix. BIO90|RoE is the comparison, using the European electricity mix.

From Figure 4.17, it can be seen that most of the midpoint impacts shoots up when changing out the Norwegian electricity mix by the European, which is explained by the European electricity mix being heavily dependent upon fossil energy [122]. That also explains why the only impact category the European electricity mix performs better than the Norwegian one, is for water usage.

The largest increase is seen for ionising radiation, eutrophication, human toxicity and fossil resource scarcity, while the increase is less for land use, ozone formation and ozone depletion. The overall impact is, however, increased when switching from Norwegian to European electricity, indicating a sensitivity to the electricity mix.

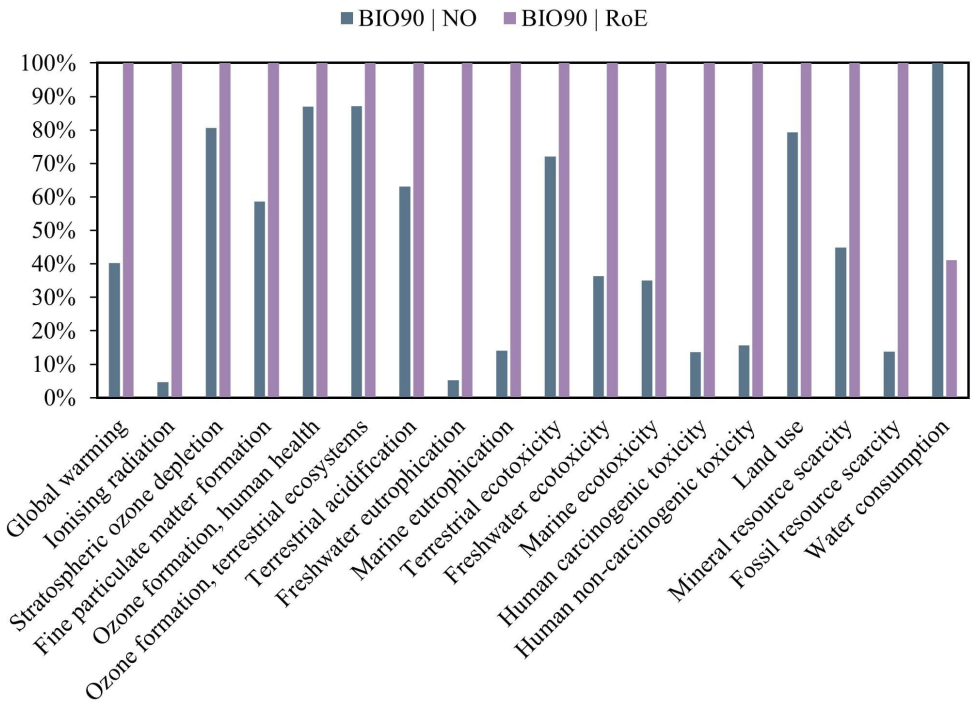

Figure 4.17: Sensitivity analysis comparing midpoint impact results of BIO90, by the Norwegian (NO) and the European electricity mix (RoE).

Chapter 5

Conclusion

During this thesis, a mass and energy balance of two different charge mixes, with three different yields, have been conducted. The results from the mass and energy balance was investigated through a life cycle assessment, to investigate the impact from different charge mixes and different yields. To answer the research question formulated in the introduction, the results from the inventory analysis and the impact analysis are considered separately.

Life Cycle Inventory Analysis

The inventory analysis revealed that material and electricity demand decreased with increasing yields, as did process emissions. The conventional charge mix was found to have a higher final silicon yield compared to the bio based mix.

Further, the conventional charge mix demanded less energy and quartz, and recovered more energy, compared to the bio based charge mix with the same yield. However, the emissions of chlorine during consumption of raw materials were found to be lower for the bio based mixes, by about one fourth compared to the conventional mixes by yield.

Life Cycle Impact Assessment

The impact assessment at endpoint level, showed that the area of protection most influenced by MG-Si production, was impact to human health. The different scenarios scored six to nine times higher on human health impact compared to impact to ecosystems, and the resource availability impact was negligible in comparison. The conventional charge mix was found to score about 1.5 times higher on damage to human health compared to the bio based mix for the same yield, while the bio based mix scored slightly higher than the conventional mix on damage to ecosystems.

Considering the contributions of midpoint impacts to the endpoint category human health, it was revealed that the main contributors were global warming and fine particulate matter formation. There was also a distinct contribution from human toxicity and water consumption. The main contributors to damage to ecosystems, were found to be land use, global warming, tropospheric ozone formation, and terrestrial acidification.

Assessing the eight midpoint impacts contributing the most to endpoint impacts, gave the following:

- **Global warming:** the bio based mix performed better than the conventional. Main contributor to BIO90, was emissions from production of charcoal, while the main contributor to MIX90, was the direct CO_2 emissions from the furnace.
- **Fine particulate matter formation:** the bio based mix performed better than the conventional. Primary contributor for both BIO90 and MIX90, was direct emissions of NO_x and SO_x from the furnace.
- **Tropospheric ozone formation:** the conventional mix performed better than the bio based one, both for impact on human health and impact on terrestrial ecosystems. The principal contributor was direct emissions of NO_x arising from the furnace to both mixes, and for both impact on human health and terrestrial ecosystems.
- **Terrestrial acidification:** the bio based mix performed better than the conventional. The main contributor was direct emissions of NO_x and SO_x from the furnace for both charge mixes.

- **Human toxicity:** the bio based mix performed better than the conventional. For both carcinogenic and non-carcinogenic human toxicity, the main contributor to the overall impact of MIX90, was waste and emissions related to mining of coal. The largest contributor to BIO90 for both human toxicity categories, was the infrastructure of electricity, but emissions arising from charcoal production also contributed substantially.

- **Land use:** the conventional mix performed better than the bio based one. The main contributor to both charge mixes was forestry related to biogenic carbon production, mainly charcoal.

Summing up the above, switching to biogenic carbon for metallurgical silicon metal production, has the potential to lower five of the eight midpoint impact categories most contributing to the endpoint impacts and damage to areas of protection. Since the midpoint impact categories where the bio based mix does not perform the best, are related to emissions of NO_x and SO_x, off gas treatment implementation can further lower the impact of a purely bio based charge mix [123, 124].

Limitations

This study is limited to a Norwegian context, and the mass balance assumed complete combustion, thus neglecting emissions related to incomplete combustion. This was accounted for by adding emission factors for some pollutants found from www.norskeutslipp.no. However, some of these emission factors, especially NO_x, are expected to be overestimated.

The sensitivity analysis revealed a sensitivity of the modelled system toward the electricity mix, where shifting towards a more fossil fuel based electricity increases most of the impact categories significantly.

Chapter 6

Further Work

Several interesting findings came out of the inventory analysis. Firstly, the fate of chlorine could be further investigated in relation to the metallurgical silicon production process. All chlorine entering the furnace, leaves with the off gas. As it is an acidic gas, it has the potential to contribute to acidification and eutrophication just like NO_x and SO_x.

Secondly, mechanisms of nitrogen combustion is of huge interest, due to its large contribution to several of midpoint impact categories. Nitrogen was not included in this mass balance, because its fate after combustion is dependent on several factors, and the distribution after combustion is not fully understood.

Thirdly, the mass balance revealed that the composition of Al and Ca in the liquid silicon before refining, was such that the phase diagram in Figure 3.1 did not cover it. The calculations further showed that if some refining agent were to be added during refining, that would have been alumina, and not quicklime. These implications could be of interest for further investigation.

Finally, conducting life cycle assessments of silicon production where more of the technological improvements regarding waste utilisation is implemented, could be interesting. Heat from cooling water have been tried utilised [45], slag generated during production is sold to silicomanganese production [119], and as mentioned in the conclusions, the off gas can be purified before emitted to air. It could be interesting to see how implementing all of these into a life cycle assessment, affects the results.

Bibliography

[1] H. K. Wedepohl. 'The Composition of the Continental Crust'. In: *Geochimica et Cosmochimica Acta* 59.7 (1995), pp. 1217–1232. DOI: https://doi.org/10.1016/0016-7037(95)00038-2.

[2] J. Marks et al. 'Metal Industry Emissions'. In: *Industrial Processes and Product Use*. Ed. by S. Eggleston et al. In collab. with R. Lanza et al. Vol. 3. 5 vols. 2006 IPCC Guidelines for National Greenhouse Gas Inventories. Japan: IGES, 2006, pp. 4.1–4.85. ISBN: 4-88788-032-4.

[3] World Bank Group. *The Growing Role of Minerals and Metals for a Low Carbon Future*. Washingtong, DC, US: World Bank Publications, 2017. URL: https://doi.org/10.1596/28312.

[4] G. Cusano et al. *Best Available Techniques (BAT) Reference Document for the Non-Ferrous Metals Industries : Industrial Emissions Directive 2010/75/EU (Integrated Pollution Prevention and Control)*. EUR 28648. ISBN: 978-92-79-69655-8. Luxembourg: European Commission Joint Research Centre, 2017. URL: https://data.europa.eu/doi/10.2760/8224.

[5] A. Monnet and A. Ait Abderrahim. *Report on Major Trends Affecting Future Demand for Critical Raw Materials*. D2.2. LGI, 22nd May 2018.

[6] EuroAlliages. *2050 Vision for the European Ferro-alloys and Silicon Sector*. Brussels, Belgium: EuroAlliages, Dec. 2019.

[7] European Commission. *Study on the EU's List of Critical Raw Materials, Factsheets on Critical Raw Materials*. 2020. URL: https://data.europa.eu/doi/10.2873/92480.

[8] CES Silicones Europe. *The Socioeconomic Impact of the Silicones Industry in Europe*. Brussels, Belgium: CES Silicones Europe, Mar. 2016.

[9] A. Ciftja, T. A. Engh and M. Tangstad. *Refining and Recycling of Silicon: A Review*. Research report. Trondheim, Norway: Faculty of Natural Science, Technology, Norwegian University of Science and Technology, Feb. 2008. URL: http://hdl.handle.net/11250/244462.

[10] A. Schei, J. K. Tuset and H. Tveit. *Production of High Silicon Alloys*. Trondheim, Norway: TAPIR, 1998. ISBN: 978-82-519-1317-1.

[11] *HS Code 28046900 - Silicon, containing, 99%*. URL: https://www.tariffnumber.com/2022/28046900 (visited on 20/03/2022).

[12] M. Tangstad and N. E. Kamfjord. 'Silicon and Ferrosilicon'. In: *Metal Production in Norway*. Ed. by M. Tangstad. Oslo, Norway: Akademika Publishing, 2013, pp. 97–120. ISBN: 978-82-321-0241-9.

[13] F. Chigondo. 'From Metallurgical-Grade to Solar-Grade Silicon: An Overview'. In: *Silicon* 10.3 (2018), pp. 789–798. DOI: https://doi.org/10.1007/s12633-016-9532-7.

[14] J. Degoulange et al. 'Multicrystalline silicon wafers prepared from upgraded metallurgical feedstock'. In: *Solar Energy Materials and Solar Cells* 92.10 (2008), pp. 1269–1273. DOI: https://doi.org/10.1016/j.solmat.2008.04.020.

[15] J. Safarian, G. Tranell and M. Tangstad. 'Processes for Upgrading Metallurgical Grade Silicon to Solar Grade Silicon'. In: *Energy Procedia*. Technoport 2012 - Sharing Possibilities and 2nd Renewable Energy Research Conference (RERC2012) 20 (2012), pp. 88–97. DOI: https://doi.org/10.1016/j.egypro.2012.03.011.

[16] W. A. Deer, R. A. Howie and J. Zussman. *An Introduction to the Rock-Forming Minerals*. 1st ed. London, UK: Longmans, Green & Co., 1966. ISBN: 0-582-44209-5.

[17] European Commission. *Study on the EU's list of Critical Raw Materials – Final Report*. Luxembourg: Publications Office of the European Union, 2020. ISBN: 978-92-76-21049-8. URL: https://data.europa.eu/doi/10.2873/11619.

[18] N. Idoine et al. *World Mineral Production 2016-2020*. Keyworth, Nottingham: British Geological Survey, 2022. ISBN: 978-0-85272-795-9.

[19] U.S. Geological Survey. *Mineral Commodity Summaries 2022*. USGS Numbered Series 2022. ISBN: 978-1-4113-4434-1. Reston, VA, US: U.S. Geological Survey, 2022. URL: https://doi.org/10.3133/mcs2022.

[20] CES Silicones Europe. *Silicones: Getting Europe to 2050*. May 2020. URL: https://www.silicones.eu/wp-content/uploads/2020/05/CES_1pager_Green-Deal.pdf (visited on 10/05/2022).

[21] European Aluminium. *Vision 2050: European Aluminium's Contribution to the EU's Mid-century Low-carbon Roadmap*. Brussels, Belgium: European Aluminium, Apr. 2019.

[22] M. Moen et al. 'Recycling of Silicon Metal Powder from Industrial Powder Waste Streams'. In: *Metal Powder Report* 72.3 (2017), pp. 182–187. DOI: https://doi.org/10.1016/j.mprp.2016.04.005.

[23] Q. He et al. 'Separating and Recycling of Elemental Silicon from Wasted Industrial Silicon Slag'. In: *Metallurgical and Materials Transactions B: Process Metallurgy and Materials Processing Science* 53.1 (2022), pp. 442–453. DOI: https://doi.org/10.1007/s11663-021-02381-6.

[24] S. Han et al. 'Electromagnetic separation of silicon from metallurgical-grade silicon refined slag during the remelting process'. In: *Separation and Purification Technology* 280 (2022), p. 119815. DOI: https://doi.org/10.1016/j.seppur.2021.119815.

[25] C. C. Farrell et al. 'Technical challenges and opportunities in realising a circular economy for waste photovoltaic modules'. In: *Renewable and Sustainable Energy Reviews* 128 (2020), p. 109911. DOI: https://doi.org/10.1016/j.rser.2020.109911.

[26] R. Bendikiene et al. 'Utilization of Industrial Solar Cells' Scrap as the Base Material to Form Coatings'. In: *Waste and Biomass Valorization* 12.5 (2021), pp. 2757–2767. DOI: https://doi.org/10.1007/s12649-020-01153-8.

[27] I. Kero, S. Grådahl and G. Tranell. 'Airborne Emissions from Si/FeSi Production'. In: *JOM* 69 (2017), pp. 365–380. DOI: https://doi.org/10.1007/s11837-016-2149-x.

[28] L. Kolbeinsen. 'Introduction to Metal Production'. In: *Metal Production in Norway*. Ed. by M. Tangstad. Oslo, Norway: Akademika Publishing, 2013, pp. 9–24. ISBN: 978-82-321-0241-9.

[29] Ø. Skreiberg, L. Wang and R. Khalil, eds. *BioCarb+ - Enabling the Biocarbon Value Chain for Energy*. Trondheim, Norway: SINTEF, 2017. ISBN: 978-82-594-3774-7.

[30] G. Fick et al. 'Using Biomass for Pig Iron Production: A Technical, Environmental and Economical Assessment'. In: *Waste and Biomass Valorization* 5.1 (2014), pp. 43–55. DOI: https://doi.org/10.1007/s12649-013-9223-1.

[31] T. Searchinger et al. 'Use of U.S. Croplands for Biofuels Increases Greenhouse Gases Through Emissions from Land-Use Change'. In: *Science* 319.5867 (2008), pp. 1238–1240. DOI: https://doi.org/10.1126/science.1151861.

[32] International Energy Agency. *Global Energy Review: CO_2 Emissions in 2021*. France: IEA, Mar. 2022.

[33] M. Dåstøl et al. 'Method for Production of White Microsilica'. European pat. 0711252B1. E. M. A. Elkem ASA. 14th Jan. 1998.

[34] G. Tranell, J. Safarian and M. Wallin. 'SisAl - A New Process for Production of Silicon'. In: *Silicon for the Chemical and Solar Industry XV: June 15 - 18, 2020, Trondheim, Norway*. Ed. by M. Tangstad et al. Silicon for the Chemical and Solar Industry XV. Trondheim, Norway: Dept. of Materials Science, Engineering, Norwegian University of Science and Technology, 2020, pp. 129–139. ISBN: 978-82-997357-9-7. URL: https://hdl.handle.net/11250/2724094.

[35] G. Sævarsdottir, T. Magnusson and H. Kvande. 'Reducing the Carbon Footprint: Primary Production of Aluminum and Silicon with Changing Energy Systems'. In: *Journal of Sustainable Metallurgy* 7.3 (2021), pp. 848–857. DOI: https://doi.org/10.1007/s40831-021-00429-0.

[36] S. M. Heidari and A. Anctil. 'Country-Specific Carbon Footprint and Cumulative Energy Demand of Metallurgical Grade Silicon Production for Silicon Photovoltaics'. In: *Resources, Conservation and Recycling* 180 (2022), p. 106171. DOI: https://doi.org/10.1016/j.resconrec.2022.106171.

[37] R. Kannan et al. 'Life Cycle Assessment Study of Solar PV Systems: An Example of a 2.7kWp Distributed Solar PV System in Singapore'.

In: *Solar Energy* 80.5 (2006), pp. 555–563. DOI: https://doi.org/10.1016/j.solener.2005.04.008.

[38] R. Gløckner et al. 'Environmental Life Cycle Assessment of the Elkem Solar Metallurgical Process Route to Solar Grade Silicon with Focus on Energy Consumption and Greenhouse Gas Emissions'. In: *Silicon for the Chemical and Solar Industry IX: Holmen Fjord Hotel, Oslo, Norway, June 23 - 26, 2008*. Ed. by H. A. Øye and Institutt for Materialteknologi. Silicon for the Chemical and Solar Industry IX. Trondheim, Norway: Dept. of Materials Technology, Norwegian University of Science and Technology, 2008, pp. 235–242. ISBN: 978-82-997357-5-9.

[39] N. J. Mohr et al. 'Environmental Life Cycle Assessment of Roof-Integrated Flexible Amorphous Silicon/Nanocrystalline Silicon Solar Cell Laminate'. In: *Progress in Photovoltaics: Research and Applications* 21.4 (2013), pp. 802–815. DOI: https://doi.org/10.1002/pip.2157.

[40] M. M. Lunardi et al. 'Life Cycle Assessment on PERC Solar Modules'. In: *Solar Energy Materials and Solar Cells* 187 (2018), pp. 154–159. DOI: https://doi.org/10.1016/j.solmat.2018.08.004.

[41] L. Ma et al. 'Assessment and Study on the Impact on Environment by Multi-Crystalline Silicon Preparation by Metallurgical Route'. In: *Silicon* 11.3 (2019), pp. 1383–1391. DOI: https://doi.org/10.1007/s12633-018-9937-6.

[42] L. Méndez et al. 'Upgraded Metallurgical Grade Silicon and Polysilicon for Solar Electricity Production: A Comparative Life Cycle Assessment'. In: *Science of The Total Environment* 789 (2021), p. 147969. DOI: https://doi.org/10.1016/j.scitotenv.2021.147969.

[43] E. P. Vallés. 'Life Cycle Assessment of Silicon Metal by Aluminothermic Reduction: an Industrial Symbiosis Approach'. Master's thesis. Trondheim: Norwegian University of Science and Technology, June 2021. URL: https://hdl.handle.net/11250/2824786.

[44] M. A. J. Huijbregts et al. *ReCiPe 2016 v1.1. Report I: Characterization.* RIVM Report 2016-0104a. Bilthoven, Netherlands: National Institute for Public Health and the Environment, 2017.

[45] N. E. Kamfjord et al. 'Energy Balance of a 45MW (Ferro-) Silicon Submerged Arc Furnace'. In: *Sustainable Future: Proceedings of the Twelfth International Ferroalloys Congress: June 6 - 9, 2010, Helsinki, Finland*. Ed. by A. Vartiainen. INFACON XII. Helsinki, Finland: Outotec Oyj, 2010, pp. 729–738. ISBN: 978-952-92-7341-6.

[46] M. Takla et al. 'Energy and Exergy Analysis of the Silicon Production Process'. In: *Energy* 58 (2013), pp. 138–146. DOI: https://doi.org/10.1016/j.energy.2013.04.051.

[47] K. A. Dill and S. Bromberg. *Molecular Driving Forces: Statistical Thermodynamics in Biology, Chemistry, Physics, and Nanoscience*. In collab. with D. Stigter. 2nd ed. Abingdon, UK: Garland Science, 2011. ISBN: 978-0-8153-4430-8.

[48] Standard Norge. *Miljøstyring - Livsløpsvurdering - Prinsipper og rammeverk*. ISO 14040:2006. 2006. URL: https://www.standard.no/no/Nettbutikk/produktkatalogen/Produktpresentasjon/?ProductID=236802.

[49] Standard Norge. *Miljøstyring - Livsløpsvurdering - Krav og retningslinjer*. ISO 14044:2006. 2006. URL: https://www.standard.no/no/Nettbutikk/produktkatalogen/Produktpresentasjon/?ProductID=236803.

[50] A. Furberg, R. Arvidsson and S. Molander. 'A Practice-Based Framework for Defining Functional Units in Comparative Life Cycle Assessments of Materials'. In: *Journal of Industrial Ecology* 26.3 (2022), pp. 718–730. DOI: https://doi.org/10.1111/jiec.13218.

[51] D. K. Panesar, K. E. Seto and C. J. Churchill. 'Impact of the Selection of Functional Unit on the Life Cycle Assessment of Green Concrete'. In: *The International Journal of Life Cycle Assessment* 22.12 (2017), pp. 1969–1986. DOI: https://doi.org/10.1007/s11367-017-1284-0.

[52] D. L. Sills et al. 'The Effect of Functional Unit and Co-Product Handling Methods on Life Cycle Assessment of an Algal Biorefinery'. In: *Algal Research* 46 (2020), p. 101770. DOI: https://doi.org/10.1016/j.algal.2019.101770.

[53] A.-M. Tillman. 'Significance of Decision-Making for LCA Methodology'. In: *Environmental Impact Assessment Review* 20.1 (2000), pp. 113–123. DOI: https://doi.org/10.1016/S0195-9255(99)00035-9.

[54] G. Wernet et al. 'The Ecoinvent Database Version 3 (part I): Overview and Methodology'. In: *The International Journal of Life Cycle Assessment* 21.9 (2016), pp. 1218–1230. DOI: https://doi.org/10.1007/s11367-016-1087-8.

[55] G. Bourgault, P. Lesage and R. Samson. 'Systematic Disaggregation: a Hybrid LCI Computation Algorithm Enhancing Interpretation Phase in LCA'. In: *The International Journal of Life Cycle Assessment* 17.6 (2012), pp. 774–786. DOI: https://doi.org/10.1007/s11367-012-0418-7.

[56] H. D. Young and R. A. Freedman. *University Physics with Modern Physics*. In collab. with A. L. Ford. 15th ed. Harlow, UK: Pearson Education, 2020. ISBN: 978-1-292-31473-0.

[57] A. G. Blackman et al. *Aylward and Findlay's SI Chemical Data*. 7th ed. Milton, Qld, Australia: Jon Wiley & Sons, 2014. ISBN: 978-0-7303-0246-9.

[58] S. Hosokai et al. 'Modification of Dulong's Formula to Estimate Heating Value of Gas, Liquid and Solid Fuels'. In: *Fuel Processing Technology* 152 (2016), pp. 399–405. DOI: https://doi.org/10.1016/j.fuproc.2016.06.040.

[59] Standard Norge. *Fast biodrivstoff - Bestemmelse av brennverdi*. ISO 18125:2017. 2017. URL: https://www.standard.no/no/Nettbutikk/produktkatalogen/Produktpresentasjon/?ProductID=928464.

[60] Standard Norge. *Fast biobrensel - Overføring av analytiske resultater fra én hovedbestanddel til en annen*. ISO 16993:2016. 2016. URL: https://www.standard.no/no/Nettbutikk/produktkatalogen/Produktpresentasjon/?ProductID=851661.

[61] A. Roine. *HSC Chemistry® 9*. Version 9.9.2.3. [software]. Metso Outotec. Pori, Finland, 2019. URL: http://www.mogroup.com/hsc.

[62] M. A. J. Huijbregts et al. 'ReCiPe2016: a Harmonised Life Cycle Impact Assessment Method at Midpoint and Endpoint Level'. In: *The International Journal of Life Cycle Assessment* 22.2 (2017), pp. 138–147. DOI: https://doi.org/10.1007/s11367-016-1246-y.

[63] M. Goedkoop et al. *ReCiPe 2008 v1.08. Report I: Characterisation*. Bilthoven, Netherlands: National Institute for Public Health and the Environment, May 2013.

[64] H. Baumann and A.-M. Tillman. *The Hitch Hiker's Guide to LCA: an Orientation in Life Cycle Assessment Methodology and Application*. Lund, Sweden: Studentlitteratur, 2004. ISBN: 91-44-02364-2.

[65] M. van Asselt and J. Rotmans. 'Uncertainty in Perspective'. In: *Global Environmental Change* 6.2 (1996), pp. 121–157. DOI: https://doi.org/10.1016/0959-3780(96)00015-5.

[66] A. L. C. Lima, J. W. Farrington and C. M. Reddy. 'Combustion-Derived Polycyclic Aromatic Hydrocarbons in the Environment—A Review'. In: *Environmental Forensics* 6.2 (2005), pp. 109–131. DOI: https://doi.org/10.1080/15275920590952739.

[67] J. C. Wakefield. *A Toxicological Review of the Products of Combustion*. HPA-CHaPD-004. ISBN: 978-0-85951- 663-1. Didcot, Oxfordshire, UK: Health Protection Agency, Centre for Radiation, Chemical, Environmental Hazards, Chemical Hazards and Poisons Division, Feb. 2010.

[68] M. J. Rogoff and F. Screve. 'Permitting Issues'. In: *Waste-to-Energy*. Ed. by M. J. Rogoff and F. Screve. 2nd ed. Oxford, UK: William Andrew Publishing, 2011, pp. 89–116. ISBN: 978-1-4377-7871-7. URL: https://doi.org/10.1016/B978-1-4377-7871-7.10008-5.

[69] S. Grådahl et al. *Miljø og ovnsprosesser. Del I*. STF24 A97568. Trondheim, Norway: SINTEF Materialteknologi, Apr. 1997.

[70] B. Ravary, C. Colomb and S. T. Johansen. 'Modelling Combustion and Thermal NO_x Formation in Electric Arc Furnaces for the Production of Ferrosilicon and Silicon-Metal'. In: *11th International Conference on Innovations in the Ferro Alloy Industry: February 18 - 21, 2007, New Delhi, India*. Ed. by Indian Ferro Alloy Producers' Association. Vol. II. II vols. INFACON XI. New Delhi, India: Macmillan, 2007, pp. 499–506. ISBN: 978-0-230-63070-3.

[71] J. E. Olsen et al. *Combustion and NO_x Formation in Silicon Pilot Furnace*. SINTEF F23783. SINTEF Materials and Chemistry, Nov. 2012.

[72] E. H. Myrhaug et al. 'NO_x Emissions from Silicon Production'. In: *Silicon for the Chemical and Solar Industry XI: June 25-29, 2012, Bergen - Ulvik, Norway*. Ed. by H. A. Øye. Silicon for the Chemical and Solar Industry XI. Trondheim, Norway: Department of Materials Science, En-

gineering, Norwegian University of Science and Technology, June 2012, pp. 95–106. ISBN: 978-82-997357-7-3.

[73] I. Solheim and N. E. Kamfjord. 'NO_x-Emissions from the Silicon Process Comparing Wet and Dry Raw Materials Pilot Scale Experiments'. In: *Efficient Technologies in Ferroalloy Industry: Proceedings of the Thirteenth International Ferroalloys Congress: June 9-12, 2013, Almaty, Kazakhstan*. Vol. II. II vols. INFACON XIII. Karaganda, Kazakhstan: P. Dipner, 2013, pp. 1029–1036. ISBN: 9965-729-36-0.

[74] V. Myrvågnes. 'Analyses and Characterization of Fossil Carbonaceous Materials for Silicon Production'. ISBN: 978-82-471-6485-3. Doctoral thesis. Trondheim: Norwegian University of Science and Technology, Jan. 2008. URL: http://hdl.handle.net/11250/248717.

[75] V. Andersen et al. 'Pilot Scale Test of Flue Gas Recirculation for the Silicon Process'. In: *REWAS 2022: Developing Tomorrow's Technical Cycles (Volume I)*. The Minerals, Metals & Materials Society. Ed. by A. Lazou et al. Vol. I. The Minerals, Metals & Materials Series. Anaheim, CA, USA: Springer International Publishing, Feb. 2022, pp. 555–564. ISBN: 978-3-030-92563-5. DOI: https://doi.org/10.1007/978-3-030-92563-5_58.

[76] V. Andersen. *Proximate, ultimate and ash analysis on coke, coal, charcoal and wood chips*. 13th May 2022.

[77] *Bituminous coal, UK HemHeath (#958)*. Phyllis2. 2016. URL: https://phyllis.nl/Biomass/View/958 (visited on 16/06/2022).

[78] *Coal (#3050)*. Phyllis2. URL: https://phyllis.nl/Biomass/View/3050 (visited on 16/06/2022).

[79] *Willow char (#2716)*. Phyllis2. 2003. URL: https://phyllis.nl/Biomass/View/2716 (visited on 16/06/2022).

[80] *Spruce, Logging residues (#3482)*. Phyllis2. 2009. URL: https://phyllis.nl/Biomass/View/3482 (visited on 16/06/2022).

[81] B. Monsen. *Delprosjekt 2. Produksjon av ferrosilisium og silisium metall i Norge*. STF24 A98537. ISBN: 82-14-00720-8. Trondheim, Norway: SINTEF, 20th May 1998.

[82] E. H. Myrhaug. 'Non-fossil reduction materials in the silicon process - properties and behaviour'. ISBN: 82-471-5619-9. Doctoral thesis. Trondheim: Norwegian University of Science and Technology, July 2003.

[83] K. Aasly. 'Properties and behavior of quartz for the silicon process'. ISBN: 978-82-471-1164-2 ISSN: 1503-8181. Doctoral thesis. Trondheim: Norwegian University of Science and Technology, Aug. 2008.

[84] V. Andersen. *Actual moist content of wood chips*. Personal communication. 7th June 2022.

[85] V. Andersen. *Quartz power consumption*. Personal communication. 13th May 2022.

[86] O. Raaness. *Delprosjekt 1. CO_2 utslipp fra forskjellige typer reduksjonsmaterialer*. STF24 A98550. ISBN: 82-14-00959-6. Trondheim, Norway: SINTEF, May 1998.

[87] V. Andersen. *Industrial practice not including C from electrodes in C needed for reduction of silica*. Personal communication. 31st May 2022.

[88] N. E. Kamfjord. 'Mass and Energy Balances of the Silicon Process: Improved Emission Standards'. ISBN: 978-82-471-3614-0. Doctoral thesis. Trondheim: Norwegian University of Science and Technology, Apr. 2012. URL: http://hdl.handle.net/11250/249043.

[89] A. Malmgren and G. Riley. 'Biomass Power Generation'. In: *Comprehensive Renewable Energy*. Ed. by A. Sayigh. Vol. 5. Oxford, UK: Elsevier, 2012, pp. 27–53. ISBN: 978-0-08-087873-7. URL: https://doi.org/10.1016/B978-0-08-087872-0.00505-9.

[90] *Orkla ndf. Svorkmo kraftstasjon — Sildre*. NVE Sildre. 13th Oct. 2021. URL: https://sildre.nve.no/station/121.59.0?stationId=121.59.0&x=237129&y=7018879&zoom=12&121.59.0.1003_period=custom&121.59.0.1003_res=1440&121.59.0.1003_to=2021-05-01&121.59.0.1003_from=2020-05-01 (visited on 21/06/2022).

[91] K. Verscheure et al. 'Furnace Cooling Technology in Pyrometallurgical Processes'. In: *New, Improved and Existing Technologies: Non-Ferrous Materials Extraction and Processing*. Ed. by F. Kongoli and R. G. Reddy. Vol. 4. Sohn International Symposium: Advanced Processing of Metals and Materials. San Diego, CA, US: Wiley, 2006, pp. 139–154. ISBN: 978-0-87339-637-0.

[92] L. Kolbeinsen et al. 'Energy Recovery in the Norwegian Ferro Alloy Industry'. In: *INFACON 7: Trondheim, June 1995*. Ed. by J. K. Tuset, H. Tveit and I. G. Page. INFACON VII. Trondheim, Norway: Norwegian Ferroalloy Research Organization (FFF), 1995, pp. 165–178. ISBN: 978-82-595-8649-0.

[93] P. Dannevig and B. Pedersen. *luft*. In: *Store Norske Leksikon*. 3rd Oct. 2019. URL: http://snl.no/luft (visited on 14/06/2022).

[94] X. Liu, H. Shen and X. Nie. 'Study on the Filtration Performance of the Baghouse Filters for Ultra-Low Emission as a Function of Filter Pore Size and Fiber Diameter'. In: *International Journal of Environmental Research and Public Health* 16.2 (Jan. 2019), p. 247. DOI: https://doi.org/10.3390/ijerph16020247.

[95] T. A. Engh, G. K. Sigworth and A. Kvithyld. *Principles of Metal Refining and Recycling*. 1st ed. Oxford, UK: Oxford University Press, 2021. ISBN: 978-0-19-185003-5. URL: https://doi.org/10.1093/oso/9780198811923.001.0001.

[96] E. L. Bjørnstad. 'Oxidative Ladle Refining of Metallurgical Grade Silicon: Refining of Ca and Al Impurities'. ISBN: 978-82-326-6676-8. Doctoral thesis. Trondheim, Norway: Norwegian University of Science and Technology, Aug. 2021. URL: https://hdl.handle.net/11250/2768770.

[97] G. Tranell and V. Andersen. *Final slag composition*. Personal communication. 1st Aug. 2022.

[98] M. K. Næss et al. 'Element Distribution in Silicon Refining: Thermodynamic Model and Industrial Measurements'. In: *JOM* 66.11 (2014), pp. 2343–2354. DOI: https://doi.org/10.1007/s11837-013-0797-7.

[99] *SimaPro*. Version 9.1.1.7 Multiuser. [software]. PRé Sustainability. 1990.

[100] *Elkem Salten*. Norske Utslipp. URL: https://www.norskeutslipp.no/no/Diverse/Virksomhet/?CompanyID=5151 (visited on 19/06/2022).

[101] *Elkem Thamshavn*. Norske Utslipp. URL: https://www.norskeutslipp.no/no/Diverse/Virksomhet/?CompanyID=6074 (visited on 19/06/2022).

[102] *Wacker Chemicals Norway*. Norske Utslipp. URL: https://www.norskeutslipp.no/no/Diverse/Virksomhet/?CompanyID=6075 (visited on 19/06/2022).

[103] C. Procaccini. 'The Chemistry of Chlorine in Combustion Systems and the Gas-Phase Formation of Chlorinated and Oxygenated Pollutants'. Doctoral thesis. Cambridge, MA, US: Massachusetts Institute of Technology, Sept. 1999. URL: http://hdl.handle.net/1721.1/9365.

[104] N. De Nevers. *Air pollution control engineering*. 2nd ed. McGraw-Hill series in water resources and environmental engineering. Boston: McGraw-Hill, 2000. 586 pp. ISBN: 978-0-07-039367-7.

[105] R. Bailis. 'Wood in Household Energy Use'. In: *Encyclopedia of Energy*. Ed. by C. J. Cleveland. New York, NY, USA: Elsevier, 2004, pp. 509–526. ISBN: 978-0-12-176480-7. URL: https://doi.org/10.1016/B0-12-176480-X/00450-2.

[106] E. Uggerud and S. Langård. *Dioksiner*. In: *Store norske leksikon*. 13th July 2021. URL: http://snl.no/dioksiner (visited on 29/06/2022).

[107] S. Grådahl et al. 'Reduction of Emissions from Ferroalloy Furnaces'. In: *11th International Conference on Innovations in the Ferro Alloy Industry: February 18 - 21, 2007, New Delhi, India*. Ed. by Indian Ferro Alloy Producers' Association. Vol. 2. 2 vols. INFACON XI. New Delhi, India: Macmillan, 2007, pp. 479–488. ISBN: 978-0-230-63070-3.

[108] K. Ravindra, R. Sokhi and R. Van Grieken. 'Atmospheric Polycyclic Aromatic Hydrocarbons: Source Attribution, Emission Factors and Regulation'. In: *Atmospheric Environment* 42.13 (2008), pp. 2895–2921. DOI: https://doi.org/10.1016/j.atmosenv.2007.12.010.

[109] V. I. Berdnikov and Y. A. Gudim. 'Formation of Dioxins in High-Temperature Combustion of Chlorine-Bearing Material'. In: *Steel in Translation* 45.2 (2015), pp. 89–93. DOI: https://doi.org/10.3103/S0967091215020035.

[110] R. van Zelm et al. 'Acidification'. In: *Life Cycle Impact Assessment*. Ed. by M. Z. Hauschild and M. A. Huijbregts. Red. by W. Klöpffer and M. A. Curran. LCA Compendium – The Complete World of Life Cycle Assessment. Dordrecht, Netherlands: Springer, 2015, pp. 163–176. ISBN: 978-94-017-9744-3. URL: https://doi.org/10.1007/978-94-017-9744-3_9.

[111] T. Y. A. Fahmy et al. 'Biomass Pyrolysis: Past, Present, and Future'. In: *Environment, Development and Sustainability* 22.1 (2020), pp. 17–32. DOI: https://doi.org/10.1007/s10668-018-0200-5.

[112] G. R. Surup, A. Trubetskaya and M. Tangstad. 'Life Cycle Assessment of Renewable Reductants in the Ferromanganese Alloy Production: A Review'. In: *Processes* 9.1 (2021), p. 185. DOI: https://doi.org/10.3390/pr9010185.

[113] G. Oberdörster, E. Oberdörster and J. Oberdörster. 'Nanotoxicology: An Emerging Discipline Evolving from Studies of Ultrafine Particles'. In: *Environmental Health Perspectives* 113.7 (2005), pp. 823–839. DOI: https://doi.org/10.1289/ehp.7339.

[114] R. Nieder and D. K. Benbi. 'Reactive Nitrogen Compounds and their Influence on Human Health: an Overview'. In: *Reviews on Environmental Health* 37.2 (2022), pp. 229–246. DOI: https://doi.org/10.1515/reveh-2021-0021.

[115] N. E. Grulke and R. L. Heath. 'Ozone Effects on Plants in Natural Ecosystems'. In: *Plant Biology* 22 (S1 2020). Ed. by S. Tausz-Posch, pp. 12–37. DOI: https://doi.org/10.1111/plb.12971.

[116] R. S. Jorge, T. R. Hawkins and E. G. Hertwich. 'Life Cycle Assessment of Electricity Transmission and Distribution — Part 1: Power Lines and Cables'. In: *The International Journal of Life Cycle Assessment* 17.1 (2012), pp. 9–15. DOI: https://doi.org/10.1007/s11367-011-0335-1.

[117] R. S. Jorge, T. R. Hawkins and E. G. Hertwich. 'Life Cycle Assessment of Electricity Transmission and Distribution — Part 2: Transformers and Substation Equipment'. In: *The International Journal of Life Cycle Assessment* 17.2 (2012), pp. 184–191. DOI: https://doi.org/10.1007/s11367-011-0336-0.

[118] P. S. Roy et al. 'Anthropogenic Land Use and Land Cover Changes—A Review on Its Environmental Consequences and Climate Change'. In: *Journal of the Indian Society of Remote Sensing* 50.8 (2022), pp. 1615–1640. DOI: https://doi.org/10.1007/s12524-022-01569-w.

[119] M. Tangstad. 'Manganese Ferroalloys'. In: *Metal Production in Norway*. Ed. by M. Tangstad and L. Kolbeinsen. Oslo, Norway: Akademika Publishing, 2013, pp. 75–96. ISBN: 978-82-321-0241-9.

[120] R. K. Rosenbaum, S. Georgiadis and P. Fantke. 'Uncertainty Management and Sensitivity Analysis'. In: *Life Cycle Assessment*. Ed. by M. Z. Hauschild, R. K. Rosenbaum and S. I. Olsen. Cham: Springer Inter-

national Publishing, 2018, pp. 271–321. ISBN: 978-3-319-56475-3. URL: https://doi.org/10.1007/978-3-319-56475-3_11.

[121] L.-M. Kristiansen and C. van der Eijk. 'Part 1: Companies and Production'. In: *Overview of the Norwegian Metallurgical Industry*. Trondheim, Norway: SFI Metal Production, 2020.

[122] International Energy Agency. *European Union 2020*. Energy Policy Review. France: IEA, June 2020. URL: https://www.iea.org/reports/european-union-2020.

[123] D. Flagiello et al. 'Advanced Flue-Gas Cleaning by Wet Oxidative Scrubbing (WOS) using $NaClO_2$ Aqueous Solutions'. In: *Chemical Engineering Journal* 447 (2022), p. 137585. DOI: https://doi.org/10.1016/j.cej.2022.137585.

[124] J. Lim and J. Kim. 'Designing and Integrating NO_x, SO_2 and CO_2 Capture and Utilization Process using Desalination Wastewater'. In: *Fuel* 327 (2022), p. 124986. DOI: https://doi.org/10.1016/j.fuel.2022.124986.

Appendix

Appendix A

Raw Material Analysis

Proximate Analysis

Table A.1: Dry based proximate analysis. Data of raw materials from [75], and of electrodes from [81].

	Moisture	**FixC**	**Volatiles**	**Ash**
Coke	11.70 %	92.00 %	6.00 %	2.00 %
Coal	10.80 %	57.70 %	40.80 %	1.50 %
Charcoal	4.70 %	85.20 %	12.70 %	2.10 %
Wood Chips	4.80[1] %	25.00 %	-	-
Electrode	0.00 %	96.00 %	0.70 %	3.00 %

Ultimate Analysis

Table A.2: Wet based ultimate analysis of carbon and hydrogen of raw materials. Calculated from Table 3.3.

	Coke	**Coal**	**Charcoal**	**Wood chips**
C [%]	79.95 %	70.40 %	79.27 %	36.21 %
H [%]	1.64 %	5.23 %	3.54 %	4.63 %

[1]This is moisture after drying. The moisture content of wood chips when utilised in silicon production is about 40%. Value provided from personal communication with Vegar Andersen (May 13, 2022).

Appendix B

Trace Elements

Quartz and Electrodes

Table B.1: Sources on trace elements in quartz, and chosen values.

		Myrhaug (2003)	Aasly (2008)	Chosen value
Al	[ppm]	2785.00	2120.00	Average
As	[ppm]	0.30	-	Myrhaug
B	[ppm]	<75	-	75/2
Ba	[ppm]	13.00	-	Myrhaug
Be	[ppm]	<0.5	0.10	Aasly
Bi	[ppm]	<0.5	-	0.5/2
Ca	[ppm]	49.00	30.00	Average
Cd	[ppm]	<0.07	-	0.07/2
Cl	[ppm]	-	-	-
Co	[ppm]	73.00	1.00	Average
Cr	[ppm]	14.00	15.00	Average
Cu	[ppm]	2.00	1.00	Average
Fe	[ppm]	1113.00	840.00	Average
Hg	[ppm]	<0.005	-	0.005/2
K	[ppm]	557.00	630.00	Average
Mg	[ppm]	51.00	50.00	Average
Mn	[ppm]	145.60	73.00	Average
Mo	[ppm]	6.00	-	Myrhaug
Na	[ppm]	128.00	30.00	Average
Ni	[ppm]	8.00	1.00	Average
P	[ppm]	<50	-	50/2
Pb	[ppm]	3.00	-	Myrhaug
S	[ppm]	927.00	-	Myrhaug
Sb	[ppm]	<0.5	-	0.5/2
Sc	[ppm]	1.00	-	Myrhaug
Se	[ppm]	<0.5	-	0.5/2
Si	[ppm]	462 000	-	Myrhaug
Sn	[ppm]	<0.5	-	0.5/2
Sr	[ppm]	12.00	-	Myrhaug
Ti	[ppm]	-	200.00	Aasly
Tl	[ppm]	<0.5	-	0.5/2
V	[ppm]	4.00	2.00	Average
W	[ppm]	75.80	-	Myrhaug
Zn	[ppm]	4.00	-	Myrhaug
Zr	[ppm]	3.30	45.00	Average

Table B.2: Sources on trace elements in electrodes, and chosen values.

		Myrhaug (2003)	Chosen values
Al	[ppm]	3 871.00	Myrhaug
As	[ppm]	<5	5/2
B	[ppm]	<75	75/2
Ba	[ppm]	62.00	Myrhaug
Be	[ppm]	<0.5	0.5/2
Bi	[ppm]	1.50	Myrhaug
Ca	[ppm]	1 509.00	Myrhaug
Cd	[ppm]	1.20	Myrhaug
Cl	[ppm]	-	-
Co	[ppm]	10.00	Myrhaug
Cr	[ppm]	19.00	Myrhaug
Cu	[ppm]	12.00	Myrhaug
Fe	[ppm]	3 366.00	Myrhaug
Hg	[ppm]	38.00	Myrhaug
K	[ppm]	183.00	Myrhaug
Mg	[ppm]	473.00	Myrhaug
Mn	[ppm]	2 939.10	Myrhaug
Mo	[ppm]	2.00	Myrhaug
Na	[ppm]	288.00	Myrhaug
Ni	[ppm]	31.00	Myrhaug
P	[ppm]	163.00	Myrhaug
Pb	[ppm]	46.00	Myrhaug
S	[ppm]	1 967.00	Myrhaug
Sb	[ppm]	0.60	Myrhaug
Sc	[ppm]	-	-
Se	[ppm]	<0.5	0.5/2
Si	[ppm]	-	-
Sn	[ppm]	1.60	Myrhaug
Sr	[ppm]	39.00	Myrhaug
Ti	[ppm]	-	-
Tl	[ppm]	<0.5	0.5/2
V	[ppm]	37.00	Myrhaug
W	[ppm]	0.50	Myrhaug
Zn	[ppm]	48.00	Myrhaug
Zr	[ppm]	1.70	Myrhaug

Coke and Coal

Table B.3: Sources on trace elements in coke, and chosen values.

		Andersen (2022)	Phyllis #958	Chosen values
Al	[ppm]	2 420.00	146.00	Average
As	[ppm]	<0.4	5.00	0.4/2
B	[ppm]	-	-	-
Ba	[ppm]	40.40	-	Andersen
Be	[ppm]	0.36	-	Andersen
Bi	[ppm]	-	-	-
Ca	[ppm]	477.00	-	Andersen
Cd	[ppm]	0.03	<1	Andersen
Cl	[ppm]	-	6 881.00	Phyllis
Co	[ppm]	0.89	<2	Andersen
Cr	[ppm]	4.68	<2	Phyllis
Cu	[ppm]	7.85	23.00	Average
Fe	[ppm]	2 240.00	2 940.00	Average
Hg	[ppm]	<0.05	<2	0.05/2
K	[ppm]	121.00	1 420.00	Average
Mg	[ppm]	322.00	-	Andersen
Mn	[ppm]	22.80	53.00	Average
Mo	[ppm]	0.85	<2	Andersen
Na	[ppm]	448.00	450.00	Average
Ni	[ppm]	4.17	3.00	Average
P	[ppm]	28.80	-	Andersen
Pb	[ppm]	1.81	20.00	Average
S	[ppm]	4 200.00	8 800.00	Average
Sb	[ppm]	-	-	-
Sc	[ppm]	1.01	-	Andersen
Se	[ppm]	-	-	-
Si	[ppm]	15 300.00	-	Andersen
Sn	[ppm]	0.07	-	Andersen
Sr	[ppm]	22.00	-	Andersen
Ti	[ppm]	89.60	-	Andersen
Tl	[ppm]	-	-	-
V	[ppm]	12.30	7.00	Average
W	[ppm]	0.18	-	Andersen
Zn	[ppm]	11.30	15.00	Average
Zr	[ppm]	4.47	-	Andersen

Table B.4: Sources on trace elements in coal, and chosen values.

		Andersen (2022)	Phyllis #3050	Chosen values
Al	[ppm]	2 280.00	13 350.40	Average
As	[ppm]	1.11	1.60	Average
B	[ppm]	-	45.50	Phyllis
Ba	[ppm]	27.50	84.90	Average
Be	[ppm]	0.22	-	Andersen
Bi	[ppm]	-	-	-
Ca	[ppm]	695.00	4 264.70	Average
Cd	[ppm]	0.03	0.10	Average
Cl	[ppm]	-	236.00	Phyllis
Co	[ppm]	0.99	2.30	Average
Cr	[ppm]	3.54	10.30	Average
Cu	[ppm]	7.03	5.90	Average
Fe	[ppm]	2 460.00	5 347.40	Average
Hg	[ppm]	<0.05	-	0.05/2
K	[ppm]	268.00	1 638.80	Average
Mg	[ppm]	398.00	916.60	Average
Mn	[ppm]	18.30	42.50	Average
Mo	[ppm]	0.59	1.40	Average
Na	[ppm]	710.00	319.40	Average
Ni	[ppm]	2.60	6.80	Average
P	[ppm]	20.00	53.60	Average
Pb	[ppm]	1.25	1.80	Average
S	[ppm]	5 200.00	8 000.00	Average
Sb	[ppm]	-	-	-
Sc	[ppm]	0.77	-	Andersen
Se	[ppm]	-	5.60	Phyllis
Si	[ppm]	6 650.00	33 988.80	Average
Sn	[ppm]	0.03	0.70	Average
Sr	[ppm]	19.20	28.00	Average
Ti	[ppm]	100.00	469.60	Average
Tl	[ppm]	-	-	-
V	[ppm]	6.42	24.20	Average
W	[ppm]	0.09	-	Andersen
Zn	[ppm]	3.32	19.30	Average
Zr	[ppm]	3.22	-	Andersen

Charcoal and Wood Chips

Table B.5: Sources on trace elements in charcoal, and chosen values.

		Andersen (2022)	Phyllis #2716	Chosen values
Al	[ppm]	225.00	223.90	Average
As	[ppm]	<0.4	3.30	Phyllis
B	[ppm]	-	15.70	Phyllis
Ba	[ppm]	82.10	4.00	Average
Be	[ppm]	0.02	-	Andersen
Bi	[ppm]	-	-	-
Ca	[ppm]	11 300.00	8 817.00	Average
Cd	[ppm]	0.05	4.80	Average
Cl	[ppm]	-	312.80	Phyllis
Co	[ppm]	0.24	0.10	Average
Cr	[ppm]	3.36	8.80	Average
Cu	[ppm]	4.23	9.20	Average
Fe	[ppm]	398.00	172.40	Average
Hg	[ppm]	<0.05	-	0.05/2
K	[ppm]	292.00	5 977.70	Average
Mg	[ppm]	824.00	1 010.10	Average
Mn	[ppm]	480.00	32.60	Average
Mo	[ppm]	0.19	-	Andersen
Na	[ppm]	114.00	498.40	Average
Ni	[ppm]	2.05	27.40	Average
P	[ppm]	515.00	2 085.60	Average
Pb	[ppm]	1.91	4.90	Average
S	[ppm]	243.00	0.04	Average
Sb	[ppm]	-	5.10	Phyllis
Sc	[ppm]	0.07	-	Andersen
Se	[ppm]	-	-	-
Si	[ppm]	1 260.00	983.90	Average
Sn	[ppm]	0.19	1.20	Average
Sr	[ppm]	39.70	38.20	Average
Ti	[ppm]	8.02	9.80	Average
Tl	[ppm]	-	-	-
V	[ppm]	0.55	0.50	Average
W	[ppm]	0.11	-	Andersen
Zn	[ppm]	32.40	151.00	Average
Zr	[ppm]	0.93	-	Andersen

Table B.6: Sources on trace elements in wood chips, and chosen values.

		Andersen (2022)	Phyllis #3482	Chosen values
Al	[ppm]	91.56	98.00	Average
As	[ppm]	<0.1	<0.05	0.05/2
B	[ppm]	-	5.90	Phyllis
Ba	[ppm]	15.40	40.00	Average
Be	[ppm]	<0.07	-	0.07/2
Bi	[ppm]	-	-	-
Ca	[ppm]	1 157.80	6 500.00	Average
Cd	[ppm]	0.08	0.30	Average
Cl	[ppm]	-	<100	100/2
Co	[ppm]	0.22	0.20	Average
Cr	[ppm]	2.56	1.60	Average
Cu	[ppm]	1.20	4.50	Average
Fe	[ppm]	67.29	130.00	Average
Hg	[ppm]	<0.01	<0.02	0.01
K	[ppm]	497.26	1 100.00	Average
Mg	[ppm]	154.39	490.00	Average
Mn	[ppm]	66.68	390.00	Average
Mo	[ppm]	0.05	0.10	Average
Na	[ppm]	47.03	<54	Andersen
Ni	[ppm]	1.56	0.80	Average
P	[ppm]	42.68	220.00	Average
Pb	[ppm]	0.43	1.50	Average
S	[ppm]	1 100.00	200.00	Average
Sb	[ppm]	-	<0.22	0.22/2
Sc	[ppm]	0.02	-	Andersen
Se	[ppm]	-	<0.05	0.05/2
Si	[ppm]	-	<1 100	1 100/2
Sn	[ppm]	-	<0.05	0.05/2
Sr	[ppm]	5.27	-	Andersen
Ti	[ppm]	5.64	<11	Andersen
Tl	[ppm]	-	-	-
V	[ppm]	0.13	0.40	Average
W	[ppm]	<0.01	-	0.01/2
Zn	[ppm]	17.10	140.00	Average
Zr	[ppm]	0.50	-	Andersen

Appendix C

Mass Balance

Daily consumption of quartz makes the foundation of all further calculations of raw materials and energy needed. Daily consumption of quartz is found by:

$$\mathrm{m_{quartz}} = \frac{45\,\mathrm{MW/d} \cdot 24\,\mathrm{h}}{4.6\,\mathrm{MWh/t_{quartz}}} = 234.78\,\mathrm{t/d}\,.$$

Operating with a quartz purity of 99.5% SiO_2 [82], total daily input to the furnace of silica is

$$\mathrm{m_{SiO_2}} = 0.95 \cdot \mathrm{m_{quartz}} = 233.61\,\mathrm{t/d}\,.$$

C.1 Submerged Electric Arc Furnace

Carbon input

Amount of Fix C needed to reduce solid SiO_2 to liquid Si is given by:

$$m_{\mathrm{Fix\ C}}\,[\mathrm{t/d}] = (1+x) \cdot \mathrm{m_{SiO_2}} \cdot \frac{\mathrm{M_C}}{\mathrm{M_{SiO_2}}}\,,$$

where M is the molar mass of the different compounds involved, and x the silicon yield. From the total mass of Fix C needed in the reaction, which varies with x, the amount of each carbon material in the charge mix is found by:

$$m_{\mathrm{C}_i}\,[\mathrm{t/d}] = m_{\mathrm{Fix\ C}} \cdot \frac{\%C_i}{\%FixC_i}\,.$$

$\%C_i$ is the percentage the different carbon sources, i, makes out of the raw material mix. $\%FixC_i$ is the amount of Fix C in raw material i.

Electrode consumption is dependent upon silicon output from the SAF [81], and is given by:

$$m_{\text{electrode}}\,[\text{t/d}] = m_{\text{Si}} \cdot 0.1\,.$$

Material output

From the furnace, there are only three material outputs considered: Liquid Si, and gaseous SiO and CO. Material balance of CO distinguishes between fossil and biogenic CO, depending on which raw material they originate from.

$$\begin{aligned} m_{\text{Si}}\,[\text{t/d}] &= x \cdot \text{m}_{\text{SiO}_2} \cdot \frac{\text{M}_{\text{Si}}}{\text{M}_{\text{SiO}_2}}\,, \\ m_{\text{SiO}}\,[\text{t/d}] &= (1-x) \cdot \text{m}_{\text{SiO}_2} \cdot \frac{\text{M}_{\text{SiO}}}{\text{M}_{\text{SiO}_2}}\,, \\ m_{\text{CO}}\,[\text{t/d}] &= m_{\text{C, total in}} \cdot \frac{\text{M}_{\text{CO}}}{\text{M}_{\text{C}}}\,. \end{aligned}$$

C.2 Combustion Zone

Input

Since air consists of, amongst others, CO_2 and water vapour, the incoming values of these were calculated to add in the LCA software. This because they are both greenhouse gases, and thus relevant to include. The amount of each was found from:

$$\begin{aligned} m_{\text{H}_2\text{O,in}}\,[\text{t/d}] &= m_{\text{air,in}} \cdot \frac{\text{M}_{\text{H}_2\text{O}} \cdot x_{\text{H}_2\text{O}}}{\text{M}_{\text{air}}}\,, \\ m_{\text{CO}_2\text{,in}}\,[\text{t/d}] &= m_{\text{air,in}} \cdot \frac{\text{M}_{\text{CO}_2} \cdot x_{\text{CO}_2}}{\text{M}_{\text{air}}}\,, \end{aligned}$$

where the molar mass M, and molar fraction x, is given in Table 3.6.

Output

The amount of combusted SiO_2 and CO_2 was added to the incoming air mass to give outgoing off gas mass. The amount of SiO_2 and CO_2 from combustion was found by:

$$m_{\mathrm{SiO_2}}\,[\mathrm{t/d}] = m_{\mathrm{SiO}} \cdot \frac{\mathrm{M_{SiO_2}}}{\mathrm{M_{SiO}}}\,,$$
$$m_{\mathrm{CO_2}}\,[\mathrm{t/d}] = m_{\mathrm{CO}} \cdot \frac{\mathrm{M_{CO_2}}}{\mathrm{M_{CO}}}\,.$$

Further, water vapour originating from the raw materials were also added to the off gas mass. Water vapour from moisture content, $MC\%$, given in the proximate analysis (Table A.2) was found by:

$$m_{\mathrm{H_2O,moisture}} = m_{\mathrm{i}} \cdot MC_{\mathrm{i}}\%\,,$$

where m_i is the mass of carbon material i. The water vapour originating from the hydrogen content in the raw materials, were found by considering the hydrogen content given in the wet based ultimate analysis (Table A.2) and assuming all hydrogen combust to oxygen according to:

$$4\,\mathrm{H} + \mathrm{O_2} \longrightarrow 2\,\mathrm{H_2O}\,,$$

giving the following:

$$m_{\mathrm{H_2O,hydrogen}} = m_{\mathrm{i}} \cdot \frac{\mathrm{M_{H_2O}}}{2\mathrm{M_H}}\,.$$

By adding $m_{\mathrm{H_2O,moisture}}$ and $m_{\mathrm{H_2O,hydrogen}}$ together for each carbon material type, the total water vapour is found.

Appendix D

Cooling Water Temperature

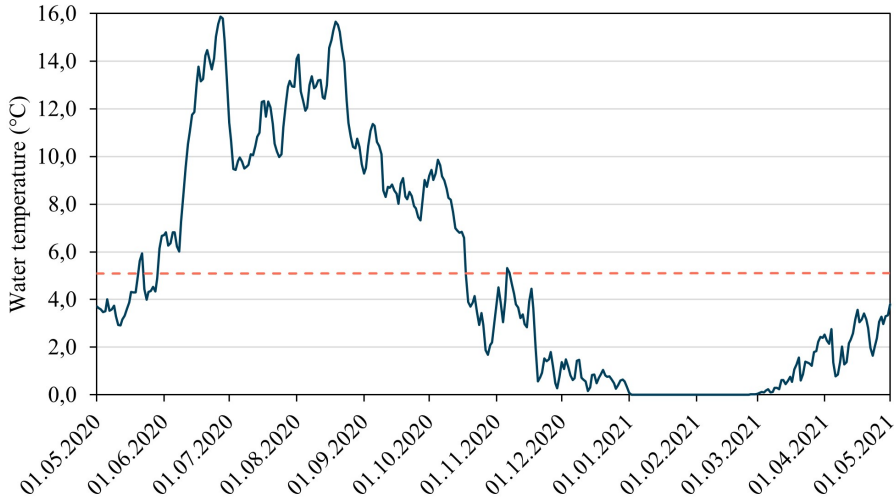

Figure D.1: Water temperature of Orkla river, measured on a daily basis close to the Svorkmo power station over the span of a year. Average yearly temperature was approximately 5 °C. Retrieved from [90].

Appendix E

Endpoint Impacts

All numbers in the following tables are given per tonne refined silicon metal.

Table E.1: Weighting results of damage categories, given in [Pt].

	BIO85	**BIO90**	**BIO95**	**MIX85**	**MIX90**	**MIX95**
Human health	151.49	144.59	138.46	224.47	215.22	207.02
Ecosystems	26.90	25.84	24.90	25.44	24.44	23.56
Resources	0.40	0.39	0.38	0.68	0.66	0.64

Resource Availability

Table E.2: Damage to resource availability, given in [US $].

	BIO85	**BIO90**	**BIO95**	**MIX85**	**MIX90**	**MIX95**
SOP	0.86	0.82	0.79	0.86	0.83	0.79
FFP	55.24	53.47	51.90	94.47	91.37	88.61
TOTAL	56.10	54.29	52.69	95.34	92.19	89.40

Ecosystem Quality

Table E.3: Damage to ecosystem quality, given in [species · year].

	BIO85	**BIO90**	**BIO95**	**MIX85**	**MIX90**	**MIX95**
GWP	7.57E-06	7.34E-06	7.14E-06	1.24E-05	1.20E-05	1.17E-05
EOFP	6.77E-06	6.38E-06	6.04E-06	6.51E-06	6.14E-06	5.82E-06
TAP	5.79E-06	5.47E-06	5.20E-06	8.19E-06	7.81E-06	7.47E-06
FEP	1.56E-07	1.50E-07	1.45E-07	8.93E-07	8.63E-07	8.35E-07
MEP	8.59E-11	8.28E-11	8.01E-11	1.67E-10	1.61E-10	1.56E-10
TETP	9.71E-08	9.35E-08	9.03E-08	8.26E-08	7.96E-08	7.69E-08
FETP	5.31E-08	5.05E-08	4.82E-08	7.34E-08	7.01E-08	6.72E-08
METP	1.05E-08	9.96E-09	9.52E-09	1.47E-08	1.41E-08	1.35E-08
LOP	2.72E-05	2.63E-05	2.54E-05	1.70E-05	1.64E-05	1.59E-05
WCP	5.36E-07	5.14E-07	4.94E-07	3.50E-07	3.33E-07	3.19E-07
TOTAL	4.82E-05	4.63E-05	4.46E-05	4.56E-05	4.38E-05	4.22E-05

Human Health

Table E.4: Damage to human health, given in [year].

	BIO85	**BIO90**	**BIO95**	**MIX85**	**MIX90**	**MIX95**
GWP	2.51E-03	2.44E-03	2.37E-03	4.12E-03	3.99E-03	3.87E-03
ODP	3.75E-06	3.60E-06	3.47E-06	2.01E-06	1.92E-06	1.84E-06
IRP	8.77E-07	8.33E-07	7.95E-07	8.84E-07	8.41E-07	8.02E-07
HOFP	4.71E-05	4.44E-05	4.20E-05	4.55E-05	4.29E-05	4.07E-05
PMFP	5.66E-03	5.36E-03	5.10E-03	7.82E-03	7.46E-03	7.14E-03
HTPc	1.25E-04	1.19E-04	1.14E-04	3.62E-04	3.49E-04	3.37E-04
HTPnc	2.25E-04	2.16E-04	2.08E-04	6.05E-04	5.83E-04	5.64E-04
WCP	4.25E-04	4.04E-04	3.85E-04	3.73E-04	3.54E-04	3.37E-04
TOTAL	9.00E-03	8.59E-03	8.22E-03	1.33E-02	1.28E-02	1.23E-02

Appendix F

Midpoint Impacts

All numbers in the following tables are given per tonne refined silicon metal.

Table F.1: Total midpoint impact score for all six scenarios.

Impact Category		**BIO85**	**BIO90**	**BIO95**	**MIX85**	**MIX90**	**MIX95**
GWP	kg CO_2 eq	2 703.53	2 622.55	2 550.63	4 437.66	4 297.88	4 173.71
IRP	kBq Co-60 eq	103.40	98.23	93.64	104.16	99.07	94.54
ODP	kg CFC-11 eq	0.01	0.01	0.01	0.00	0.00	0.00
PMFP	kg $PM_{2.5}$ eq	9.00	8.53	8.11	12.45	11.87	11.36
HOFP	kg NO_x eq	51.72	48.76	46.13	50.02	47.19	44.68
EOFP	kg NO_x eq	52.48	49.50	46.85	50.48	47.63	45.10
TAP	kg SO_2 eq	27.30	25.82	24.52	38.66	36.83	35.22
FEP	kg P eq	0.23	0.22	0.22	1.33	1.29	1.25
MEP	kg N eq	0.05	0.05	0.05	0.10	0.10	0.09
TETP	kg 1,4-DCB	8 512.91	8 195.86	7 917.63	7 245.76	6 979.86	6 746.66
FETP	kg 1,4-DCB	76.79	73.01	69.66	106.04	101.35	97.18
METP	kg 1,4-DCB	99.59	94.78	90.51	139.78	133.70	128.30
HTPc	kg 1,4-DCB	37.53	35.89	34.44	109.01	104.99	101.42
HTPnc	kg 1,4-DCB	986.38	946.21	910.51	2 654.64	2 558.73	2 473.52
SOP	kg Cu eq	3.72	3.55	3.41	3.73	3.57	3.42
FFP	kg oil eq	176.50	170.68	165.51	686.65	663.63	643.18
WCP	m^3	373.16	354.13	337.23	339.35	321.84	306.29
LOP	m^2a crop eq	3 066.03	2 960.80	2 867.35	1 917.13	1 851.18	1 792.58

Global Warming

Table F.2: Inventory flow contributions to global warming of each scenario, given in unit [kg CO_2 eq].

	BIO85	**BIO90**	**BIO95**	**MIX85**	**MIX90**	**MIX95**
Process emissions	433.09	429.48	426.28	2 925.35	2 837.38	2 759.23
Quartz	141.42	133.08	125.68	134.15	126.22	119.19
Coke	0.00	0.00	0.00	174.63	168.75	163.53
Coal	0.00	0.00	0.00	298.23	288.18	279.26
Charcoal	1 851.45	1 788.79	1 733.13	660.74	638.49	618.72
Wood chips	69.12	66.78	64.70	49.34	47.68	46.20
Electrode material	7.95	7.92	7.89	7.67	7.63	7.60
Quicklime (refining)	0.00	0.00	0.00	2.81	2.37	1.99
Electricity consumed	277.78	261.31	246.69	264.35	248.73	234.85
Silica recovered (byproduct)	-20.88	-13.11	-6.20	-20.24	-12.83	-6.25
Electricity recovered (byproduct)	-57.77	-53.02	-48.81	-60.31	-55.62	-51.46
Slag (waste)	1.36	1.31	1.27	0.95	0.90	0.85

Ionising Radiation

Table F.3: Inventory flow contributions to ionising radiation of each scenario, given in unit [kBq Co-60 eq].

	BIO85	**BIO90**	**BIO95**	**MIX85**	**MIX90**	**MIX95**
Process emissions	0.00	0.00	0.00	0.00	0.00	0.00
Quartz	1.79	1.68	1.59	1.70	1.60	1.51
Coke	0.00	0.00	0.00	2.39	2.31	2.24
Coal	0.00	0.00	0.00	12.25	11.83	11.47
Charcoal	10.63	10.27	9.95	3.79	3.66	3.55
Wood chips	1.68	1.63	1.58	1.20	1.16	1.13
Electrode material	0.54	0.54	0.53	0.52	0.52	0.51
Quicklime (refining)	0.00	0.00	0.00	0.02	0.01	0.01
Electricity consumed	112.35	105.69	99.78	106.92	100.60	94.99
Silica recovered (byproduct)	-0.26	-0.17	-0.08	-0.26	-0.16	-0.08
Electricity recovered (byproduct)	-23.36	-21.45	-19.74	-24.39	-22.50	-20.81
Slag (waste)	0.04	0.04	0.03	0.03	0.02	0.02

Stratospheric Ozone Depletion

Table F.4: Inventory flow contributions to stratospheric ozone depletion of each scenario, given in unit [kg CFC-11 eq].

	BIO85	**BIO90**	**BIO95**	**MIX85**	**MIX90**	**MIX95**
Process emissions	9.40E-04	8.84E-04	8.35E-04	8.95E-04	8.42E-04	7.95E-04
Quartz	4.73E-05	4.45E-05	4.21E-05	4.49E-05	4.23E-05	3.99E-05
Coke	0.00	0.00	0.00	5.84E-05	5.65E-05	5.47E-05
Coal	0.00	0.00	0.00	1.77E-04	1.71E-04	1.66E-04
Charcoal	5.29E-03	5.11E-03	4.95E-03	1.89E-03	1.83E-03	1.77E-03
Wood chips	4.25E-05	4.11E-05	3.98E-05	3.03E-05	2.93E-05	2.84E-05
Electrode material	4.34E-06	4.32E-06	4.30E-06	4.18E-06	4.16E-06	4.15E-06
Quicklime (refining)	0.00	0.00	0.00	3.37E-07	2.84E-07	2.38E-07
Electricity consumed	9.38E-04	8.83E-04	8.33E-04	8.93E-04	8.40E-04	7.93E-04
Silica recovered (byproduct)	-6.99E-06	-4.39E-06	-2.08E-06	-6.77E-06	-4.29E-06	-2.09E-06
Electricity recovered (byproduct)	-1.95E-04	-1.79E-04	-1.65E-04	-2.04E-04	-1.88E-04	-1.74E-04
Slag (waste)	8.73E-07	8.42E-07	8.15E-07	6.07E-07	5.74E-07	5.45E-07

Fine Particulate Matter Formation

Table F.5: Inventory flow contributions to fine particulate matter formation of each scenario, given in unit [kg PM2.5 eq].

	BIO85	**BIO90**	**BIO95**	**MIX85**	**MIX90**	**MIX95**
Process emissions	7.35	6.94	6.57	10.32	9.82	9.37
Quartz	0.28	0.27	0.25	0.27	0.25	0.24
Coke	0.00	0.00	0.00	0.70	0.67	0.65
Coal	0.00	0.00	0.00	0.49	0.48	0.46
Charcoal	1.02	0.99	0.95	0.36	0.35	0.34
Wood chips	0.09	0.09	0.08	0.06	0.06	0.06
Electrode material	0.02	0.02	0.02	0.02	0.02	0.02
Quicklime (refining)	0.00	0.00	0.00	0.00	0.00	0.00
Electricity consumed	0.35	0.33	0.31	0.33	0.31	0.30
Silica recovered (byproduct)	-0.04	-0.03	-0.01	-0.04	-0.03	-0.01
Electricity recovered (byproduct)	-0.07	-0.07	-0.06	-0.08	-0.07	-0.07
Slag (waste)	0.00	0.00	0.00	0.00	0.00	0.00

Tropospheric Ozone Formation, Human Health

Table F.6: Inventory flow contributions to tropospheric ozone formation (human health) of each scenario, given in unit [kg NO_x eq].

	BIO85	**BIO90**	**BIO95**	**MIX85**	**MIX90**	**MIX95**
Process emissions	47.88	45.04	42.52	45.56	42.87	40.48
Quartz	0.71	0.66	0.63	0.67	0.63	0.60
Coke	0.00	0.00	0.00	0.69	0.67	0.65
Coal	0.00	0.00	0.00	1.64	1.59	1.54
Charcoal	2.40	2.32	2.25	0.86	0.83	0.80
Wood chips	0.35	0.34	0.33	0.25	0.24	0.24
Electrode material	0.04	0.04	0.04	0.04	0.04	0.04
Quicklime (refining)	0.00	0.00	0.00	0.00	0.00	0.00
Electricity consumed	0.54	0.51	0.48	0.52	0.49	0.46
Silica recovered (byproduct)	-0.10	-0.07	-0.03	-0.10	-0.06	-0.03
Electricity recovered (byproduct)	-0.11	-0.10	-0.10	-0.12	-0.11	-0.10
Slag (waste)	0.01	0.01	0.01	0.01	0.01	0.01

Tropospheric Ozone Formation, Terrestrial Ecosystems

Table F.7: Inventory flow contributions to tropospheric ozone formation (terrestrial ecosystems) of each scenario, given in unit [kg NO_x eq].

	BIO85	**BIO90**	**BIO95**	**MIX85**	**MIX90**	**MIX95**
Process emissions	47.88	45.04	42.52	45.56	42.87	40.48
Quartz	0.72	0.67	0.64	0.68	0.64	0.60
Coke	0.00	0.00	0.00	0.83	0.81	0.78
Coal	0.00	0.00	0.00	1.66	1.61	1.56
Charcoal	3.12	3.01	2.92	1.11	1.08	1.04
Wood chips	0.38	0.37	0.35	0.27	0.26	0.25
Electrode material	0.04	0.04	0.04	0.04	0.04	0.04
Quicklime (refining)	0.00	0.00	0.00	0.00	0.00	0.00
Electricity consumed	0.55	0.52	0.49	0.53	0.50	0.47
Silica recovered (byproduct)	-0.11	-0.07	-0.03	-0.10	-0.07	-0.03
Electricity recovered (byproduct)	-0.12	-0.11	-0.10	-0.12	-0.11	-0.10
Slag (waste)	0.01	0.01	0.01	0.01	0.01	0.01

Terrestrial Acidification

Table F.8: Inventory flow contributions to terrestrial acidification of each scenario, given in unit [kg SO_2 eq].

	BIO85	**BIO90**	**BIO95**	**MIX85**	**MIX90**	**MIX95**
Process emissions	24.43	23.04	21.82	34.72	33.02	31.52
Quartz	0.71	0.67	0.63	0.67	0.63	0.60
Coke	0.00	0.00	0.00	0.71	0.69	0.67
Coal	0.00	0.00	0.00	1.38	1.33	1.29
Charcoal	1.37	1.33	1.29	0.49	0.47	0.46
Wood chips	0.21	0.20	0.19	0.15	0.14	0.14
Electrode material	0.04	0.04	0.04	0.04	0.04	0.04
Quicklime (refining)	0.00	0.00	0.00	0.00	0.00	0.00
Electricity consumed	0.80	0.76	0.71	0.77	0.72	0.68
Silica recovered (byproduct)	-0.11	-0.07	-0.03	-0.10	-0.06	-0.03
Electricity recovered (byproduct)	-0.17	-0.15	-0.14	-0.17	-0.16	-0.15
Slag (waste)	0.01	0.01	0.01	0.00	0.00	0.00

Freshwater Eutrophication

Table F.9: Inventory flow contributions to freshwater eutrophication of each scenario, given in unit [kg P eq].

	BIO85	**BIO90**	**BIO95**	**MIX85**	**MIX90**	**MIX95**
Process emissions	0.00	0.00	0.00	0.00	0.00	0.00
Quartz	2.62E-02	2.47E-02	2.33E-02	2.49E-02	2.34E-02	2.21E-02
Coke	0.00	0.00	0.00	1.73E-01	1.67E-01	1.62E-01
Coal	0.00	0.00	0.00	1.00E+00	9.70E-01	9.40E-01
Charcoal	9.97E-02	9.63E-02	9.33E-02	3.56E-02	3.44E-02	3.33E-02
Wood chips	1.19E-02	1.15E-02	1.11E-02	8.49E-03	8.20E-03	7.95E-03
Electrode material	2.30E-03	2.29E-03	2.29E-03	2.22E-03	2.21E-03	2.20E-03
Quicklime (refining)	0.00	0.00	0.00	5.68E-05	4.79E-05	4.01E-05
Electricity consumed	1.23E-01	1.15E-01	1.09E-01	1.17E-01	1.10E-01	1.04E-01
Silica recovered (byproduct)	-3.87E-03	-2.43E-03	-1.15E-03	-3.75E-03	-2.38E-03	-1.16E-03
Electricity recovered (byproduct)	-2.55E-02	-2.34E-02	-2.15E-02	-2.66E-02	-2.46E-02	-2.27E-02
Slag (waste)	1.47E-04	1.42E-04	1.38E-04	1.03E-04	9.70E-05	9.21E-05

Marine Eutrophication

Table F.10: Inventory flow contributions to marine eutrophication of each scenario, given in unit [kg N eq].

	BIO85	BIO90	BIO95	MIX85	MIX90	MIX95
Process emissions	0.00	0.00	0.00	0.00	0.00	0.00
Quartz	1.96E-03	1.85E-03	1.75E-03	1.86E-03	1.75E-03	1.66E-03
Coke	0.00	0.00	0.00	1.13E-02	1.10E-02	1.06E-02
Coal	0.00	0.00	0.00	6.26E-02	6.05E-02	5.87E-02
Charcoal	3.85E-02	3.72E-02	3.60E-02	1.37E-02	1.33E-02	1.29E-02
Wood chips	2.12E-03	2.05E-03	1.99E-03	1.51E-03	1.46E-03	1.42E-03
Electrode material	1.74E-04	1.73E-04	1.72E-04	1.67E-04	1.67E-04	1.66E-04
Quicklime (refining)	0.00	0.00	0.00	4.32E-06	3.64E-06	3.05E-06
Electricity consumed	1.02E-02	9.57E-03	9.03E-03	9.68E-03	9.10E-03	8.60E-03
Silica recovered (byproduct)	-2.90E-04	-1.82E-04	-8.62E-05	-2.81E-04	-1.78E-04	-8.68E-05
Electricity recovered (byproduct)	-2.11E-03	-1.94E-03	-1.79E-03	-2.21E-03	-2.04E-03	-1.88E-03
Slag (waste)	1.24E-05	1.20E-05	1.16E-05	8.62E-06	8.15E-06	7.74E-06

Terrestrial Ecotoxicity

Table F.11: Inventory flow contributions to terrestrial ecotoxicity of each scenario, given in unit [kg 1,4-DCB eq].

	BIO85	BIO90	BIO95	MIX85	MIX90	MIX95
Process emissions	3 759.07	3 614.32	3 489.09	3 237.19	3 117.96	3 015.06
Quartz	918.77	864.58	816.46	871.49	820.02	774.30
Coke	0.00	0.00	0.00	171.88	166.09	160.95
Coal	0.00	0.00	0.00	340.57	329.10	318.91
Charcoal	1 370.93	1 324.53	1 283.32	489.25	472.78	458.14
Wood chips	693.77	670.28	649.43	495.18	478.51	463.69
Electrode material	53.45	53.24	53.05	51.53	51.32	51.12
Quicklime (refining)	0.00	0.00	0.00	4.61	3.89	3.26
Electricity consumed	2 324.79	2 186.99	2 064.61	2 212.43	2 081.67	1 965.51
Silica recovered (byproduct)	-135.64	-85.15	-40.31	-131.47	-83.35	-40.61
Electricity recovered (byproduct)	-483.47	-443.78	-408.53	-504.72	-465.52	-430.70
Slag (waste)	11.25	10.85	10.50	7.83	7.40	7.02

Freshwater Ecotoxicity

Table F.12: Inventory flow contributions to freshwater ecotoxicity of each scenario, given in unit [kg 1,4-DCB eq].

	BIO85	**BIO90**	**BIO95**	**MIX85**	**MIX90**	**MIX95**
Process emissions	0.09	0.09	0.09	0.06	0.06	0.06
Quartz	2.93	2.76	2.60	2.78	2.61	2.47
Coke	0.00	0.00	0.00	6.65	6.43	6.23
Coal	0.00	0.00	0.00	32.91	31.80	30.82
Charcoal	7.89	7.62	7.39	2.82	2.72	2.64
Wood chips	1.25	1.20	1.17	0.89	0.86	0.83
Electrode material	0.28	0.28	0.28	0.27	0.27	0.27
Quicklime (refining)	0.00	0.00	0.00	0.00	0.00	0.00
Electricity consumed	81.76	76.91	72.61	77.80	73.21	69.12
Silica recovered (byproduct)	-0.43	-0.27	-0.13	-0.42	-0.27	-0.13
Electricity recovered (byproduct)	-17.00	-15.61	-14.37	-17.75	-16.37	-15.15
Slag (waste)	0.03	0.03	0.03	0.02	0.02	0.02

Marine Ecotoxicity

Table F.13: Inventory flow contributions to marine ecotoxicity of each scenario, given in unit [kg 1,4-DCB eq].

	BIO85	**BIO90**	**BIO95**	**MIX85**	**MIX90**	**MIX95**
Process emissions	2.43	2.34	2.26	1.90	1.83	1.77
Quartz	4.36	4.11	3.88	4.14	3.90	3.68
Coke	0.00	0.00	0.00	9.17	8.86	8.59
Coal	0.00	0.00	0.00	45.27	43.74	42.39
Charcoal	11.07	10.70	10.37	3.95	3.82	3.70
Wood chips	1.99	1.93	1.87	1.42	1.38	1.33
Electrode material	0.39	0.39	0.39	0.38	0.38	0.38
Quicklime (refining)	0.00	0.00	0.00	0.01	0.01	0.01
Electricity consumed	100.92	94.94	89.63	96.05	90.37	85.33
Silica recovered (byproduct)	-0.64	-0.40	-0.19	-0.62	-0.40	-0.19
Electricity recovered (byproduct)	-20.99	-19.27	-17.73	-21.91	-20.21	-18.70
Slag (waste)	0.04	0.04	0.04	0.03	0.03	0.03

Human Toxicity, Carcinogenic

Table F.14: Inventory flow contributions to human toxicity (carcinogenic) of each scenario, given in unit [kg 1,4-DCB eq].

	BIO85	**BIO90**	**BIO95**	**MIX85**	**MIX90**	**MIX95**
Process emissions	0.15	0.15	0.14	0.13	0.13	0.12
Quartz	3.51	3.30	3.12	3.33	3.13	2.95
Coke	0.00	0.00	0.00	12.14	11.73	11.37
Coal	0.00	0.00	0.00	67.48	65.21	63.19
Charcoal	9.06	8.75	8.48	3.23	3.12	3.03
Wood chips	1.44	1.40	1.35	1.03	1.00	0.97
Electrode material	0.33	0.33	0.33	0.32	0.32	0.31
Quicklime (refining)	0.00	0.00	0.00	0.01	0.01	0.01
Electricity consumed	29.69	27.93	26.36	28.25	26.58	25.10
Silica recovered (byproduct)	-0.52	-0.32	-0.15	-0.50	-0.32	-0.15
Electricity recovered (byproduct)	-6.17	-5.67	-5.22	-6.44	-5.94	-5.50
Slag (waste)	0.04	0.04	0.04	0.03	0.03	0.02

Human Toxicity, Non-carcinogenic

Table F.15: Inventory flow contributions to human toxicity (non-carcinogenic) of each scenario, given in unit [kg 1,4-DCB eq].

	BIO85	**BIO90**	**BIO95**	**MIX85**	**MIX90**	**MIX95**
Process emissions	129.52	125.04	121.03	83.62	80.71	78.09
Quartz	104.43	98.27	92.80	99.06	93.21	88.01
Coke	0.00	0.00	0.00	248.63	240.26	232.83
Coal	0.00	0.00	0.00	1668.58	1612.39	1562.48
Charcoal	237.37	229.33	222.20	84.71	81.86	79.32
Wood chips	34.16	33.01	31.98	24.38	23.56	22.83
Electrode material	7.17	7.14	7.12	6.91	6.88	6.86
Quicklime (refining)	0.00	0.00	0.00	0.19	0.16	0.14
Electricity consumed	616.66	580.11	547.65	586.86	552.17	521.36
Silica recovered (byproduct)	-15.42	-9.68	-4.58	-14.94	-9.47	-4.62
Electricity recovered (byproduct)	-128.24	-117.71	-108.36	-133.88	-123.48	-114.25
Slag (waste)	0.73	0.70	0.68	0.51	0.48	0.46

Mineral Resource Scarcity

Table F.16: Inventory flow contributions to mineral resource scarcity of each scenario, given in unit [kg Cu eq].

	BIO85	**BIO90**	**BIO95**	**MIX85**	**MIX90**	**MIX95**
Process emissions	0.00	0.00	0.00	0.00	0.00	0.00
Quartz	0.30	0.28	0.27	0.28	0.27	0.25
Coke	0.00	0.00	0.00	0.18	0.17	0.17
Coal	0.00	0.00	0.00	0.58	0.57	0.55
Charcoal	0.76	0.73	0.71	0.27	0.26	0.25
Wood chips	0.23	0.22	0.22	0.17	0.16	0.16
Electrode material	0.02	0.02	0.02	0.02	0.02	0.02
Quicklime (refining)	0.00	0.00	0.00	3.82E-04	3.22E-04	2.70E-04
Electricity consumed	3.09	2.90	2.74	2.94	2.76	2.61
Silica recovered (byproduct)	-0.04	-0.03	-0.01	-0.04	-0.03	-0.01
Electricity recovered (byproduct)	-0.64	-0.59	-0.54	-0.67	-0.62	-0.57
Slag (waste)	4.19E-03	4.04E-03	3.91E-03	2.91E-03	2.76E-03	2.62E-03

Fossil Resource Scarcity

Table F.17: Inventory flow contributions to fossil resource scarcity of each scenario, given in unit [kg oil eq].

	BIO85	**BIO90**	**BIO95**	**MIX85**	**MIX90**	**MIX95**
Process emissions	0.00	0.00	0.00	0.00	0.00	0.00
Quartz	36.38	34.24	32.33	34.51	32.47	30.66
Coke	0.00	0.00	0.00	96.44	93.20	90.31
Coal	0.00	0.00	0.00	475.10	459.10	444.89
Charcoal	77.96	75.33	72.98	27.82	26.89	26.05
Wood chips	22.60	21.83	21.15	16.13	15.59	15.10
Electrode material	2.22	2.21	2.20	2.14	2.13	2.12
Quicklime (refining)	0.00	0.00	0.00	0.26	0.22	0.19
Electricity consumed	53.02	49.88	47.08	50.46	47.47	44.82
Silica recovered (byproduct)	-5.37	-3.37	-1.60	-5.21	-3.30	-1.61
Electricity recovered (byproduct)	-11.03	-10.12	-9.32	-11.51	-10.62	-9.82
Slag (waste)	0.72	0.69	0.67	0.50	0.47	0.45

Water Use

Table F.18: Inventory flow contributions to water use of each scenario, given in unit [m^3 water consumed].

	BIO85	**BIO90**	**BIO95**	**MIX85**	**MIX90**	**MIX95**
Process emissions	47.01	44.90	43.02	47.28	45.20	43.35
Quartz	1.06	1.00	0.95	1.01	0.95	0.90
Coke	0.00	0.00	0.00	0.61	0.59	0.58
Coal	0.00	0.00	0.00	1.05	1.02	0.99
Charcoal	21.10	20.39	19.75	7.53	7.28	7.05
Wood chips	0.22	0.22	0.21	0.16	0.15	0.15
Electrode material	0.04	0.04	0.04	0.04	0.04	0.04
Quicklime (refining)	0.00	0.00	0.00	0.00	0.00	0.00
Electricity consumed	383.63	360.89	340.70	365.09	343.51	324.34
Silica recovered (byproduct)	-0.16	-0.10	-0.05	-0.15	-0.10	-0.05
Electricity recovered (byproduct)	-79.78	-73.23	-67.41	-83.29	-76.82	-71.07
Slag (waste)	0.03	0.03	0.03	0.02	0.02	0.02

Land Use

Table F.19: Inventory flow contributions to land use of each scenario, given in unit [$m^2 \cdot$ year annual crop land].

	BIO85	**BIO90**	**BIO95**	**MIX85**	**MIX90**	**MIX95**
Process emissions	0.00	0.00	0.00	0.00	0.00	0.00
Quartz	42.08	39.60	37.40	39.92	37.56	35.46
Coke	0.00	0.00	0.00	47.10	45.51	44.10
Coal	0.00	0.00	0.00	312.09	301.57	292.24
Charcoal	1 872.26	1 808.90	1 752.61	668.16	645.67	625.68
Wood chips	1 020.94	986.38	955.69	728.69	704.16	682.36
Electrode material	3.34	3.33	3.32	3.22	3.21	3.20
Quicklime (refining)	0.00	0.00	0.00	0.11	0.09	0.08
Electricity consumed	168.39	158.41	149.54	160.25	150.78	142.37
Silica recovered (byproduct)	-6.21	-3.90	-1.85	-6.02	-3.82	-1.86
Electricity recovered (byproduct)	-35.02	-32.14	-29.59	-36.56	-33.72	-31.20
Slag (waste)	0.24	0.23	0.22	0.17	0.16	0.15

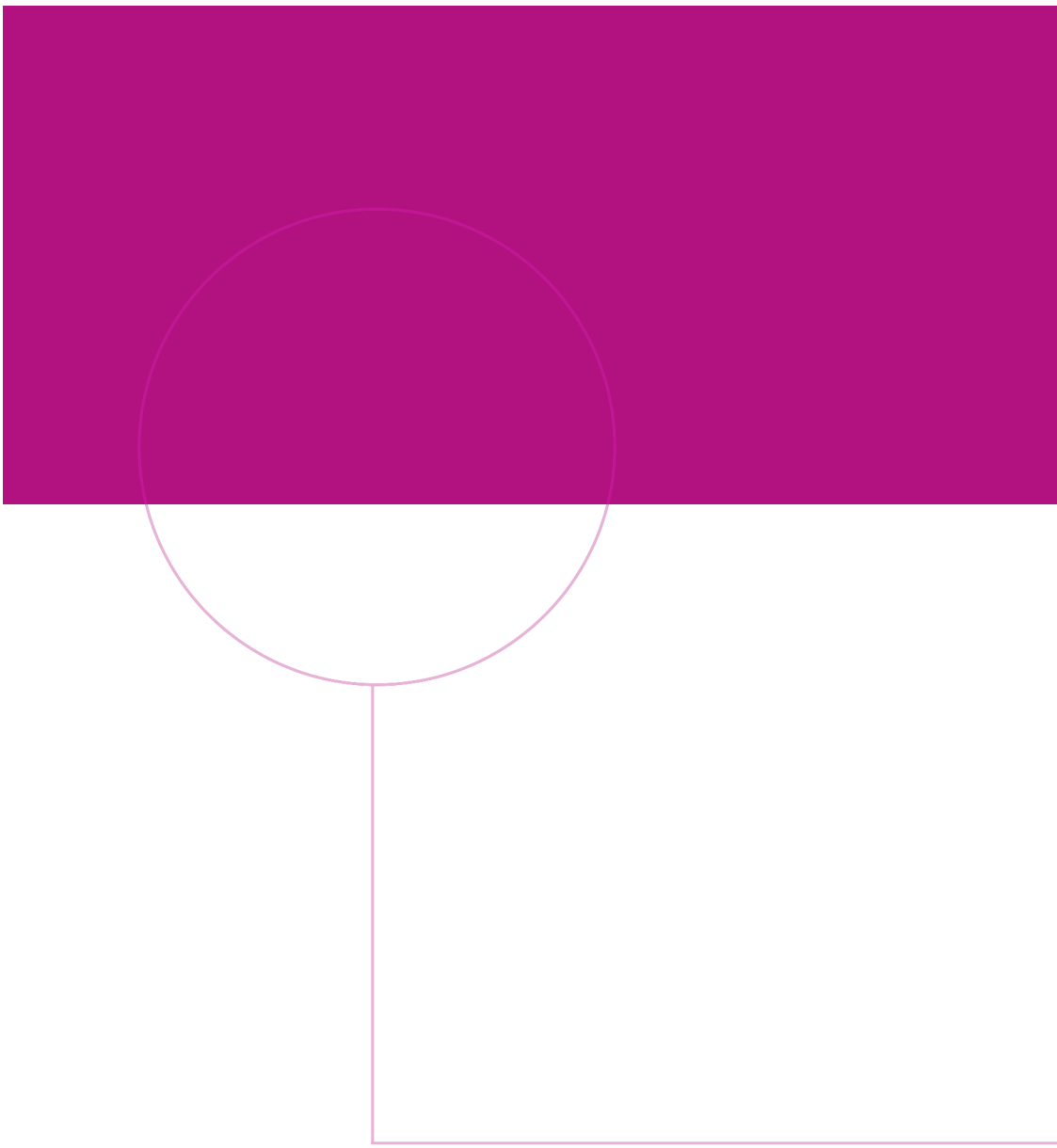

NTNU

Norwegian University of
Science and Technology